Synthesis, spectral and reactivity studies of ruthenium complexes with 2,6-*bis*(benzimidazol-2-yl)pyridine

Thesis

submitted in partial fulfillment of the requirements for the degree of

Doctor of Philosophy

By

Amardeep
(*Roll No. 05612215*)

Supervisor

Dr. Biplab Mondal

Department of Chemistry
Indian Institute of Technology Guwahati
Guwahati, Assam-781039, India
October, 2009

Dedicated to my

Parents

INDIAN INSTITUTE OF TECHNOLOGY GUWAHATI
Guwahati, Assam-781 039, India
Department of Chemistry

STATEMENT

I do hereby declare that the matter embodied in this thesis is the result of investigations carried out by me in the Department of Chemistry, Indian Institute of Technology Guwahati, Guwahati, Assam, India under the supervision of Dr. Biplab Mondal, Department of Chemistry, Indian Institute of Technology Guwahati, Guwahati, Assam, India.

In keeping with the general practice of reporting scientific observations, due acknowledgement has been made wherever the work described is based on the findings of other investigators.

October, 2009

(Amardeep)

INDIAN INSTITUTE OF TECHNOLOGY GUWAHATI
Guwahati, Assam-781 039, India
Department of Chemistry

CERTIFICATE

This is to certify that the work contained in the thesis entitled **"Synthesis, spectral and reactivity studies of ruthenium complexes with 2,6-*bis*(benzimidazol-2-yl)pyridine"** by Amardeep, a PhD student of the Department of Chemistry, Indian Institute of Technology Guwahati, for the award of degree of Doctor of Philosophy has been carried out under my supervision and this work has not been submitted elsewhere for a degree.

October, 2009

Dr. Biplab Mondal

INDIAN INSTITUTE OF TECHNOLOGY GUWAHATI
Guwahati, Assam-781 039, India
Department of Chemistry

CERTIFICATE OF COURSE WORK

This is to certify that Amardeep has satisfactorily completed all the courses required for the Ph. D degree program. These courses include

1) CH 605 : Applied Crystallography
2) CH 627 : New Reagents in Organic Chemistry
3) CH 611 : Bioinorganic Chemistry
4) CH 630 : A Fundamental Approach to Physical Chemistry

Prof. A. Chattopadhyay
Head,
Department of Chemistry

Prof. T. Punniyamurthy
Secretary,
Departmental Post Graduate Program Committee
Department of Chemistry

ACKNOWLEDGMENT

First, I would like to express my deep sense of gratitude to my supervisor, Dr. Biplab Mondal, for his excellent guidance, helping to learn chemistry and always believing in me. He provided me the opportunity and resources to be creative, inspired me to do my best, making sure I am progressing along a forward path. It is these things that have given me the most confidence in my scientific abilities.

I am thankful to my Doctoral Committee members, Prof. J. B. Baruah, Dr. Gopal Das and Dr. Parameswar K. Iyer for helping me in various ways with their suggestions.

Next, I would like to take the opportunity to thank all the faculty members who had helped me in one way or another to finish this PhD work for and all the initial help with learning chemistry.

I am thankful to the Head of Department for allowing me to use the Instruments Facilities ie. FT-IR and UV-visible spectrophotometer and Cyclic Voltammetry Techniques. The Head of Central Instruments Facility (CIF) for providing me Instruments facilities ie. NMR. EPR and Mass spectrometer, Chandan-da, Kula-da and kishore-da for the NMR, EPR and Mass spectroscopic measurements. Mr. Babulal Das, Mrs. Lipika, Mrs. Abhilasha, Mr. Prikshit, Mr. Anirudh, Mr. Neelu, Mr. Diganta, Mr. Shyamal, Mr. Shantanu and Mr. Subal for their anytime help.

I would like to thank my past and present labmates Pushpendra, Partha, Ananya, Bidraha, Dadu, Abhimanyu, Subrahmanium, Moushumi, Rajib, Pankaj, Apurba, Lovish, Anuj, Neeraj, Satish, Madhav, Kaushik and Debabrata for fruitful discussion on my chemistry.

I am also thankful to all Research Scholars, friends, M.Sc. and B.Tech. students: Papori-di, Panda-da, Bolin-da, Ballav, Rik, Sonit, Gunin, Prashant, Shaitanya, Anirban, Shahzad, Murgadoss, Jashmini, Shiva, Subash, Suri Babu, Pramod, Ramesh, Bhasker,. Joyshree, Ali, Hari, Faizi, Mohan, Musawwer, Rezzak, Prasenjit, Priyanka, Rupam, Marjit, Devendra, Atul, Nihar, Reddy, Somu, Himanshu, Rosi, Vijendra, Raihana, Shristi, Franciss, Sadhucharan, Subhojit, Deb, Arvind, Ziya Khan, Chaitanya, Nani, Rajan, Anil, Himanshu Jha, Dilip, Satchi, Rajendra, Prabhanjan, Rajesh, Gourav, Nar Singh, Atul,

Achilesh, Sanjay, Vigya, Ravi, Akhilesh, Ashok, Anand, Brij Bhusan, Avneesh, Madhumita, Praveen, Varsha, Mayank, Garima, Ram Niwas, Rajiv, Amit, Rajan, Nitin, Lekhraj, Surendra, Hema, Abhey, Nidhi, Tushar, Gourav, Sajid, Medhi and Joyshree(Deka), who made my stay here and there more enjoyable.

My special thanks to Late Prof. M. K. Maheshwari who left encouraging path for me.

I thank my father though, he is no more, but his remembrance has always given me inspiration, encouragement and strength.

I thank my sisters, Premlata, Kunti, and my brother, Jitender, brother in law, Mr. Raghuvir Singh, my Nephews, Ashu and Shanu, my niece, Shikha and Chitra for their love and moral support during my research work.

Finally, I thank my mother. Without her love, support and encouragement, this work would not have been completed.

October, 2009 **Amardeep**

CONTENTS

Statement I

Certificate II

Certificate for course work III

Acknowledgement IV

Synopsis X

Chapter 1: Introduction

1.1 Introduction 1

1.2 Objective of the present work 03

1.3 References 16

Chapter 2: Ruthenium complexes of 2,6-*bis*(benzimidazol-2-yl)pyridine with terpyridine: Synthesis, spectral properties and crystal structure

Abstract 20

2.1 Introduction 21

2.2 Results and Discussion 22

2.3 Conclusion 37

2.4 Experimental Section 38

2.5 References 41

Chapter 3: Proton dependent valence state distribution in ruthenium *o*-quinonoids with 2,6-*bis*(benzimidazol-2-yl)pyridine ancillary

Abstract 44

3.1 Introduction 45

3.2 Results and Discussion 47

3.3 Conclusion 68

3.4 Experimental Section 69

3.5 References 73

Chapter 4: Valence state distribution in ruthenium complexes of 2,6-*bis*(benzimidazol-2-yl)pyridine with catechol and acetylacetone

Abstract 78

4.1 Introduction 79

4.2 Results and Discussion 79

4.3 Conclusion 87

4.4 Experimental Section 87

4.5 References 89

Chapter 5a: Reduction of coordinated acetonitrile to ethylamine in [Ru^{II}(bbp)(*o*-phen)(CH_3CN)] by *p*-phenylenediamine and hydroquinone

Abstract 91

5a.1 Introduction 92

5a.2 Results and Discussion 93

5a.3 Conclusion 101

5a.4 Experimental Section 101

5a.5 References 104

Chapter 5b: Nucleophilic addition reaction on coordinated acetonitrile in [Ru^{II}(bbp)(*o*-phen)(CH_3CN)]

Abstract 106

5b.1 Introduction 107

5b.2 Results and Discussion 108

5b.3 Conclusion 112

5b.4 Experimental Section 112

5b.5 References 114

Chapter 6: Synthesis of ruthenium complexes [Ru^{II}(bbp)(*o*-phen)(Cl)], [Ru^{II}(bbp)(*o*-phen)(H_2O)], [Ru^{II}(bbp)(*o*-phen)(DMSO)] and [Ru^{II}(bbp)(*o*-phen)(CH_3CN)]: Structural and spectral studies

Abstract 115

6.1 Introduction 116

6.2 Results and Discussion 116

6.3 Conclusion 131

6.4 Experimental Section 132

6.5 References 136

Chapter 7: Synthesis, spectral and electrochemical studies of ruthenium complexes with substituted 2,6-*bis*(benzimidazol-2-yl)pyridine ligands

Abstract 140

7.1 Introduction 141

7.2 Results and Discussion 142

7.3 Conclusion 152

7.4 Experimental Section 153

7.5 References 156

The thesis entitled, "**Synthesis, spectral and reactivity studies of ruthenium complexes with 2,6-*bis*(benzimidazol-2-yl)pyridine"** is divided into seven chapters.

Chapter-1 presents a brief introduction of the 2,6-*bis*(benzimidazol-2-yl)pyridine (bbp) as a tridentate ligand. The common polypyridyl ligands used in ruthenium chemistry are 2,2′-bipyridine(bpy), 1,10-phenonthroline(phen) and 2,2′:6′,2″-terpyridine (trpy) and their substituted analogous. From the structural point of view, the tridentate terpyridine type ligands are generally better than the bidentate one as their complexes are associated with less number of geometrical isomers. The 2,6-*bis*(benzimidazol-2-yl)pyridine is structurally analogous to 2,2′:6′,2″-terpyridine (Figure 1) and like trpy, due to the extensive π-delocalization, it affords well defined structure of it's complexes.

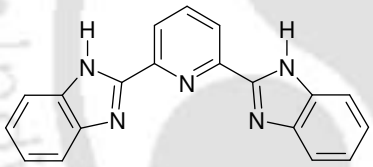

bbp

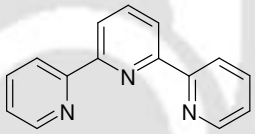

trpy

Figure 1

It can bind the metal centers in meridional fashion with an average bite angle of ~ 79° which is comparable to that of trpy. At the same time, bbp can offer a combination of moderate π-acceptor pyridine nitrogen and π-donor imidazole nitrogen, also. In addition, this ligand can provide one or more dissociable protons which can be used as a trigger for proton-induced tuning of redox as well as chemical properties of its complexes (scheme 1).

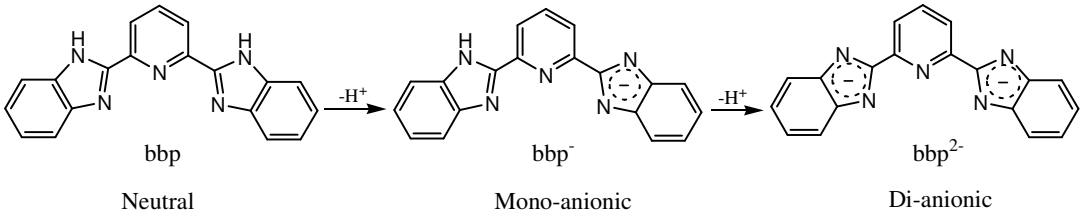

Scheme 1

Hence, one could think of substitute trpy ligand by the bbp and indeed, the present project originates from our interest to study the effect of use of bbp instead of trpy in ruthenium complexes and in addition, the effect of the presence or absence of proton on bbp on the binding, spectral, electrochemical as well as chemical behaviour of it's ruthenium complexes in combination with other bidentate ancillaries.

Chapter-2 discusses the redox and spectral properties of ruthenium-bbp complex with trpy as ancillary ligand. In this regard, as a starting point, the ruthenium monoterpyridine complexes $[Ru(trpy)(bbp)]^{2+}$, $[\mathbf{1}]^{2+}$ and $[Ru(trpy)(bbp^{2-})]$, **2** with the proposed bbp ligand have been synthesized and characterized using various spectroscopic techniques and by single crystal structure determination (Figure 2). Complexes $[\mathbf{1}]^{2+}$ and **2** exhibit strong

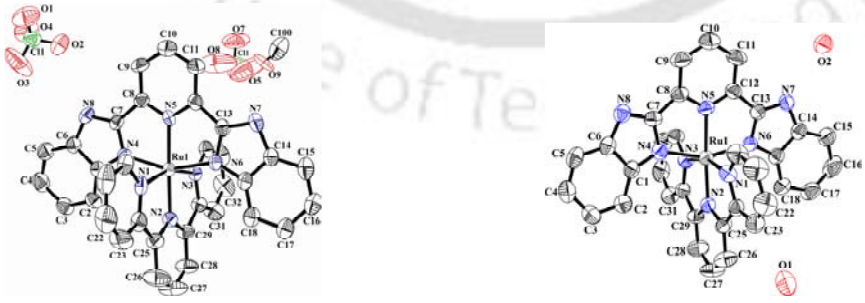

1 **2**

Figure 2: ORTEP diagrams of complexes **1** and **2** (50% thermal ellipsoids plot).

MLCT transitions at 475 and 510 nm, respectively and are found to be very much

dependent on solution pH. The successive pH dependent dissociation of the N-H protons of benzimidazole moiety of bbp in **1** lead to the formation of **2** (Figure 3). The proton induced reversible interconversion of **1** and **2** has been observed via electrochemical studies, also (Figure 4).

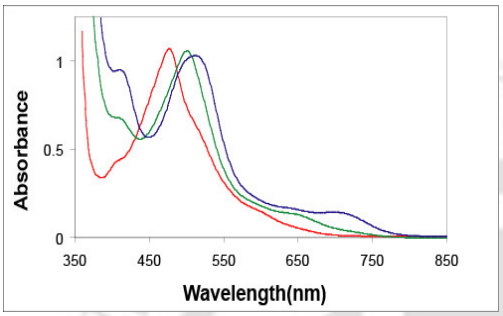

Figure 3: UV-visible spectra of $[\mathbf{1}]^{2+}$ (red), $[\mathbf{1a}]^{+}$ (blue) and **2** (black) in acetonitrile: water (1:4 v/v) at pH: 1.25, 6.50 and 12, respectively.

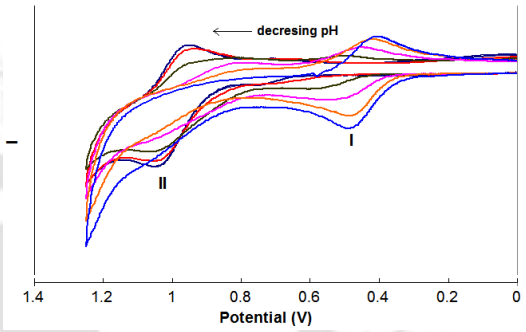

Figure 4: pH (1.02 to 12.5) dependent cyclic voltammograms in acetonitrile : water (1:4 v/v).

Chapter-3 describes the valance state distribution in Ru-bbp complexes with oxolene ancillaries. The protonation/deprotonation of the bbp has been observed to play the key role in controlling the metal binding mode of these quinonoid type non-innocent ligands. The neutral complexes $[Ru(bbp)(X)(CH_3CN)]$ (**3a**-**5a**) and monocationic complexes $[Ru(bbp)(Y)(CH_3CN)]^{+}$ (**3b**-**5b**) (X = quinone form of *o*-phenylenediamine, *o*-aminophenol and *o*-aminothiophenol, respectively and Y = semiquinonate form of *o*-phenylenediamine, *o*-aminophenol and *o*-aminothiophenol, respectively) have been synthesized by the reaction of $[Ru(bbp)Cl_3]$ with *o*-phenylenediamine, *o*-aminophenol and *o*-aminothiophenol, respectively. The unsymmetrical nature of *o*-phenylenediamine, *o*-aminophenol and *o*-aminothiophenol are expected to give two isomeric products, **A** and **B** (scheme 2). However, in the present case only isomer, **B** was obtained preferentially.

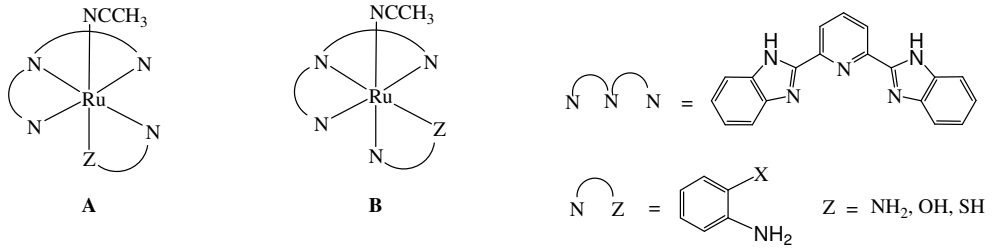

Scheme 2

The complexes **3a–5a** are found to be neutral in acetonitrile whereas **3b-5b** exhibit 1:1 electrolytic nature. The ESI-mass spectral studies also confirm the formation of the complexes. Complexes **3a–5a** are found to be diamagnetic in nature whereas **3b-5b** display one-electron paramagnetism.

The neutral, diamagnetic complexes can arise from any of the following combinations: (i) [Ru^{II}(bbp)(*cat*)], (ii) [Ru^{III}(bbp^{-})(*sq*)], (iii) [Ru^{II}(bbp^{2-})(*qu*)]. Hence, in the present case, the charge distribution on the redox active ligand has become of interest. The structures of the complexes **3a** and **4b** were authenticated by their single crystal X-ray structures (Figure 5). The crystal structures reveal that the bbp ligand is bonded to the metal in di-anionic form and the ancillary ligands are present in neutral quinone form.

As the complex is neutral and non-conducting, it is evident that the ruthenium is in +II oxidation state.

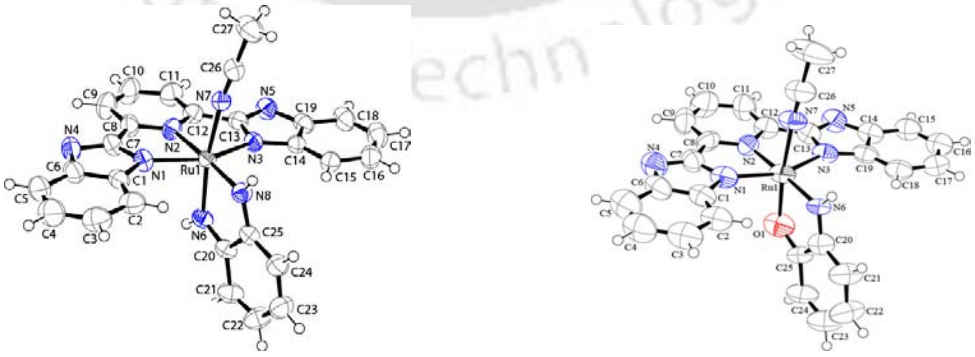

3a **4a**

Figure 5: ORTEP diagrams of complexes **3a** and **4a** (50% thermal ellipsoids plot).

^{1}H-NMR study shows expected number of aromatic protons with a sharp singlet at $\delta \approx$ 2.04 ppm corresponding to three protons from coordinated acetonitrile. All these complexes show reversible responses for Ru^{II}/Ru^{III} couple in cyclic voltammetric studies. The representative voltammograms of complex **3a** are shown in figure 6. The voltammogram exhibits two quasi-reversible red-ox couples in the positive side of SCE and these can be attributed to the $Ru^{II/III}$ and *sq-qu* processes. The redox couples in the negative side are due to the reduction of oxolene and bbp ligands.

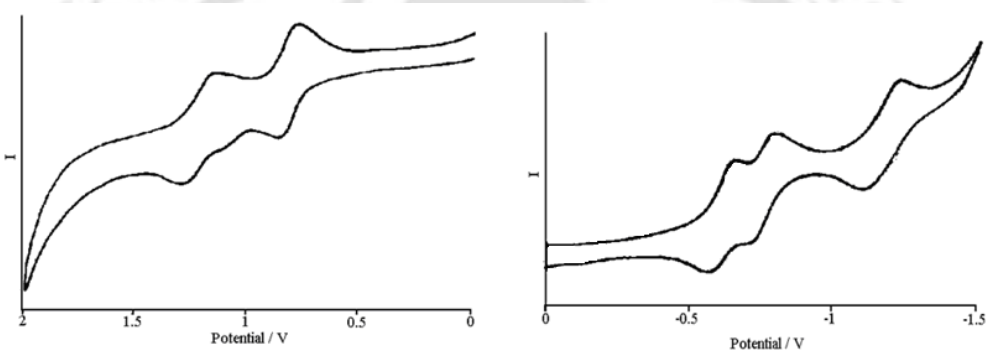

Figure 6: Cyclic voltammograms of complex **3a** in acetonitrile solvent (SCE: Reference electrode; Glassy Carbon: working electrode; Supporting electrolyte: TBAP).

Though we are unable to crystallize **5a**, all the spectral properties match well with **3a** and **4a**, it is logical to assume that **5a** also have the same valence state configuration.

On the other hand, the paramagnetism in complexes **3b-5b** is attributed to the presence of $[Ru^{II}(bbp)(sq)(CH_3CN)]^+$ form. The isotropic signal in X-band EPR spectral studies at low temperature (77K) indicate presence of radical in the ligand framework (Figure 7).

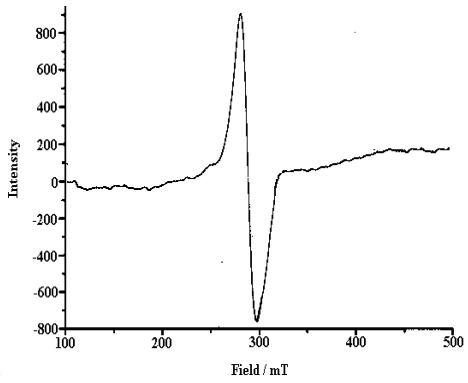

Figure 7: X-band EPR spectrum for complex **3b** in acetonitrile/toluene at 77K.

The deviation of the *g* values from 2.005 for the free semiquinone moiety to 2.220 - 2.233 in complexes **3b-5b**, respectively, is attributed to the slight mixing of the metal *d*-orbital to the oxolene molecular orbitals.

Chapter-4 deals with synthesis and spectral studies of Ru-bbp complexes with catechol and acetylacetone. A set of two complexes with catechol and acetylacetone have been synthesized to study the variation of their physicochemical properties depending on the ancillary ligands i.e. catecholato (*cat*) and acetylacetoneto (*acac*), respectively. The complexes [Ru(bbp)(*cat*)(CH_3CN)] (**6**) and [Ru(bbp)(*acac*)(CH_3CN)] (**7**) were prepared by the reaction of [Ru(bbp)Cl_3] with the respective ligands in ethanolic medium (Scheme 3). followed by chromatographic separation using silica gel column. Both the complexes were isolated as neutral molecules. Though the actual electronic structure in complex **7** is bit straight forward, in complex **6** it could be either Ru^{II}(*sq*) or Ru^{III}(*cat*) or lies between these two resonance forms. Both the complexes exhibit broad and unresolved signals in ^{1}H-NMR spectra. This is because of the presence of paramagnetic centers in the complexes. In magnetic moment measurement, both the complexes display magnetic susceptibility corresponding to one unpaired electron.

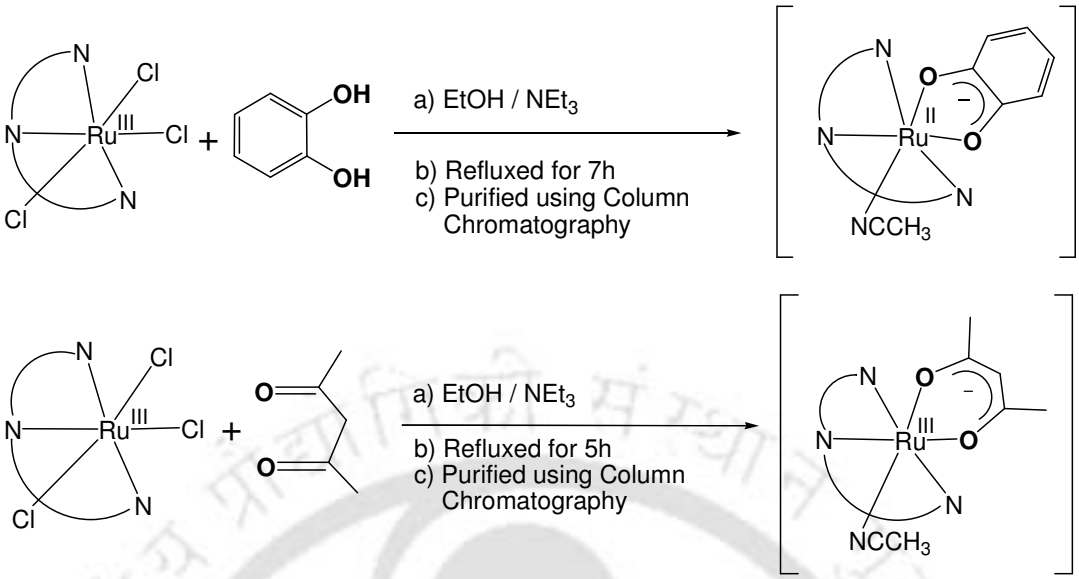

Scheme 3

The X-band EPR spectrum of the frozen solution of complex **6** shows an isotropic signal with g = 2.103 at 77K which can be attributed to the presence of the semiquinonate radical. The higher g value from the free semiquinonate anion radical indicates the partial mixing of the metal *d*-orbital with the molecular orbitals from catechol moiety which are of comparable energy. Hence for complex **6**, one could think of a Ru^{II}-*sq* charge distribution. The complex **7** exhibits a broad signal at g = 2.284 with a degree of anisotropic character (Figure 8).

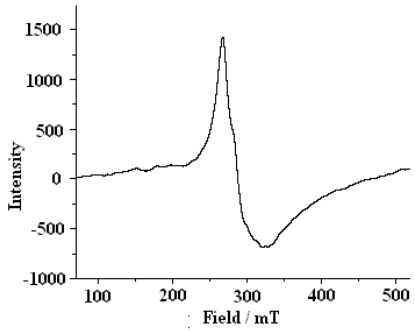

Figure 8: X-band EPR spectrum for complex **7** in acetonitrile/toluene at 77K.

This unresolved anisotropic signal indicates the presence of the unpaired electron on the metal center. Hence in complex **7**, the Ru(III)-acetylacetoneto charge distribution is more probable.

Chapter-5 describes the various reactions of and on the coordinated acetonitrile solvent in complex **3a**. In complexes **3a–5a**, as the solvent acetonitrile is coordinated to the metal center, hence, one could think of solvent substitution with different donor ligands. In this regard, we have tried with a set of ligands starting from neutral pyridine to anionic azide, thiocyanato etc. In acetonitrile medium. However, in all the cases, it has been found to end up with complex, $[Ru(bbp)(CH_3CN)_3](ClO_4)_2$, which is the result of the replacement of oxolene ligand rather than solvent substitution (Figure 9).

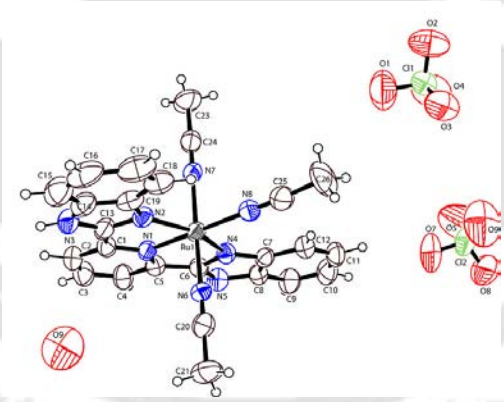

Figure 9: ORTEP diagram of complex $[Ru(bbp)(CH_3CN)_3](ClO_4)_2$ (50% thermal ellipsoids plot) obtained from the reaction of complex **3a** with NaN_3 in acetonitrile solvent.

Reduction of coordinated acetonitrile

As the replacement of coordinated acetonitrile by other ligands has not been observed, one could think of the reduction of the coordinated acetonitrile. From literature, this reduction has been reported to carry out either by hydrogen or by hydride sources (e.g. NaH, $NaBH_4$, $LiAlH_4$, $LiHBEt_3$ etc.). However, in the present case with complex **3a**, the

reduction of coordinated acetonitrile to ethylamine in $[Ru^{II}(bbp^{2-})(Y)(CH_3CH_2NH_2)]$ (**8**) [Y : *o*-phenylenediamine in quinone form] has been found to take place in presence of *p*-phenylenediamine or hydroquinone.

The complex **3a**, on refluxing with three equivalent of *p*-phenylenediamine in ethanol solvent for 4h followed by chromatographic purification yields the complex **8**. In the positive ion ESI mass spectrum, the molecular ion peak appears at 562.74 which indicates the reduction of coordinated acetonitrile to ethylamine. The formation of **8** is further confirmed by its single crystal structure (Figure 10).

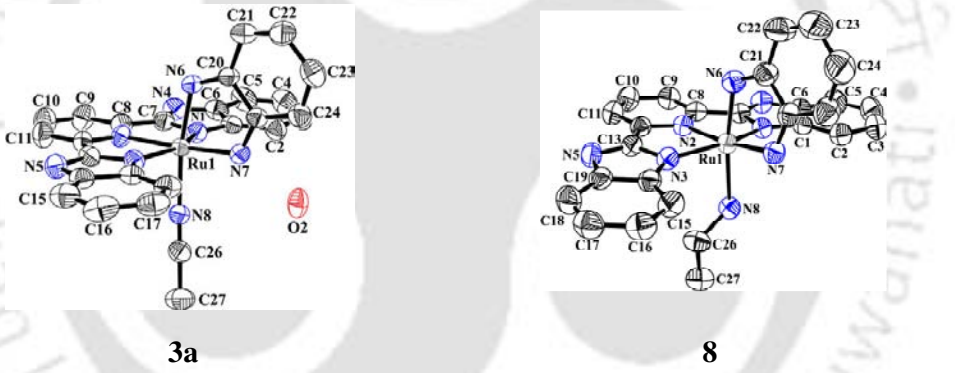

Figure 10: ORTEP diagrams of complexes **3a** and **8** (50% thermal ellipsoids plot).

The reduction of the acetonitrile to ethylamine is evidently a $4e^-/4H^+$ process; hence, it results into the oxidation of two equivalent of *p*-phenylenediamine to corresponding aminoquinone (in case of hydroquinone, to corresponding quinone) (quantitatively determined by isolated product analysis). It is important to note that the same reduction has not been observed with benzonitrile or acrylonitrile analogues.

The nucleophilic addition of $NaOCH_3$ to the metal coordinated acetonitrile in complex **3a** has been studied. The reaction resulted into the formation of metal coordinated imido

derivative, [Ru(bbp)(L){NH=CO(CH_3)CH_3}] (**9**). The formation of the imido-complex has been confirmed by various spectroscopic techniques.

Chapter-6 presents the comparison of the spectral and electrochemical properties of complex **3a** with its chloro-analogue, complex **10**. In addition, the chloro complex **9**, has been converted to the aqua-derivative, complex **11**, by treating with aqueous $AgNO_3$ solution. The complex **11** on refluxing in EtOH:DMSO (1:4 v/v) (or CH_3CN) resulted into the complexes **12** (or **3a**). All the complexes are characterized by various spectroscopic techniques. The single crystal structure of complex **10** confirms the formulation (Figure 11). We have tried to grow the crystals of complex **11** and we failed. However, the X-ray quality crystals was grown from DMSO solvent which shows the presence of coordinated DMSO solvent in the molecule (Figure 11).

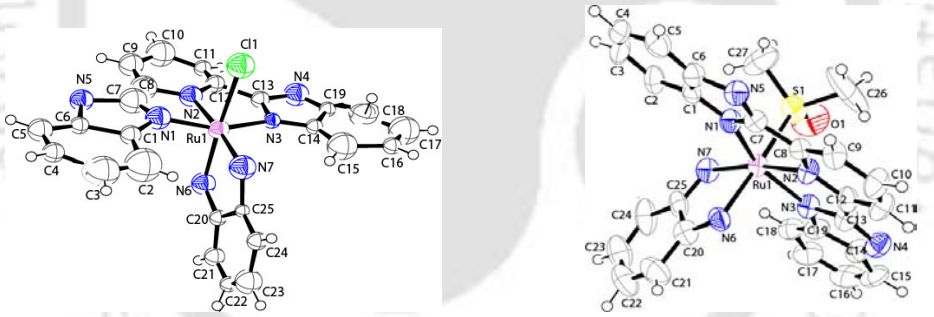

10 **12**

Figure 11: ORTEP diagrams of complexes **10** and **12** (50% thermal ellipsoids plot).

This aqua derivative can be used for various solvent substitution reactions and make them more effective for electrochemical devices.

Chapter-7 describes the synthesis and characterization Ru-dioxolene complexes with substituted bbp ligand to study the effect of the absence of proton.

In this regard, the bbp ligand has been modified by substituting the benzyl, ethyl and methyl group on N-center in it's imidazole frame work. The modified ligands have been characterized by various spectroscopic techniques as well as single crystal structure (Figure 12).

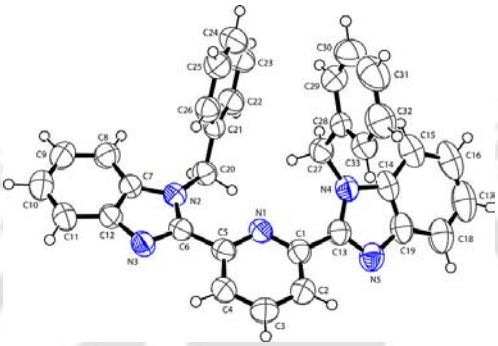

Figure 12: ORTEP diagram of the benzyl-substituted bbp ligand (50% thermal ellipsoids plot).

These substituted ligands have been used to synthesis the ruthenium oxolene complexes to compare the valence state distribution pattern with the earlier observed results. It is interesting to note that the oxolene ligands are coordinated to metal in catecholato form rather than quinone and semiquinone form.

1.1 Introduction

Ruthenium(II) polypyridyl complexes have been the subject matter of considerable attention over the last few decades and perhaps, have been investigated in greater detail than any other class of luminescent metal complexes.[1,2] In this direction, a considerable number of compounds have been prepared to study their utility in photophysics, electrochemistry, solar cells, biosensors, modified electrodes, displays, etc.[3] The enormous popularity of this class of compounds and also, of the related osmium, rhodium and iridium compounds has been driven by their wide range of applications. Investigation into this chemistry of ruthenium has started in earnest in the late 1950's with the report of the dinuclear complex $[(NH_3)_5Ru_2pz]^{2+}$ (pz = pyrazine) by Creutz and Taube[2] and the first report of luminescence of the paradigm complex $[Ru(bpy)_3]^{2+}$ (bpy = 2,2′- bipyridine) by Paris and Brandt.[4] However, the study of ruthenium polypyridyl complexes really exploded in the next decade with the realization that the combination of excited state and electrochemical properties of $[Ru(bpy)_3]^{2+}$ would enable it to split water into hydrogen and oxygen.[5] Although the initial expectations of photochemical water splitting were not easily achieved, the physical properties of these compounds were sufficiently promising to encourage the search for potential applications in other areas.[6]

The interest in mimicking the photo-induced charge separation occurring in natural photosynthesis has guided many research groups in the design of synthetic analogues. This has led to the development of multicomponent systems containing donor and/or acceptor units attached to the photo sensitizer, creating long-lived charge separated states in which solar energy is stored as chemical energy.[7-9] The photoactive transition metal complexes, especially the polypyridines of ruthenium(II) and osmium(II), have played a major role due to their favorable photophysical behavior.[1,10-13] Both ruthenium(II)*bis*(terpyridine), $[Ru(trpy)_2]^{2+}$ and ruthenium(II)*tris*(bipyridine), $[Ru(bpy)_3]^{2+}$ have been widely used as sensitizers, where the $[Ru(trpy)_2]^{2+}$ unit offers the

advantage of a C_2 axis running through the 4′-position of the terpyridine ligand.[13] For the $[Ru(bpy)_3]^{2+}$ analogue, the arrangement of one donor and one acceptor component in the 4′-position on two bipyridines unavoidably leads to isomers.[14] This has important consequences, since only one possible isomer, the *trans* isomer, has the optimum arrangement of the donor/acceptor components in terms of separation distance. The advantage of the $[Ru(bpy)_3]^{2+}$ unit is a longer excited state lifetime as compared to the $[Ru(trpy)_2]^{2+}$, due to low-lying *d-d* states of the latter.[13] A number of different acceptors have been linked to the ruthenium(II) polypyridine sensitizer. All of these offer different possibilities in terms of synthesis, redox and spectroscopic properties, and stability.

In this direction, a variety of ruthenium complexes incorporating different kinds of bidentate and tridentate ancillary ligands have been synthesized in a recent years. Ziessel et al. reported heteroleptic terpyridine complexes $[Ru(trpy(trpy\text{-}Br)]^{2+}$ and they investigated the reactivity with substituted trpy ligands.[15] Koizumi et al. reported the electrochemical properties of ruthenium complexes bearing terpyridine-analogous (N,N,C)-tridentate ligands.[16] Abrahamsson et al. investigated the new strategy for the improvement of photophysical properties in mononuclear ruthenium(II)*bis*(terpyridine) type complexes.[17] Tseng et al. reported the mononuclear ruthenium(II) complexes that catalyze the water oxidation.[18] Manner et al. reported the proton-electron transfers in ruthenium(II)terpyridine-4′-carboxylate complex $[Ru^{II}(pydic)(trpyCOOH)]$ [trpyCOOH = 2,2′:2′,6″-terpyridine-4′-carboxylic acid and Na_2pydic = disodium pyridine-2,6-dicarboxylate] with a long distance between the redox and basic sites.[19]

The facile electron transfer properties of this class of compounds has also attracted the attention of the chemists to develop biomimetic catalysts involving proton coupled electron transfer processes and also in designing molecular electronics based on proton movements.[20] Several molecular devices such as fluorescent logic gates and molecular shuttles have been developed on the basis of proton movement as an external stimulus.[21-

[23] Electronic control of proton transport from the polymer or monolayer films has been reported.[24,25]

1.2 Objective of the present work

The proton coupled electron transfer processes, by virtue, demand the presence of coordinated H_2O or OH-group in the molecule as the trigger point.[26] To avoid the synthetic complexity of these compounds, one could think of designing the ligand which can bind the metal in similar fashion like trpy and at the same time, can provide one or more dissociable proton centers as trigger to tune the molecular properties.

The present work originates from our interest to substitute trpy by tridentate 2,6-*bis*(benzimidazol-2-yl)pyridine (bbp) unit for synthesizing various ruthenium complexes effective for proton coupled electron transfer processes.

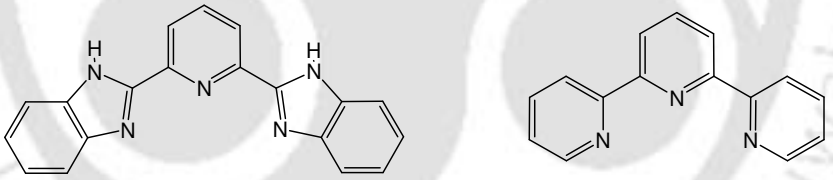

(a) bbp (b) trpy

Figure 1.1: (a) 2,6-*bis*(benzimidazol-2-yl)pyridine (bbp) and (b) terpyridine (trpy).

The factors that make the bbp ligand as a potential substitute for trpy are: (i) similar chelating unit like trpy; (ii) due to extensive π-delocalization, its rigidity and planarity give well defined structure for metal complexes; (iii) in addition, bbp ligand shows the reversible proton dependency (Scheme 1.1) which can tune the properties of metal complexes.[27]

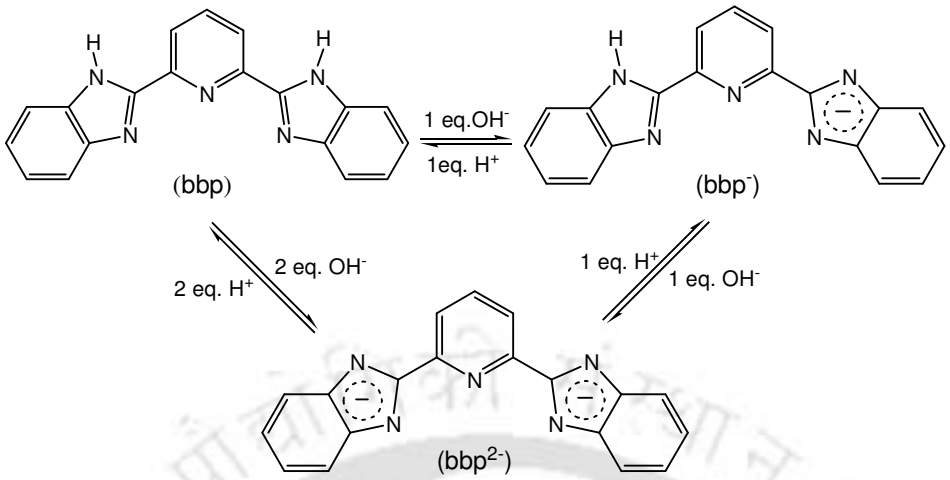

Scheme 1.1

Furthermore, it is easy to synthesize from cheap starting materials with a good yield.[28,27b,41]

The mononuclear ruthenium chemistry with bbp ligand in combination with ancillary ligands are not much explored though its chemistry with some transition metals like copper, iron, zinc and cadmium have been studied well.[29-33]

Liu and co-workers synthesized the Cd and In complexes with 2,6-*bis*(benzimidazol-2-yl)pyridine and shown the blue luminescent properties.[34]

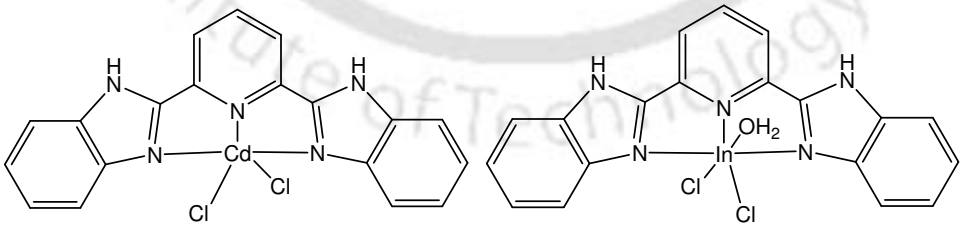

(a) (b)

Figure 1.2: Structures of **(a)** [Cd(bbp)Cl_2] and **(b)** [In(bbp)Cl_2(H_2O)].

Wang et al. also synthesized Mn and Cd complexes with same ligand.[30] Hasegawa and co-workers reported the temperature dependant fluorescence spectra of Fe(II) spin crossover complexes with bbp.[35]

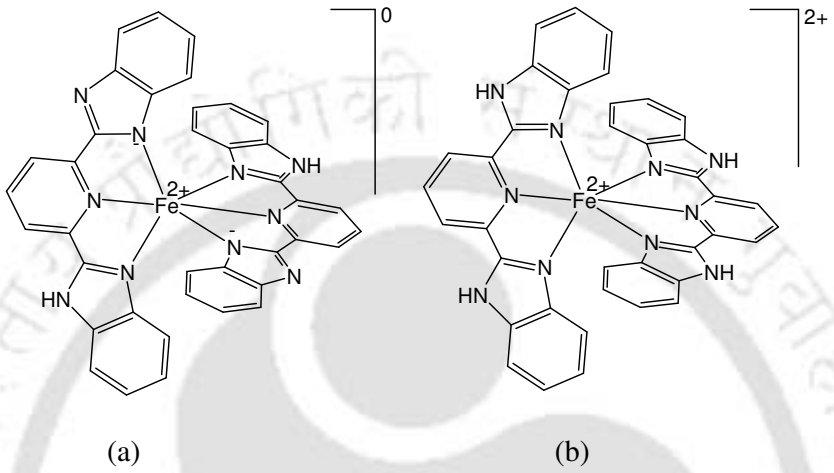

Figure 1.3: Structures of **(a)** $[Fe(bbp^{-})_2]$ and **(b)** $[Fe(bbp)_2]^{2+}$.

Boca and co-workers synthesized the iron(II) complexes of substituted and deprotonated bbp and shown extensive spin crossover above room temperature.[31] Boca et al. also investigated the exceptional spin transition in $[Fe(bbp)_2](ClO_4)_2\ 0.25H_2O$ complex, also.[36]

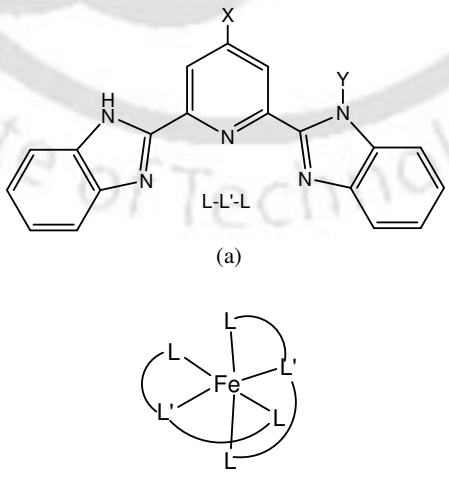

Figure 1.4: (a) Structure of the ligands bbp (X, Y=H), bbp (X= benzimidazole) and bbp^{-} (Y = none) and (b) $[Fe(bbp)_2](ClO4)_2\ 0.25H_2O$.

Aghatabay and co-workers synthesized and shown the antimicrobial activity of Fe(II), Zn(II), Cd(II) and Hg(II) complexes with 2,6-*bis*(benzimidazol-2-yl)pyridine ligand.[37]

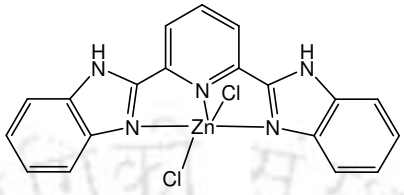

Figure 1.5: Structure of $[Zn(bbp)Cl_2]$ complex.

Butcher and co-workers reported the mononuclear and mixed valence binuclear oxovanadium complexes with benzimidazole-derived chelating agents.[38]

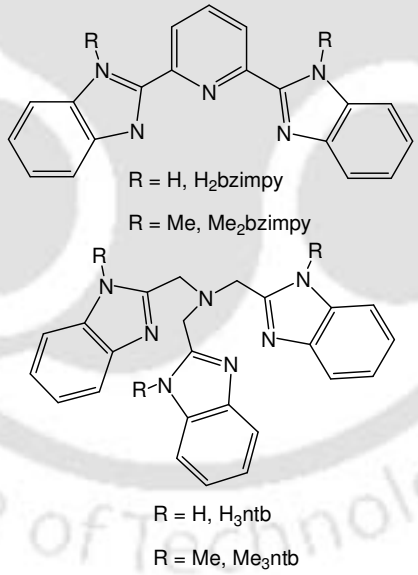

Figure 1.6: Structures of benzimidazole derivatives.

Zhang et al. reported the ethylene oligomerization and polymerization of $CrCl_3$ with bbp and their substituted.[39]

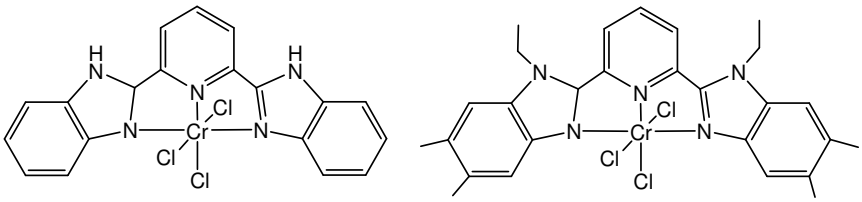

(a) (b)

Figure 1.7: Structures of Cr(III) complexes with **(a)** bbp and **(b)** substituted bbp.

Chetia et al. reported the bbp ligand as a neutral receptor enables the formation of highly stable supramolecular complexes with urea *via* self assembly.[41]

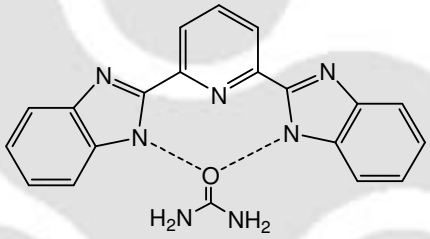

Figure 1.8: Structure of bbp with urea.

Chetia et al. also employed the bbp ligand as a chemosensor for detection of fluoride ions.[41]

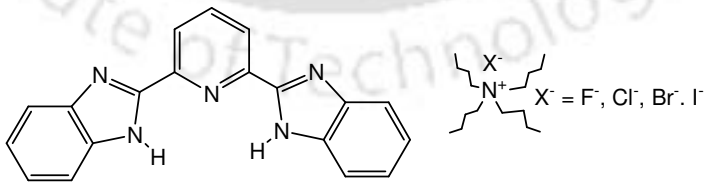

Figure 1.9: bbp and various ions.

Haga and co-workers reported ruthenium (II) complexes with tetradentate 6,6'-*bis*(oxazolinyl or benzimidazolyl)-2,2'-bipyridine.[42]

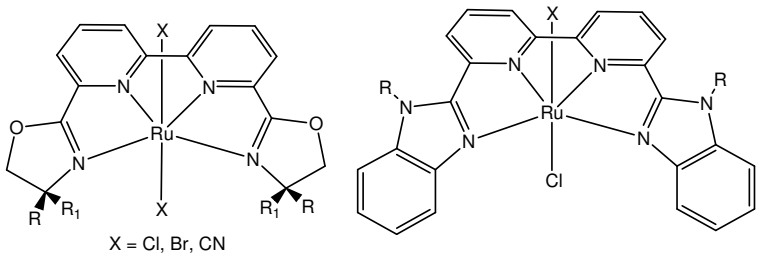

(a) (b)

Figure 1.10: Stuctures of ruthenium(II) complexes with **(a)** 6,6'-*bis*(oxazolinyl)-2,2'-bipyridine and **(b)** 6,6'-*bis*(benzimidazolyl)-2,2'-bipyridine.

Ruthenium complexes of biimidazole, bibenzimidazole, 2-pyridylbenzimidazole, 2,2-*bis*(2-pyridyl)bibenzimidazole and 2,6-*bis*(benzimidazolyl)pyridine as well as 2,6-*bis*(imidazolyl)pyridine have been explored in recent past.[43-47]

Mishra et al. reported an infinite double columnar supramolecule by strong intermolecular H-bonding in the solid state of ruthenium complex trans-$[Ru(PPh_3)_2(bbp)Cl]Cl.CHCl_3.H_2O$.[48]

Haga and co-workers reported the proton coupled electron transfer reaction of self assembled mono layers of ruthenium(II) complex containing tridentate bbp ligand on gold surface.[49]

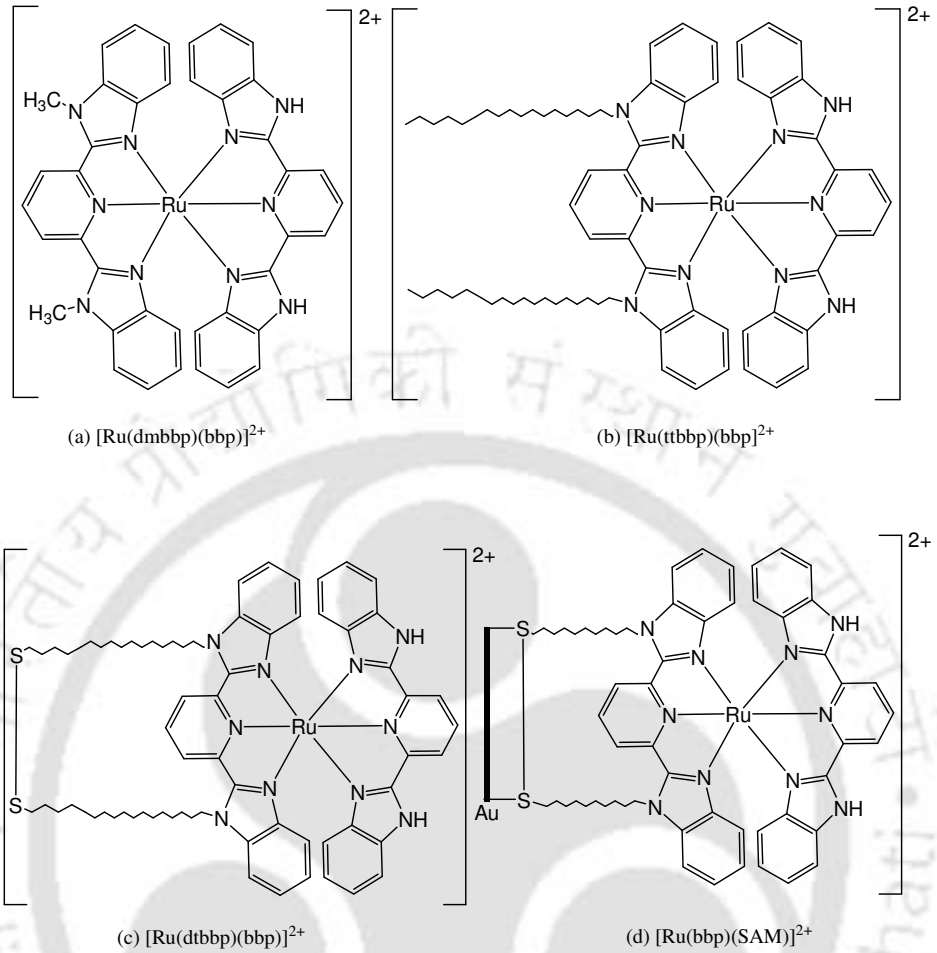

Scheme 1.2: Self assembled mono layers of ruthenium (II) complexes (a) $[Ru(dmbbp)(bbp)]^{2+}$, (b) $Ru(ttbbp)(bbp)]^{2+}$, (c) $[Ru(dtbbp)(bbp)]^{2+}$, (d) $[Ru(bbp)(SAM)]^{2+}$ containing bbp ligand on gold surface.

Haga and co-workers reported the molecular design of a proton-induced molecular switch based on rod-shaped Ru-dinuclear complexes with *bis*-tridentate 2,6-*bis*(benzimidazol-2-yl)pyridine derivatives and observed the stability of immobilized Ru(II) complex for electrochromic applications.[50]

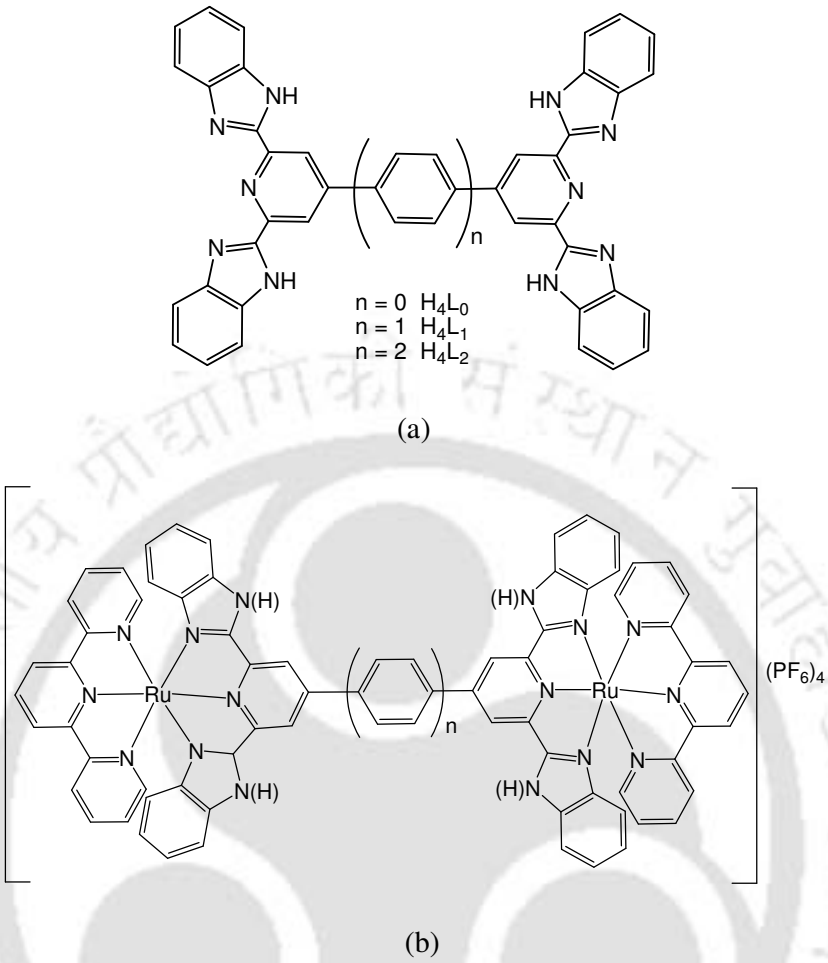

Scheme 1.3: (a) *bis*-tridentate 2,6-*bis*(benzimidazol-2-yl)pyridine derivatives, (b) $[Ru_2(btbbp)(trpy)_2](PF_6)_4$.

Terada et al. reported the new trinuclear ruthenium complexes bearing both 1,3,5-*tris*(2,2′:6′,2″-terpyridyl)benzene and *bis*(benzimidazol-2-yl)pyridine with six phosphonate anchors and immobilized on an ITO electrode (Indium Tin Oxide Electrode).[51]

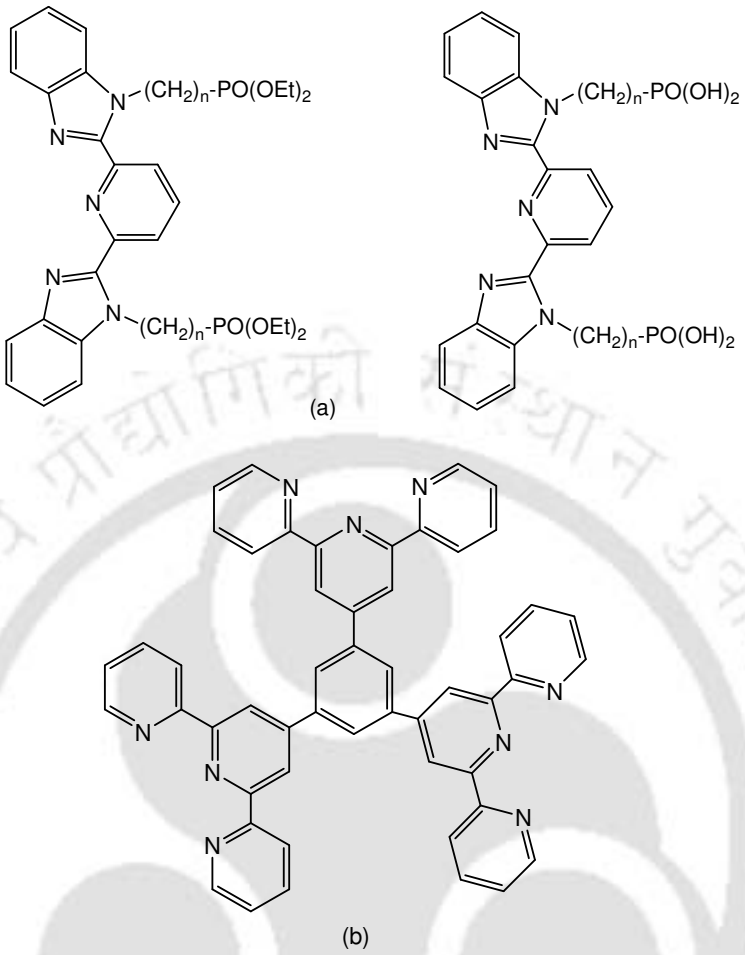

Scheme 1.4: (a) bbp with six phosphonate anchors and (b) 1,3,5-*tris*(2,2′:6′,2″-terpyridyl)benzene.

Nair et al. synthesized and characterized the ruthenium (II) complex $[Ru(bbp)_2]Cl_2$ and studied their DNA binding and cleavage properties.[52]

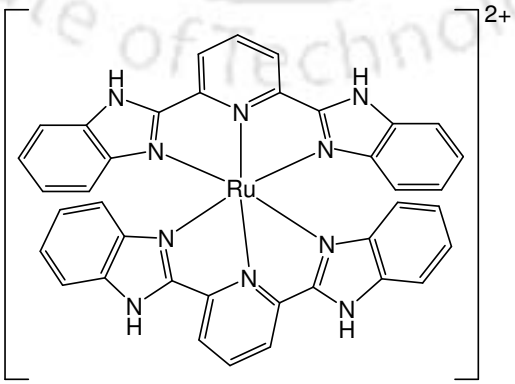

Figure 1.12: Structure of $[Ru(bbp)_2]^{2+}$.

Nair et al. also reported the mixed ligand complexes of ruthenium (II) $[Ru(bbp)(bpy)(H_2O)]^{2+}$ and $[Ru(bbp)(phen)(H_2O)]^{2+}$ and electrochemically generated ruthenium(IV) species and found to be effective in oxidative cleavage of DNA.[53]

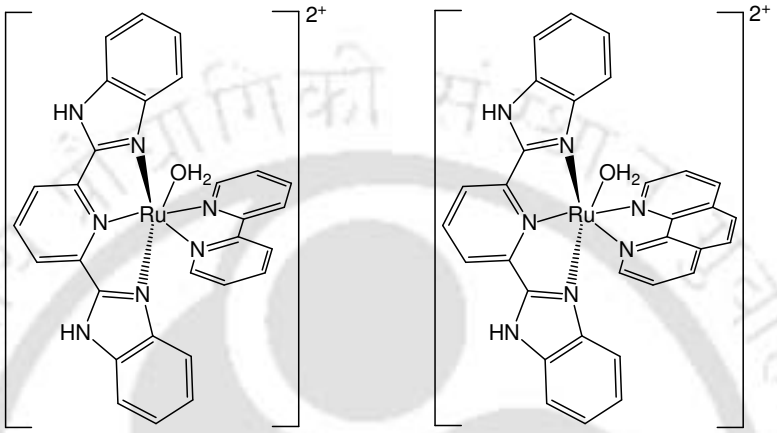

(a) (b)

Figure 1.13: Structures of (a) $[Ru(bbp)(H_2O)]^{2+}$ and (b) $[Ru(bbp)(phen)(H_2O)]^{2+}$.

In addition, the trpy ligand binds the metal ions, almost always in tridentate fashion but bidentate and monodentate coordination of trpy derivatives to the monovalent metals are also known.[13] Similarly the bbp ligand can also coordinate to the metal ion in tridentate as well as bidentate fashion due to their structural features.

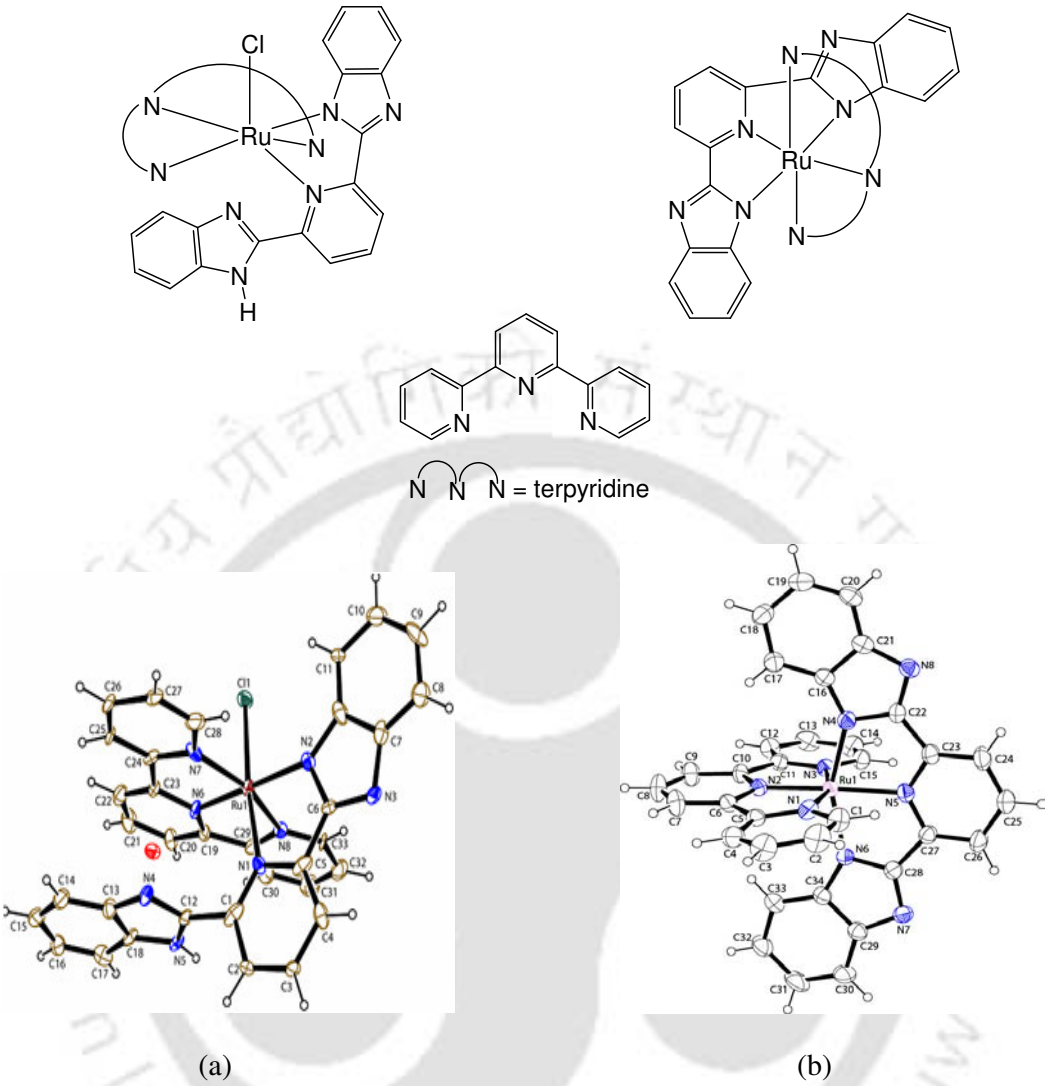

Figure 1.14: Structures of (a) [Ru(bbp^{-})(trpy)(Cl)] and (b) [Ru(bbp^{2-})(trpy)].

The work presented in the proceeding chapters of the thesis will be primarily focused on the following aspects:

(a) synthesis, spectral and reactivity studies of ruthenium complexes with 2,6-*bis*(benzimidazol-2-yl)pyridine (bbp) as a ancillary in combination with trpy ligand which can display novel chemical, spectro-electrochemical and physical properties.

(b) structural and spectral studies of valence state distribution in ruthenium complexes of 2,6-*bis*(benzimidazol-2-yl)pyridine with oxolene ancillary ligands.

(c) the ruthenium complexes with catechol and acetylacetone in combination with bbp ligand to study their physicochemical and electrochemical properties.

(d) reduction of coordinated acetonitrile solvent to ethylamine in a synthesized ruthenium complex in the presence of *p*-phenylenediamine or hydroquinone.

(e) nucleophilic addition reaction at the coordinated acetonitrile in a synthesized ruthenium complex by $NaOCH_3$.

(f) the comparison of the spectral and electrochemical properties of acetonitrile coordinated ruthenium complex with it's chloro-, aquo- and DMSO-analogues.

(g) a set of substituted benzimidazole based ligand have been synthesized to study the effect of absence of dissociable protons. These substituted ligands have been used to synthesize the ruthenium oxolene complexes to compare the valence state distribution pattern with the earlier observed results.

(h) the detailed structural, spectroscopic and electrochemical aspects of the all complexes have been examined**.**

1.3 References

1. Juris, A.; Balzani, V.; Barigelletti, F.; Campagna, S.; Belser, P.; VonZelewsky, A. *Coord. Chem. Rev.* **1988**, *84*, 85.

2. Creutz, C.; Taube, H. *J. Am. Chem. Soc.* **1969**, *91*, 3988.

3. (a) Xiong, Y.; He, X. F.; Zhon, X. H.; Wu, J. Z.; Chen, X. M.; Ji, L. N.; Li, R. H.; Zhon, J. Y.; Yu, K. B. *J. Chem. Soc., Dalton Trans.* **1999**, 19. (b) Yam, V. W. W.; Chu, B. W. K.; Cheung, K. K. *J. Chem. Soc., Chem. Commun.* **1998**, 2261. (c) Coe, B. J.; Friessen, D. A.; Thompson, D. W.; Meyer, T. J. *Inorg. Chem.* **1996**, *35*, 4575. (d) Bardwell, D. A.; Cargill-Thompson, A. M. W.; Jeffery, J. C.; McCleverty, J. A.; Ward, M. D. *J. Chem. Soc., Dalton Trans.* **1996**, 873 (e) Ward, M. D. *Inorg. Chem.* **1996**, *35*, 1712. (f) Santra, B. K.; Menon, M.; Pal, C. K.; Lahiri, G. K. *J. Chem. Soc., Dalton Trans.* **1997**, 1387. (g) Barigelletti, F.; Flamigni, L.; Calogero, G.; Hammarstrom, L.; Sauvage, J.-P.; Collin, J.-P. *J. Chem. Soc., Chem. Commun*. **1998**, 2333. (h) Kulkarni, S. S.; Santra, B. K.; Munshi, P.; Lahiri, G. K. *Polyhedron* **1998**, *17*, 4365. (i) Bhattacharya, D.; Chakraborty, S.; Munshi, P.; Lahiri, G. K. *Polyhedron* **1999**, *18*, 2951. (j) Newkome, G. R.; He, E.; Godinez, L. A.; Baker, G. R. *J. Am. Chem. Soc.* **2000**, *122*, 9993. (k) Hirano, T.; Ueda, K.; Mukaida, M.; Nagao, H.; Oui, T. *J. Chem. Soc., Dalton Trans.* **2001**, 2341. (l) Chakraborty, S.; Laye, R. H.; Paul, R. L.; Gonnade, R. G.; Puranik, V. G.; Ward, M. D.; Lahiri, G. K. *J. Chem. Soc., Dalton Trans.* **2002**, 1172.

4. Paris, J. P.; Brandt, W. W. *J. Am. Chem. Soc.* **1959**, *81*, 5001.

5. (a) De Cola, L.; Belser, P. *Coord. Chem. Rev.* **1998**, *177*, 301. (b) Balzani, V.; Scandola, F. *Supramolecular Photochemistry*, Ellis Horwood, New York, **1991**.

6. (a) Sprintschnik, G.; Sprintschnik, H. W.; Kirsch, P. P.; Whitten, D. G. *J. Am. Chem. Soc*. **1976**, *98*, 2337. (b) G. Sprintschnik, G.; Sprintschnik, H. W.; Kirsch, P. P.; Whitten, D. G. *J. Am. Chem. Soc*. **1977**, *99*, 4949.

7. Gust, D.; Moore, T. A.; Moore, A. L. Covalently Linked Systems Containing Porphyrin Units. In *Electron Transfer in Chemistry*; Balzani, V., Ed.; WILEY-VCH: Weinheim, **2001**, pp 272-336.

8. Scandola, F.; Chiorboli, C.; Indelli, M. T.; Rampi, M. A. Covalently Linked Systems Containing Metal Complexes. In *Electron Transfer in Chemistry*; Balzani, V., Ed.; WILEY-VCH: Weinheim, **2001**, pp 337-408.

9. Wasielewski, M. R. *Chem. Rev.* **1992**, *92*, 435.

10. Balzani, V.; Juris, A.; Venturi, M.; Campagna, S.; Serroni, S. *Chem. Rev.* **1996**, *96*, 759.

11. Kalyanasundaram, K. *Photochemistry of Polypyridine and Porphyrin Complexes*; Academic Press Limited: London, **1992**.

12. Meyer, T. J. *Acc. Chem. Res.*, **1989**, *22*, 163.

13. Sauvage, J.-P.; Collin, J.-P.; Chambron, J.-C.; Guillerez, S.; Coudret, C.; Balzani, V.; Barigelletti, F.; De Cola, L.; Flamigni, L. *Chem. Rev.* **1994**, *94*, 993.

14. Keene, F. R. *Coord. Chem. Rev.* **1997**, *166*, 121.

15. Ziessel, R.; Grosshenny, V.; Hissler, M.; Stroh, C. *Inorg. Chem.* **2004**, *43*, 4262.

16. Koizumi, T.-A.; Tomon, T.; Tanaka, K. *Organometallics* **2003**, *22*, 970.

17. Abrahamsson, M.; Wlpher, H.; Johansson, O.; Larson, J.; Kritikos, M.; Erriksson, L.; Norrby, P-O.; Bergquist, J.; Kermark, B.; Hammarstrm, L. *Inorg. Chem.* **2005**, *44*, 3215.

18. Tseng, H.-W.; Zong, R.; Muckerman, J. T.; Thummel, T. *Inorg. Chem.* **2008**, *47*, 11763.

19. Manner, V. W.; DiPasquale, A. G.; Meyer, J. M. *J. Am. Chem. Soc.* **2008**, *130*, 7210.

20. (a) Nakamoto, M.; Tanaka, K.; Tanaka, T. *Bull. Chem. Soc. Jpn.* **1988**, *61*, 4099. (b) Niemz, A.; Rotello, V. M. *Acc. Chem. Res.* **1999**, *32*, 44. (c) Tam-Chang, S.-W.; Mason, J.; Iverson, I.; Hwang, K.-O.; Leonard, C. *Chem. Commun.* **1999**, 65.

21. Credi, A.; Balzani, V.; Langford, S. J.; Stoddart, J. F. *J. Am. Chem. Soc.* **1997**, *119*, 2679.

22. Collier, C. P.; Jeppesen, J. O.; Luo, Y.; Perkins, J.; Wong, E. W.; Heath, J. R.; Stoddart, J. F. *J. Am. Chem. Soc.* **2001**, *123*, 12632.

23. De Silva, A. P.; Gunaratne, H. Q.; McCoy, C. P. *J. Am. Chem. Soc.* **1997**, *119*, 7891.

24. Cameron C. G.; Pickup, P. G. *J. Am. Chem. Soc.* **1999**, *121*, 7710.

25. Cameron, C. G.; Pittman, T. J.; Pickup, P. G. *J. Phys. Chem. B* **2001**, *105*, 8838.

26. (a) Wada, T.; Tsuge, K.; Tanaka, K. *Inorg. Chem.* **2001**, *40*, 329. (b) Sens, C.; Romeo, I.; Rodriguez, M.; Llobet, A.; Parella, T.; B-Buchholz, J. *J. Am. Chem. Soc.* **2004**, *126*, 7799.

27. (a) Lebeau, E. L.; Binsetead, R. A.; Meyer, T. J. *J. Am. Chem. Soc.* **2001**, *123*, 10535. (b) Singh, A.; Chetia, B.; Mobin, S. M.; Das, G.; Iyer, P. K.; Mondal, B. *Polyhedron* **2008**, *27*, 1983.

28. Addison, A. W.; Burke, P. J. *J. hetrocycl. Chem.* **1981**, *12*, 4455.

29. Wang, S.; Luo, Q.; Zhou, X.; Zeng, Z. *Polyhedron* **1993**, *12*, 1945.

30. (a) Wang, S.; Zhu, Y.; Zhang, F.; Wang, Q.; Wang, L. *Polyhedron* **1992**, *11*, 1909. (b) Wang, S.; Cuo, Y.; Tan, R.; Luo, Q.; Shi, J.; Wu, Q. *Polyhedron* **1994**, *13*, 1661.

31. (a) Boca, R.; Boca, M.; Dlhan, L.; Falk, K.; Fuess, H.; Haase, W.; Jarosciak, R.; Papankova, B.; Renz, F.; Vrbova, M.; Werner, R. *Inorg. Chem.* **2001**, *40*, 3025. (b) Boca, R.; Boca, M.; Dlhan, L'.; Falk, K.; Fuess, H.; Haase, W.; Jarosciak, R.; Papankova, B.; Renz, F.; Vrbova, M.; Werner, R. *Inorg. Chim. Acta* **1997**, *260*, 129.

32. (a) Ruttimann, S.; Moreau, C. M.; Williams, A. F; Bernardinelli, G.; Addison, A. W. *Polyhedron* **1992**, *11*, 635. (b) Piguet, C.; Bocquet, B.; Mueller, E.; Williams, A. F. *Helv. Chimica Acta* **1989**, *72*, 323.

33. Wang, J.; Shuai, L.; Xiao, X.; Zeng, Y.; Li, Z.; T. Matsumura-Inoue, T. *J. Inorg. Biochem.* **2005**, *99*, 883.

34. Liu, S-G.; Zuo, J-L.; Li, Y-Z.; You, X-Z. *J. Mol. Str.* **2004**, *705*, 153.

35. Hasegawa, M.; Renz, F.; Hara, T.; Kikuchi, Y.; Fukuda, Y.; Okubo, J.; Hoshi, T.; Linert, W. *Chem. Phys.* **2002**, *277*, 21.

36. R. Boca, R.; F. Renz, F.; M. Boca, M.; H. Fuess, H.; W. Haase, W.; G. Kickelbick, G.; Linert, W.; Scikora, M. V. *Inorg. Chem. Commun.* **2005**, *8*, 227.

37. Aghatabay, N. M.; Neshat, A.; Karabiyik, T.; Somer, M.; Haciu, D.; Dulger, B. *Eur. J. Med. Chem.* **2007**, *42*, 205.

38. Ghosh, S.; Nanda, K. K.; Addison, K. A. W.; Butcher, R. J. *Inorg. Chem.* **2002**, *41*, 2243.

39. Zhang, W.; Sun, W-H.; Zhang, S.; Hou, J.; Wedeking, K.; Schultz, S.; Fro¨hlich, R.; Song, H. *Organometallics* **2006,** *25,* 1961.

40. Groppo, E.; Lamberti, C.; Bordiga, S.; Spoto, G.; Zecchina, A. *Chem. Rev.* **2005**, *105*, 115.

41. (a) Chetia, B.; Iyer, P. K. *Tetrahedron Lett.* **2006**, *47*, 8115. (b) Chetia, B.; Iyer, P. K. *Tetrahedron Lett.* **2008**, *49*, 94.

42. Mizushira, K.; Nakaura, M.; Park, S.-B.; Nishiyama, H.; Monjushiro, H.; Harada, K.; Haga, M-a. *Inorg. Chim. Acta* **1997***, 261*, 175.

43. Haga, M.-a.; Takasugi, T.; Tomie, A.; Ishizuya, M.; Yamada, T.; Hossain, M.D.; Inoue, M. *J. Chem. Soc., Dalton Trans.* **2003**, 2069.

44. Rau, S.; Büttner, T.; Temme, C.; Ruben, M.; Görls, H.; Walther, D.; Duati, M.; Fanni, S.; Vos, J. G. *Inorg. Chem.* **2000**, *39*, l62l.

45. Rillema, D. P.; Sahai, R.; Matthews, P.; Edwards, A. K.; Shaver, R. J.; Morgan, L. *Inorg. Chem.* **1990**, *29*, l67.

46. Xiaoming, X.; Haga, M.-a.; Inoue, T. M.; Ru, Y.; Addison, A. W.; Kano, K. *J. Chem. Soc., Dalton Trans.* **1993**, 2477.

47. Haga, M.-a.; Ano, T.-a.; Kano, K.; Yamabe, S. *Inorg. Chem.* **1991**, *30*, 3483.

48. Mishra, D.; Naskar, S.; Chattopadhyay, S. K.; Majhi, M.; Sengupta, P.; Dinda, R.; Ghosh, S.; Mak, T. C. W. *Trans. Met. Chem.* **2005**, *30*, 352.

49. Haga, M.-a.; Hong, H.-Gi.; Shiozawa, Y.; Kawata, Y.; Monjushiro, H.; Fukuo, T.; Arakawa, R. *Inorg. Chem.* **2000**, *39*, 4566.

50. Haga, M.-a.; Takasugi, T.; Tomie, A.; Ishizuya, M.; Yamada, T.; Hossain, M. D.; Inoue, M. *J. Chem. Soc., DaltonTrans.* **2003**, 2069.

51. Terada, K.; Kobayashi, K.; Haga, M.-a. *J. Chem. Soc*., *Dalton Trans.* **2008**, 4846.

52. Vaidyanathan, V. G.; Nair, B. U. *J. Inorg. Biochem.* **2002**, *91*, 405.

53. Vaidyanathan, V. G.; Nair, B. U. *J. Chem. Soc., Dalton Trans.* **2005**, 2842.

Abstract

Ruthenium monoterpyridine complexes with the tridentate 2,6-*bis*(benzimidazol-2-yl)pyridine (bbp), $[Ru(trpy)(bbp)](ClO_4)_2$ (**1**) and $[Ru(trpy)(bbp^{2-})]$ (**2**) (trpy = 2,2′:6′,2″-terpyridine) have been synthesized. The complexes have been authenticated by elemental analyses, UV-visible, FT-IR, ^{1}H-NMR spectra and their single crystal X-ray structures. Complexes **1** and **2** exhibit strong MLCT band near 475 and 510 nm, respectively and are found to be very much dependent on solution pH. The successive pH dependent dissociations of the N-H protons of benzimidazole moiety of bbp in **1** lead to the formation of **2**. The proton induced inter-convertibility of **1** and **2** has been monitored via UV-visible spectroscopy and cyclic voltammetry. The two pK_a values, 5.75 and 7.70, for complex **1** have been determined spectroscopically.

2.1 Introduction

Protons play an important role in biological processes. Proton transfer and its gradients through biomembranes are the subject of fundamental importance in bioenergetics.[1] In photosynthetic processes, the electron flow can be directly coupled to the proton flow through the membrane to maintain the proton gradients. Thus, the combination of proton and electron transfer processes has drawn a considerable attention not only for developing the biomimic catalysts, but also in designing molecular electronics based on proton movements.[2-4] Several examples of proton coupled electron transfer (PCET) processes have been reported so far indicating that in transition metal complexes, the ligand based protonation/deprotonation processes influence the metal redox potential to a great extent.[5-9] A number of studies have been made using various imidazole based ligands which can provide one or more dissociable protons.[5] However, the examples of mononuclear complexes with ruthenium mono-terpyridine frameworks are not known.

In this chapter, we report ruthenium mono-terpyridine complexes with the well documented benzimidazole based tridentate ligand (bbp, Scheme 2.1) which can offer a combination of moderate π-acceptor pyridine nitrogen and π- donor imidazole

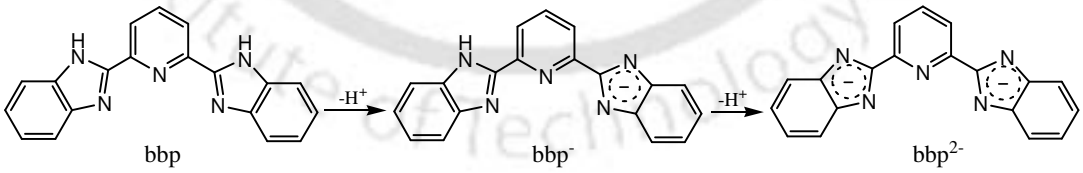

Scheme 2.1

nitrogen and their proton-induced tuning of redox as well as chemical properties.[10-13]

2.2 Results and Discussion

The ligand has been synthesized following a reported procedure.[14] The reaction of bbp ligand with the ruthenium precursor complex, $Ru(trpy)Cl_3$, in ethanol afforded a dark solution, from which a dark colored solid mass has been isolated on addition of excess saturated aqueous $NaClO_4$ solution (Scheme 2.2). Chromatographic purification of the crude product on a silica gel column using CH_2Cl_2 : CH_3CN(4:1, v/v)

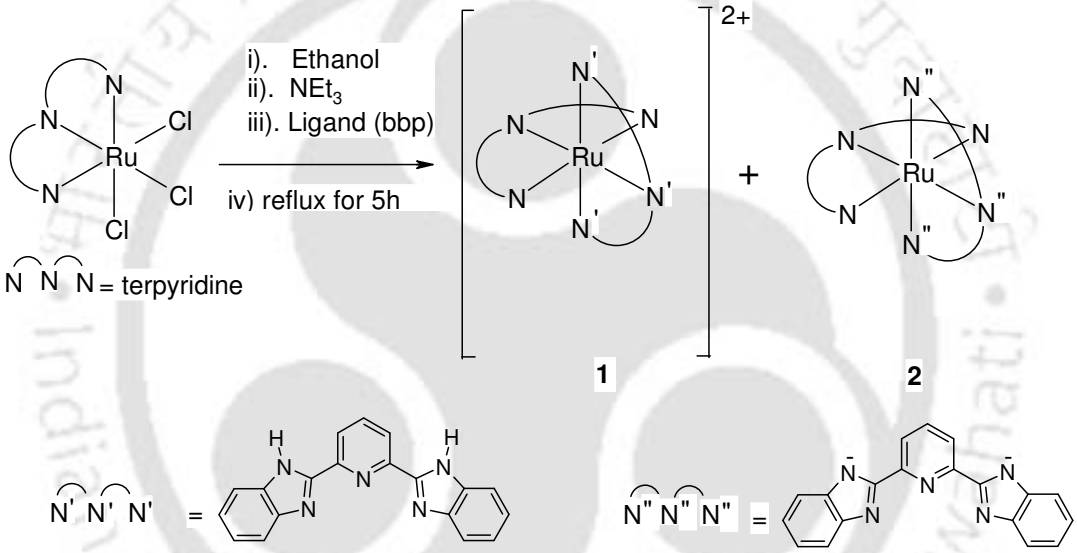

Scheme 2.2

mixture as eluent results in initially the reddish complex **1** (112 mg, yield, 30%) followed by the pink colored neutral complex **2** (114 mg, yield, 40%). The complex **1** has been synthesized by other group in a different process.[15]

The complexes exhibit satisfactory elemental analyses (see Experimental Section) and **1** shows 1:2 conductivity [$\Lambda_M(\Omega^{-1}cm^2mol^{-1})$, 248] in acetonitrile solution whereas **2** is neutral. The formulation of the complexes have been further supported by the FT-IR and ^{1}H-NMR spectral features. **1**, in presence of one equivalent of base affords **1a** which on successive addition of another equivalent of base gives **2**. The formation of

1 and **2** have been authenticated by their single crystal X-ray structures.

2.2.1 X-ray Crystallography

Single crystal of complex **1** was grown by slow diffusion of an acetonitrile solution of it in benzene followed by slow evaporation and for complex **2**, a dichloromethane solution of it was allowed to diffuse slowly in hexane followed by slow evaporation. The crystal structures of **1** and **2** are shown in figure 2.1 and the crystal data are listed in table 2.1.

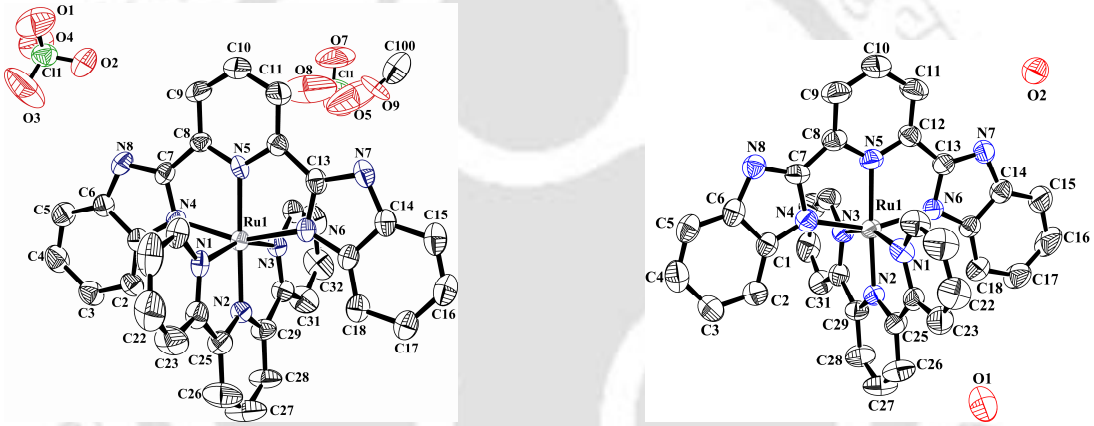

Figure 2.1: ORTEP plot with atom numbering scheme of complexes (a) **1** and (b) **2**. (Hydrogen atoms are omitted for clarity)(50% thermal ellipsoids plot).

The single crystal of complex **1** contains one methanol and complex **2** contains water as solvent of crystallization in the ratio of **2**: H_2O = 1:2. The important bond lengths and angles are listed in table 2.2 and 2.3, respectively. The RuN_6 chromophores in **1** and **2** are in distorted octahedral arrangement as can be seen from the angles subtended at the metal ions in table 2.3. It is found that the ligands bbp and bbp^{2-} in **1** and **2** are coordinated in the usual meridional fashion and terpyridine and bbp or bbp^{2-} in **1** or **2**, respectively, are in planes perpendicular to each other. The pyridine nitrogen of bbp or bbp^{2-} in **1** or **2** is in *trans* orientation with respect to the central pyridine nitrogen of terpyridine. Bond

distances and angles associated with **1** and **2** match well with the reported analogous ruthenium- terpy complexes.[16-20] The geometrical constrains imposed on the meridional configurations of terpyridine and bbp in **1** and terpyridine and bbp^{2-} in **2** are reflected in the respective *trans* angles: N(1)-Ru(1)-N(3), 158.6(3)°/N(4)-Ru(1)-N(6), 156.0(3)° and N(1)-Ru(1)-N(3), 159.5(3)°/ N(4)-Ru(1)-N(6), 156.8(3)°. Consequently, Ru(1)-N(2) (central pyridine nitrogen of terpyridine) distances in **1** and **2**, 1.964(7) Å and 1.951(7) Å, respectively, and the distance between ruthenium center and the central pyridine nitrogen (N_p) of the ancillary ligand (bbp and bbp^{2-}) in **1** and **2** are 2.017(7) Å and 2.029(8) Å, respectively, which are approximately 0.05 Å shorter than the corresponding terminal Ru-N bonds (Table 2.2). The average bite angles involving terpyridine/bbp in **1** and terpyridine/bbp^{2-} in **2** are 79.30°/78.00° and 79.75°/78.40°, respectively. It might be expected that an anionic ligand would be a better donor compared to the neutral and hence that will lead to shorter bonds. For complex **1**, the crystal quality was not very good. We have tried several times to grow crystals from different solvent systems and at different conditions (e.g. at room temperature, at low temperature etc.), also. However, we got the same results. The insignificant difference in the Ru-N bond distances in the two complexes might be because of this.

A poorly refined single crystal structure of complex **1** has been published previously along with spectroscopic and electrochemical measurements by Chattopadhyay et. al.[15]

In the solid-state there is no π-stacking interactions due to the orthogonal orientation of the lignads in both the complexes. However, in complex **1**, imidazole nitrogens are hydrogen bonded with perchlorate and methanol oxygen atoms. In addition to that they form several weak C-H••••O and C-H••••π type hydrogen bond interactions. It is interesting to note that in solid-state it forms alternate hydrophobic and hydrophilic layers in the *bc* plane (Figure 2.2).

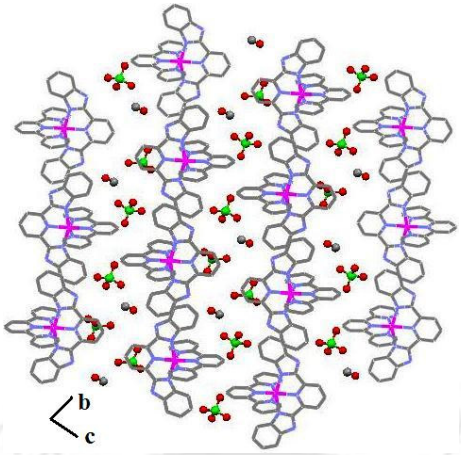

Figure 2.2: Packing diagram of complex **1** viewed along *a* axis.

On the other hand, complex **2** forms square boxes along *ab* plane in the solid-state with average dimension of the boxes is ~ 6 Å (Figure 2.3). Each box is filled with four water molecules of crystallization (Figure 2.4).

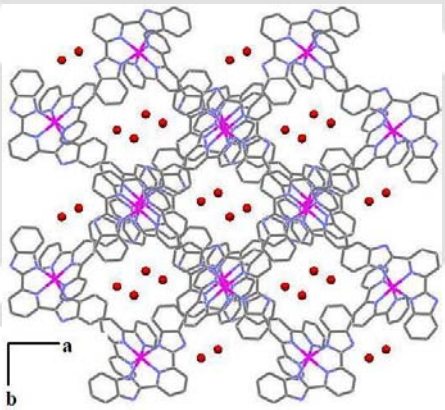

Figure 2.3: Packing diagram of complex **2** viewed along *c* axis.

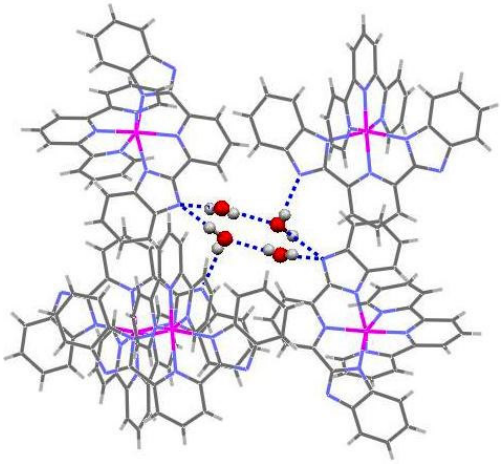

Figure 2.4: Tetrameric water clusters inside hydrophilic pocket in complex **2**.

One water molecule (O1) is double hydrogen bond donor while other one (O2) is as double hydrogen bond donor and single hydrogen bond acceptor. They form cylic tetrameric water cluster with alternate arrangement of two symmetrically independent water molecules. This water cluster is highly stabilized by strong hydrogen bond between ligands.

Table 2.1: Crystallographic data for complexes **1** and **2**

	1.CH_3OH	**2. $2H_2O$**
Formulae	$C_{35}H_{28}Cl_2N_8O_9Ru$	$C_{34}H_{26}N_8O_2Ru$
Mol. wt.	876.62	679.67
Crystal system	Triclinic	Monoclinic
Space group	P-1	P2(1)/n
Temperature /K	298(2)	298(2)
Wavelength /Å	0.71073	0.71073
a /Å	8.9369(5),	14.8580(4)
b /Å	12.9441(6	13.2833(3)
c /Å	16.6331(8)	18.4269(5)
α/°	79.843(3)	90.00
β/°	76.981(2),	106.779(2)
γ/°	81.413(3)	90.00
V/ $Å^3$	1833.20(16)	3481.96(15)
Z	2	4
Density/Mgm^{-3}	1.582	1.292
Abs. Coeff. /mm^{-1}	0.637	0.493
F(000)	805	1500
Total no. of reflections	8899	8575
Reflections, I > 2σ(I)	6243	4920
Max. 2θ/°	28.27	28.35

Ranges (h, k, l)	-11<h>11 -16<k>17 -22<l>22	-19<h>19 -17<k>17 -24<l>22
Complete to 2θ (%)	98.8	98.4
Refinement method	Full-matrix least-squares on F^2	Full-matrix least-squares on F^2
Data/ Restraints/Parameters	8899/0/501	8575/0/422
WR_2(all data)	0.2087	0.2084
Goof (F^2)	1.051	1.009
R indices [I > 2σ(I)]	0.0495	0.0757
R indices (all data)	0.0713	0.0931

Table 2.2: Selected bond lengths (Å) of complexes **1** and **2**

Bond lengths	**1**	**2**
Ru(1)-N(1)	2.071(7)	2.051(8)
Ru(1)-N(2)	1.964(7)	1.951(7)
Ru(1)-N(3)	2.072(7)	2.050(8)
Ru(1)-N(4)	2.067(7)	2.064(8)
Ru(1)-N(5)	2.017(7)	2.029(8)
Ru(1)-N(6)	2.070(7)	2.075(7)
N(1)-C(20)	1.340(11)	1.355(13)
N(1)-C(24)	1.340(11)	1.373(12)
N(2)-C(12)	1.337(11)	-
N(2)-C(25)	-	1.355(12)
N(2)-C(29)	-	1.348(12)
N(2)-C(40)	1.364(11)	-
N(3)-C(29)	1.350911)	
N(3)-C(30)	-	1.373(12)
N(3)-C(34)	-	1.343(12)
N(3)-C(40)	1.330(11)	-
N(4)-C(1)	1.395(10)	1.361(12)
N(4)-C(7)	1.344(11)	1.374(12)
N(5)-C(8)	1.340(11)	1.362(12)
N(5)-C(12)	1.330(10)	1.338(12)
N(6)-C(13)	1.348(11)	1.361(12)
N(6)-C(19)	1.378(11)	1.366(12)

Table 2.3: Selected bond angles (°) for complexes **1** and **2**

Bond angle (°)	**1**	**2**
N(1)-Ru(1)-N(3)	158.6(3)	159.5(3)
N(1)-Ru(1)-N(4)	-	91.8(3)
N(1)-Ru(1)-N(6)	-	91.4(3)
N(2)-Ru(1)-N(1)	79.5(3)	79.9(3)
N(2)-Ru(1)-N(3)	79.1(3)	79.6(3)
N(2)-Ru(1)-N(4)	103.9(3)	103.3(3)
N(2)-Ru(1)-N(5)	177.8(3)	-
N(2)-Ru(1)-N(6)	100.1(3)	99.9(3)
N(3)-Ru(1)-N(4)	-	92.5(3)
N(3)-Ru(1)-N(6)	-	92.4(3)
N(4)-Ru(1)-N(1)	90.8(3)	-
N(4)-Ru(1)-N(3)	94.3(3)	-
N(4)-Ru(1)-N(6)	156.0(3)	-
N(5)-Ru(1)-N(1)	99.5(3)	96.7(3)
N(5)-Ru(1)-N(3)	101.8(3)	103.8(3)
N(5)-Ru(1)-N(4)	78.1(3)	78.6(3)
N(5)-Ru(1)-N(6)	77.9(3)	78.2(3)
N(6)-Ru(1)-N(3)	90.6(3)	-
N(6)-Ru(1)-N(4)	-	156.8(3)

2.2.2 UV-visible Spectroscopy

Complex **1** exhibits metal to ligand charge transfer (MLCT) transition at 475 nm and intra-ligand $\pi \rightarrow \pi^*$ transitions appear at 347 and 314 nm at pH ~5 in acetonitrile / water (1:4, v/v) mixture. The MLCT band position is observed to change with the solution pH. It appears at 475 nm at a pH ≤ 5; with increasing pH, 5-7, it is red shifted to 498 nm and finally, above pH 7, the band shifts further to 510 nm (Figure 2.5). It is believed that in the acidic pH range of ≤ 5, the di-protonated form of bbp exists in **1** in solution, which with increasing pH gets transformed to **1a** containing the mono-protonated form of bbp^- and the doubly-deprotonated form bbp^{2-} stabilizes in **2** in the alkaline pH range of 7-13 (Scheme 2.3, Figure 2.6).

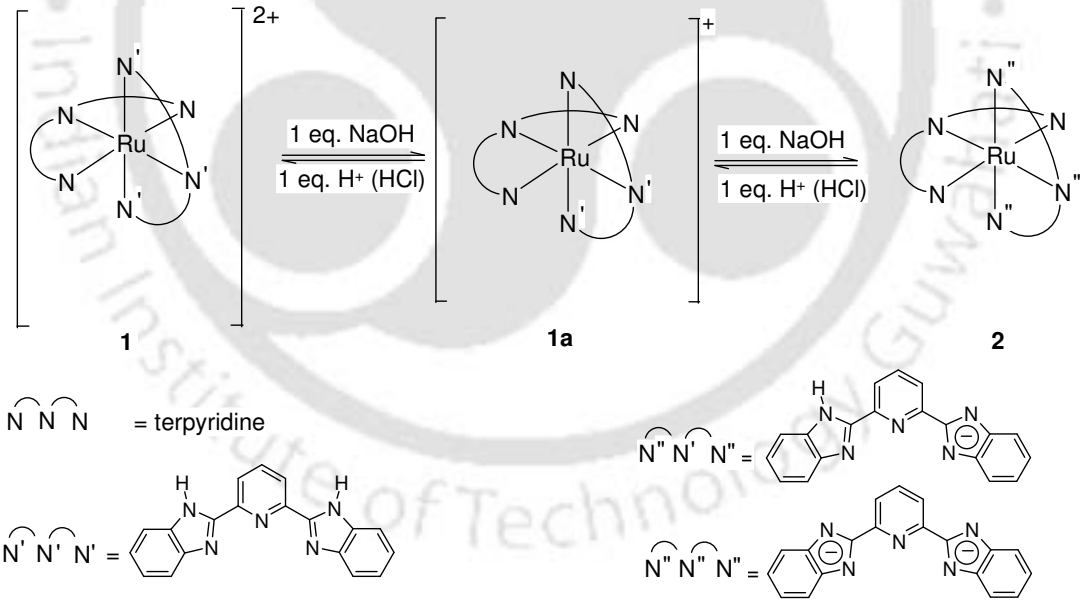

Scheme 2.3

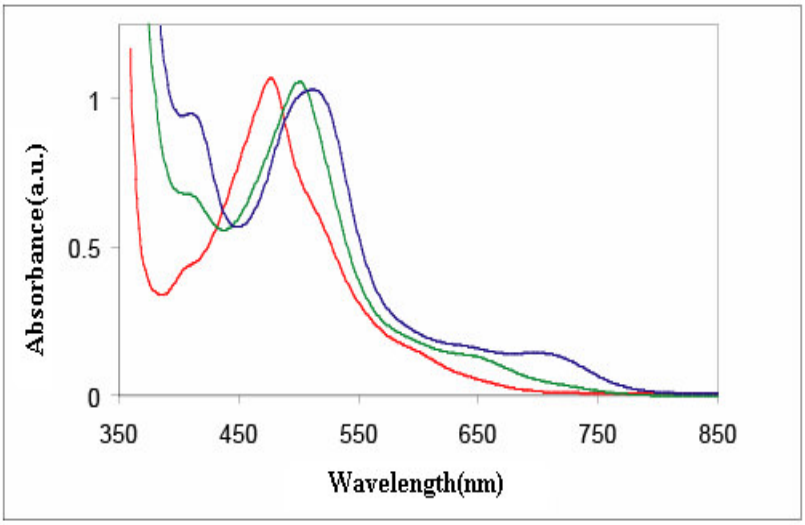

Figure 2.5: UV-visible spectra of **1** (red), **1a** (green) and **2** (blue) in acetonitrile:water (1:4 v/v) at pH: 1.25, 6.50 and 12, respectively.

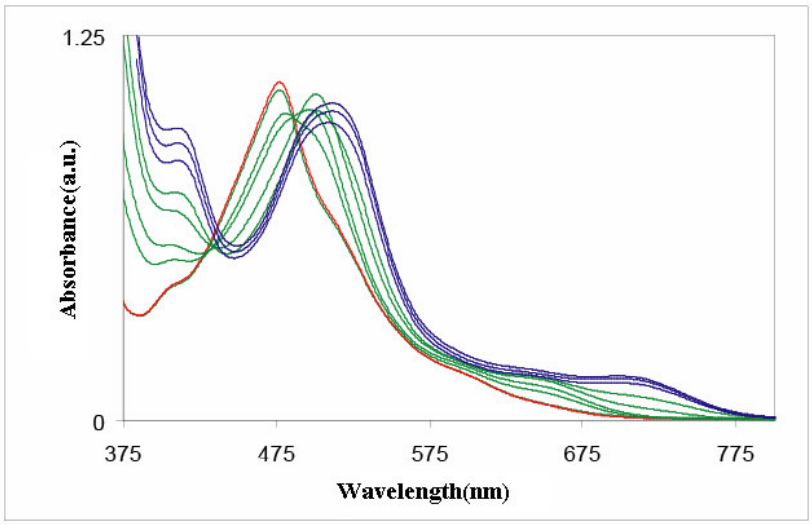

Figure 2.6: pH dependent UV-visible spectra in acetonitrile:water (1:4 v/v) with increasing pH from 1.25 to 12, respectively.

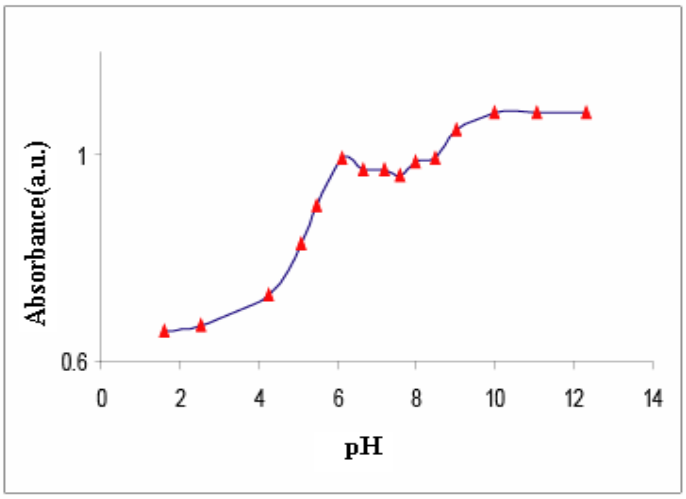

Figure 2.7: Plot of absorbance *vs* pH.

The two pK_a values, 5.75 and 7.70 are determined from the spectral changes with the pH of the solution. The similar spectral changes were reported for $[Ru(dtbimpy)(bimpyH_2)]^{2+}$ and $[Ru(dmbimpy)(bimpyH_2)]^{2+}$ in acetonitrile/buffer (1:1 v/v) with the pK_a values of 5.70, 7.33 and 6.35, 7.87, respectively.[21] Haga et al have reported similar pK_a values for $[Os(bpy)_2(BiBzImH_2)]^{2+}$ and $[Ru(bpy)_2(BiBzImH_2)]^{2+}$. The pK_a values are also comparable to those of $[Ru(L_{18})(bimpyH_2)]^{2+}$ (L_{18} = 2,6-*bis*(1-octadecylbenz imid- azol-2-yl)pyridine) in a micelle solution (10mM Triton/0.1 M Na_2SO_4) (pK_a = 5.35 and 6.94).[22]

2.2.3 FT-IR Spectroscopy

The FT-IR spectra of the complexes were recorded in KBr pellets. The strong, sharp perchlorate vibrations at ~ 1100 cm^{-1} and ~ 625 cm^{-1} of complex **1** were found to be absent in **2**, indicating the dianionic nature of the ligand bbp in complex **2**.

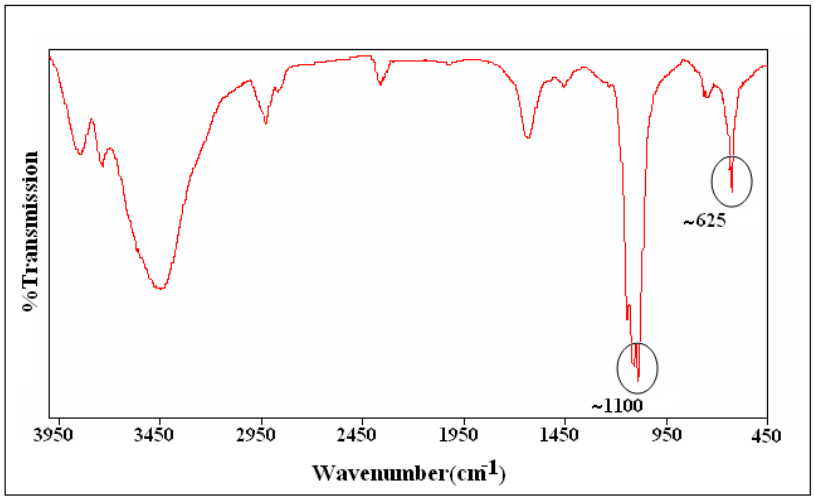

Figure 2.8: FT- IR spectrum complex **1** in KBr pellet.

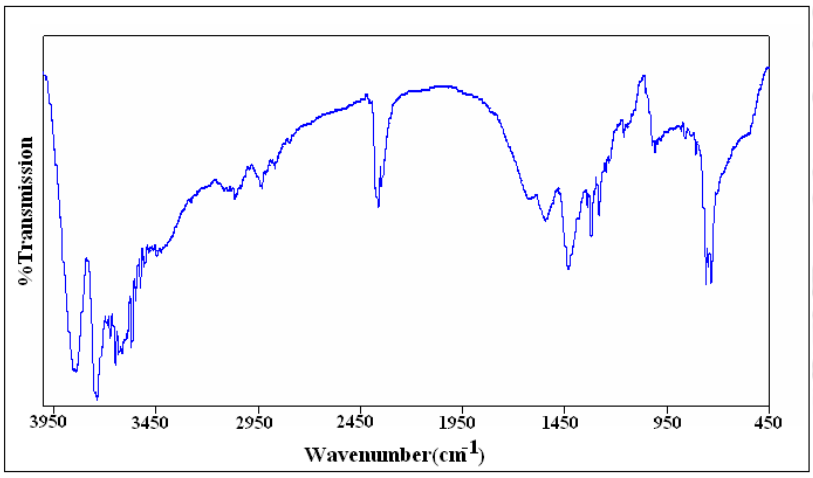

Figure 2.9: FT- IR spectrum complex **2** in KBr pellet.

3.2.4 ^{1}H-NMR Spectroscopy

The ^{1}H-NMR spectra of complexes **1** and **2** in $(CD_3)_2SO$ solvent show the calculated number of twenty four and twenty two aromatic protons, respectively (overlapping between 5.5 – 9.2 ppm); eleven from the terpyridine group in each case; thirteen from the ancillary ligand bbp in case of complex **1** and eleven from bbp^{2-} in **2**.

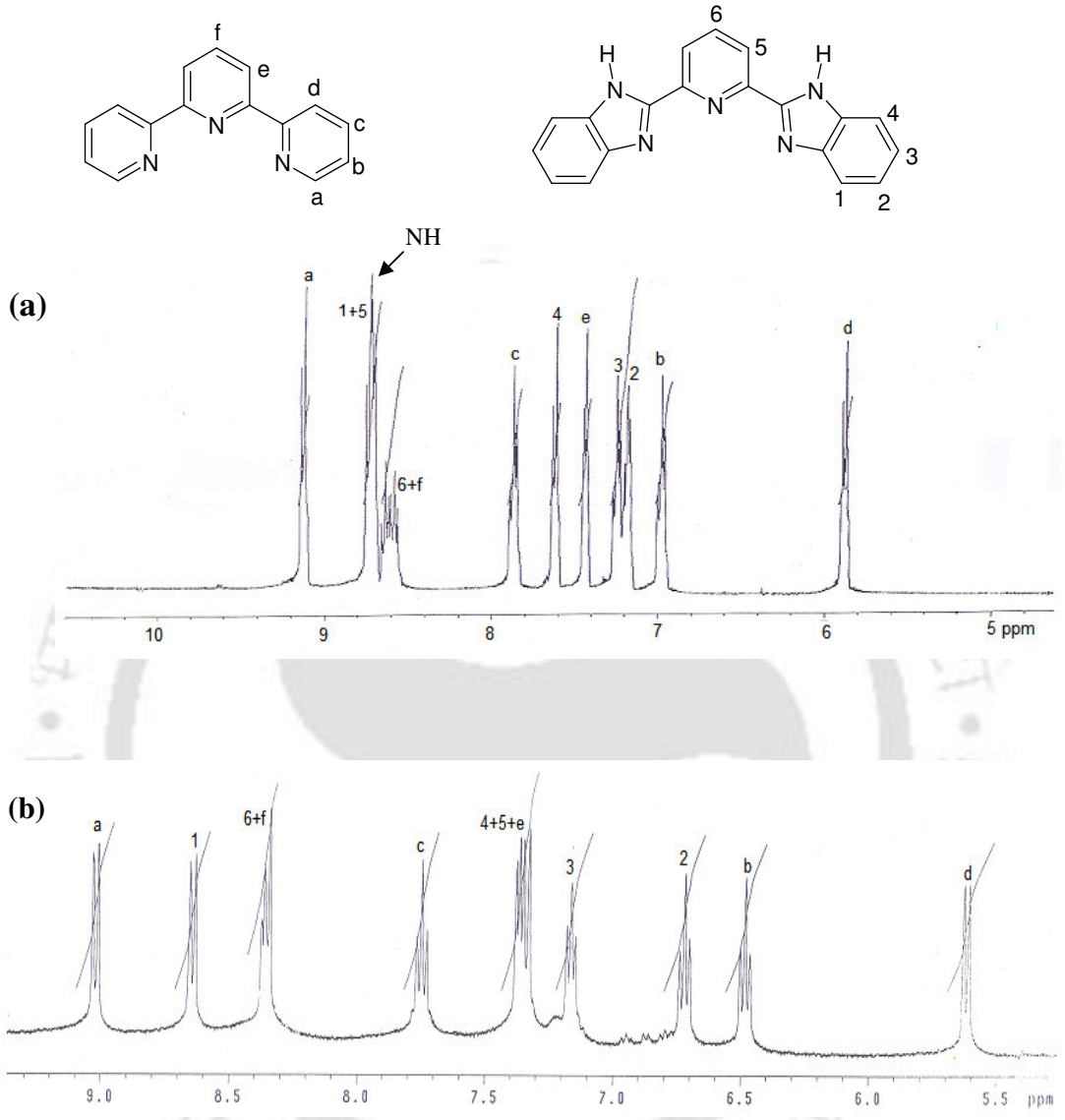

Figure 2.10: ^{1}H-NMR spectra of (a) **1** and (b) **2** in $(CD_3)_2SO$ solvent. (Only the aromatic region is shown for clarity).

The NH protons of bbp in **1** are observed at 8.8 ppm, which have, as expected, disappeared on D_2O exchange.[23] The observed signals have been assigned to individual aromatic hydrogens with the aid of ^{1}H-NMR correlation spectroscopic (COSY) experiments.

2.2.5 Electrochemical studies

Electrochemical studies have been performed in 1:4 acetonitrile-water solvent mixture since the complexes are not fully soluble in water. The Ru^{II}/Ru^{III} couple for **2** with fully deprotonated bbp^{2-} has been observed at 0.45 V *vs.* SCE (I in Figure 2.11) whereas the same for **1** with doubly-protonated bbp appears at 0.99 V (II in Figure 2.11).

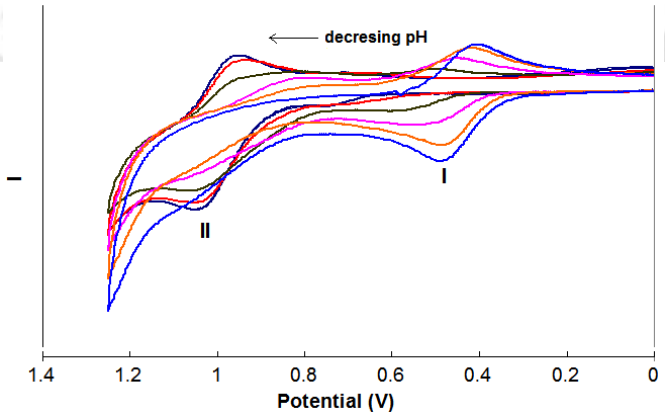

Figure 2.11: pH dependent cyclic voltammograms in acetonitrile:water (1:4 v/v) (pH from 1.02 to 12.5).

It is interesting to note that Ru^{II}/Ru^{III} couple for $[Ru(trpy)_2]^{2+}$ was reported to appear at 1.30 V.[24] Thus a decrease in potential of 0.30 V in case of **1** and 0.85 V in case of **2** has been observed depending on the protonated (bbp) or deprotonated (bbp^{2-}) form of the ancillary ligand. This can be attributed by the better σ-donor characteristic of the benzimidazol as compared to pyridine groups in trpy.[25,26] With the decrease in pH the redox wave (I in Figure 2.11) of the fully deprotonated complex **2** is found to diminish with a gradual growth of a new redox wave at a higher anodic potential (II in Figure 2.11, pH ~ 5) corresponding to **1** with doubly-protonated bbp and no more significant change is observed with further decrease in pH. Thus Ru^{II}/Ru^{III} couple remains pH

independent in the range of < 5 and > 8.5. The major Ru(II) species in these limits of pH are $[Ru(trpy)(bbp)]^{2+}$ (**1**) and $[Ru(trpy)(bbp^{2-})]$ (**2**), respectively and the electrode processes can be defined as :

$$[Ru^{II}(trpy)(bbp)]^{2+} \rightleftharpoons [Ru^{III}(trpy)(bbp)]^{3+} + e^- \quad (pH < 5) \qquad (i)$$

$$[Ru^{II}(trpy)(bbp^{2-})] \rightleftharpoons [Ru^{III}(trpy)(bbp^{2-})]^{+} + e^- \quad (pH > 8.5) \qquad (ii)$$

Although pH dependent UV-visible spectral changes clearly indicate the formation of singly protonated intermediate **1a** (Figure 2.5, Scheme 2.2), the voltammogram involving the singly-protonated species **1a** is not apparently (Figure 2.11) involved. Haga et al. has also reported same observation with $[Ru(bpy)(BiBzImH_2)]^{2+}$.[7] Significantly, the shift in redox potential of the Ru^{II}/Ru^{III} couple with the change in pH is reversible in nature.

The plot of Ru^{II}/Ru^{III} potential as a function of pH is shown in Figure 2.12. The redox process at 0.99 V going from region A to D involves only the protonated species, **1** and the process at 0.45 V going from region C to F involves only the deprotonated species, **2** [equations (i) and (ii)].

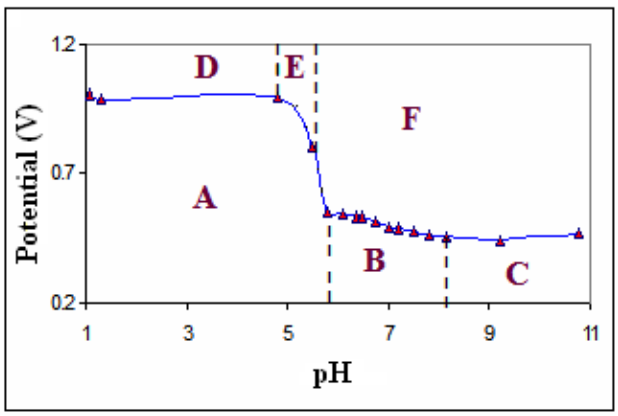

Figure 2.12: The half-wave potential, $E_{1/2}$ vs. pH diagram for **1** in acetonitrile:water (1:4 v/v).

The slope of the lines indicate the pH dependent processes in which proton transfer process is coupled with electron transfer (PCET). According to Nernst equation for a reversible electrode process, the slope of $\Delta E_{1/2}/\Delta pH = (m/n)59$ mV/pH-unit where m and n represent the number of protons and electrons involved in the process. From the plot (Figure 2.12), it is evident that three distinct PCET processes are involved in the present case. The slope of 53 mV/pH in the region A to E implies one-electron/one-proton transfer process as follows (equation iii):

$$[Ru^{II}(trpy)(bbp)]^{2+} \rightleftharpoons [Ru^{III}(trpy)(bbp^{-})]^{2+} + H^{+} + e^{-} \quad \text{(iii)}$$

The change in slope to 114 mV/pH in the region A to F correlates with the expected two-proton/one-electron transfer process (equation iv):

$$[Ru^{II}(trpy)(bbp)]^{2+} \rightleftharpoons [Ru^{III}(trpy)(bbp^{2-})]^{+} + 2H^{+} + e^{-} \quad \text{(iv)}$$

Finally, the electrode reaction in the region B to F comes back to a one-proton/one-electron process with a slope 51 mV/pH (equation v):

$$[Ru^{II}(trpy)(bbp^{-})]^{+} \rightleftharpoons [Ru^{III}(trpy)(bbp^{2-})]^{+} + H^{+} + e^{-} \quad \text{(v)}$$

Similar observations were reported by Ayers et al. and Haga et al. with $[Ru(bpy\text{-}bzimH)_2]^{2+}$ and $[(bpy)_2Ru(bibzimH_2)]^{2+}$ (where bpy-bzimH = 6-(2-benzimidazole)-2,2′-bipyridyl; bpy = 2,2′-bipyridine and bibzimH = 2,2′-bibenzimidazole).[7,24]

2.3 Conclusion

In conclusion, this chapter demonstrated an example of a set of ruthenium monoterpyridine complexes, **1** and **2**, with both the fully-protonated and depropotonated ancillary ligand. Both the complexes have been isolated as solid crystals. The complexes were characterized completely using various spectroscopic techniques and single crystal structures. The complex **1**, in solution, behaves as a

dibasic acid. It, on successive addition of two equivalent of OH^-, results into complex **2**. The conversion of **1** to **2** is found to be completely reversible in nature. The proton (or pH) dependency of the spectral and redox properties of the complexes have been studied in detail.

2.4 Experimental Section

2.4.1. Materials

The starting complex $Ru(trpy)Cl_3$ was prepared according to the reported procedure.[14] 2, 2′: 6′, 2″-terpyridine, 2,6-pyridinedicarboxylic were obtained from Aldrich, USA. 1,2-phenylenediammine was purchased from Loba Chemie, India. Other chemicals and solvents were reagent grade and used as received. For spectroscopic and electrochemical studies HPLC grade solvents were used. Commercial tetraethyl ammonium bromide was converted into pure tetrabutyl ammonium perchlorate by following available procedure.[27]

2.4.2 Physical Measurements

UV-visible spectra were recorded with a Perkin Elmer Lambda-25 spectrophotometer. FT-IR spectra were taken on a Perkin Elmer spectrophotometer with samples prepared as KBr pellets. Solution electrical conductivity was checked using a Systronic 305 conductivity bridge. ^{1}H-NMR spectra were obtained with a 400 MHz Varian FT spectrometer. Cyclic voltammetric, differential pulse voltammetric and coulometric measurements were carried out using a PAR model 273A electrochemistry system. Glassy carbon working, platinum auxiliary electrodes and an aqueous saturated calomel reference electrode (SCE) were used in a three electrode configuration. The supporting electrolyte was $[NBu^t_4]ClO_4$ and the solute concentration was ~10^{-3} M. The

half- wave potential E^0_{298} was set equal to $0.5(E_{pa} + E_{pc})$, where E_{pa} and E_{pc} are anodic and cathodic cyclic voltammetric peak potentials respectively. All experiments were carried out under a dinitrogen atmosphere and were uncorrected for junction potentials. The elemental analyses were carried out with Perkin Elmer elemental analyser.

2.4.3 Crystallography

Single crystals were grown by slow diffusion followed by slow evaporation technique. The intensity data were collected using a Bruker SMART APEX-II CCD diffractometer, equipped with a fine focus 1.75 kW sealed tube MoK_α radiation (λ = 0.71073 Å) at 273(3) K, with increasing ω (width of 0.3° per frame) at a scan speed of 3s/frame. The SMART software was used for data acquisition. Data integration and reduction were undertaken with SAINT and XPREP software.[28] Multi-scan empirical absorption corrections were applied to the data using the program SADABS.[29] Structures were solved by direct methods using SHELXS-97 and refined with full-matrix least squares on F^2 using SHELXL-97.[30] All non-hydrogen atoms were refined anisotropically. The hydrogen atoms were located from the difference Fourier maps and refined. Structural illustrations have been drawn with ORTEP-3 for Windows.[31]

2.4.4 Synthesis of the ligand, bbp

The tridentate ligand, bbp has been synthesized in a modified reported route.[14] A mixture 2,6-pyridinedicarboxylic acid (835 mg, 5 mmol) and *o*-phyenlenediamine (540 mg, 5 mmol) in 10 ml orthophosphoric acid was refluxed for 8h. Then cool down to room temperature and poured into 200 ml pre-cooled water with constant stirring which gives a light blue precipitate. On washing with 200 ml with 20% sodium

carbonate solution, pink precipitate of the ligand bbp was obtained. It was then recrystallized from hot methanolic solution [Yield = 80% (668 mg)]. Elemental analysis: Calcd. (%) ($C_{19}H_{13}N_5$): C, 73.30; H, 4.21; N, 22.49. Found (%): C, 73.21; H, 4.23; N, 22.51.

2.4.5 Synthesis of the complexes 1 and 2

$Ru^{III}(trpy)Cl_3$ (200 mg, 0.44 mmol) and bbp ligand (142 mg, 0.46 mmol) was dissolved in 20 ml ethanol and NEt_3 (0.7 mmol) was added dropwise in the mixture. It was then heated to reflux with constant stirring for 4h. Then the volume of mixture was reduced to 5 ml under reduced pressure and a precooled saturated aqueous $NaClO_4$ solution was added. The mixture was kept in refrigerator for overnight. The dark precipitate was then filtered off and washed with ice cold distilled water. The product was dried in vacuo over P_4O_{10}. It was then purified by column chromatography using the silica gel column with CH_2Cl_2/CH_3CN solvent mixture. The redish brown color complex, **1** was separated first with 4:1 CH_2Cl_2:CH_3CN followed by complex **2**. Yield: Complex **1**, 30% and **2**, 40%. Analyses: **1. $2H_2O$** : Calcd.(%) : C, 46.05; H, 3.84; N, 12.64. Found (%): C, 46.11; H, 3.86; N, 12.61. For **2. $2H_2O$** : Calcd.(%) : C, 59.38; H, 4.98; N, 16.29. Found (%): C, 59.35; H, 4.96; N, 16.25.

2.5 References

1. (a) Nakamoto, M.; Tanaka, K.; Tanaka, T. *Bull. Chem. Soc. Jpn*. **1988**, *61*, 4099. (b) Link, T. A. In Electron and Proton Transfer through the Mitochondrial Respiratory Chain; Muller, A., Ratajczak, H., Junge, W., Diemann, E., Eds.; Elsevier Science Publishers: Amsterdam, **1992**, *78*, 197.
2. Niemz, A.; Rotello, V. M. *Acc. Chem. Res.* **1999**, *32*, 44.
3. Tam-Chang, S.-W.; Mason, J.; Iverson, I.; Hwang, K.-O.; Leonard, C. *Chem. Commun.* **1999**, 65.
4. Thorp, H. H.; Chemtracts: *Inorg. Chem.* **1991**, *3*, 171.
5. Trammell, S. A.; Wimbish, J. C.; Odobel, F.; Gallagher, L. A.; Narula, P. M.; Meyer, T. J. *J. Am. Chem. Soc.* **1998**, *120*, 13248.
6. Bond, A. M.; Haga, M. *Inorg. Chem.* **1986**, *25*, 4507.
7. Haga, M.; Ano, T.; Kano, K.; Yamabe, S. *Inorg. Chem.* **1991**, *30*, 3843.
8. Haga, M.; Ali, M. M.; Koseki, S.; Fujimoto, K.; Yoshimura, A.; Nozaki, K.; Ohno, T.; Nakajima, K.; Stufkens, D. *Inorg. Chem.* **1996**, *35*, 3335.
9. Constable, E. C.; Steel, P. J. *Coord. Chem. Rev.* **1989**, *93*, 205.
10. Rillema, D. P.; Sahai, R.; Matthews, P.; Edwards, A. K.; Shaver, R. J.; Morgan, L. *Inorg. Chem.* **1990**, *29*, 167.
11. Haga, M.; Bond, A. M.; *Inorg. Chem.* **1991**, *30*, 475.
12. . Haga, M.; Matsumura-Inoue, T.; Yamabe, S. *Inorg. Chem.* **1987**, *26*, 4145.
13. Hutchison, K.; Morris, J. C.; Nile, T. A.; Walsh, J. L.; Thompson, D. W.; Petersen, J. D.; Schoonover, J. R. *Inorg. Chem.* **1999**, *38*, 2516.
14. (a) Addison, A. W.; Burke, P. J. *J. Heterocycl. Chem.* **1981**, *12*, 4455. (b) Mishra, D.; Barbieri, A.; Sabatini, C.; Drew, M. G. B.; Figgie, H. M.; Sheldrick, W. S.; Chattopadhyay, S. K. *Inorg. Chim. Acta* **2007**, *360*, 2231.

15. Mondal, B.; Puranik, V. G.; Lahiri, G. K. *Inorg. Chem.* **2002**, *41*, 5831.

16. Mondal, B.; Paul, H.; Puranik, V. G.; Lahiri, G. K. *J. Chem. Soc., Dalton Trans.* **2001**, 481.

17. Sarkar, S.; Sarkar, B.; Chanda, N.; Kar, S.; Mobin, S. M.; Fiedler, J.; Kaim, W.; Lahiri, G. K. *Inorg. Chem.* **2005**, *44*, 6092.

18. Chanda, N.; Paul, D.; Kar, S.; Mobin, S. M.; Dutta, A.; Puranik, V. G; Rao, K. K.; Lahiri, G. K. *Inorg. Chem.* **2005**, *44*, 3499.

19. Sans, C.; Rodriguez, M.; Romero, I.; Llobet, A. *Inorg. Chem.* **2003**, *42*, 8385.

20. Haga, M.; Hong, H.-G.; Shiozaka, Y.; Kawata, Y.; Monjushiro, H.; Fukuo, T.; Arakwa, R. *Inorg. Chem.* **2000**, *39*, 4566.

21. Golzhauser, A .; Panov, S.; Woll, C. *Surf. Sci.* **1994**, *314*, 849.

22. Sarkar, B.; Laye, R. H.; Mondal, B.; Chakraborty, S.; Paul, R. L.; Jeffery, J. C.; Puranik, V. G;. Ward M. D.; Lahiri, G. K. *J. Chem. Soc., Dalton Trans.* **2002**, 2097.

23. Thummel, R. P.; Chirayil, S. *Inorg. Chim. Acta* **1988**, *154*, 77.

24. Haga, M.; Takasugi, T.; Tomie, A.; Ishizuya, M.; Yamada, T.; Hossain, M. D.; Inoue, M. *J. Chem. Soc. Dalton Trans.* **2003**, 2069.

25. Maestri, M.; Armaroli, N.; Balzani, V.; Constable, E. C.; Thompson, A. M. W. C. *Inorg. Chem.* **1995**, *34*, 2759.

26. Ayers, T.; Caylor, N.; Ayers, G.; Godwin, C.; Hathcock, D. J.; Stuman, V.; Slattery, S. J. *Inorg. Chim. Acta* **2002**, *328*, 33.

27. Sawyer, D. T.; Sobkowiak, A.; Roberts, J. L. Jr. Electrochemistry for Chemists, 2nd ed., Wiley, New York, **1995**.

28. SMART, SAINT and XPREP, Siemens Analytical X-ray Instruments Inc., Madison, Wisconsin, USA, **1995**.

29. Sheldrick, G. M. SADABS: software for Empirical Absorption Correction, University of Gottingen, Institut fur Anorganische Chemieder Universitat, Tammanstrasse 4, D-3400 Gottingen, Germany, **1999–2003**.

30. Sheldrick, G. M. SHELXS-97, University of Gottingen, Germany, **1997.**

31. Farrugia, L. J. *J. Appl. Crystallogr.* **1997**, *30*, 565.

Abstract

Ruthenium complexes of 2,6-*bis*(benzimidazol-2-yl)pyridine (bbp) with dioxolene ligands (L) {L = *o*-phenylenediamine, *o*-aminophenol, *o*-aminothiophenol} were prepared and characterized by ^{1}H-NMR, IR, UV-visible, Mass spectroscopic studies and single crystal X-ray structure determination. The spectral and structural characterizations were used to assign the charges on the metal ion and ligand frameworks. It has been noticed that the di-negative form of the bbp ligand stabilizes the Ru(II)-quinone charge distribution whereas the neutral bbp favors the Ru(II)-semiquinonate valence state.

3.1 Introduction

Quinonoid ligands and their analogues are very well-known in coordination chemistry because of their non-innocent nature.[1] These ligands and their metal complexes has been the subject matter of continuous research activity because of their biological importance, redox and magnetic properties.[2] They can bind to the metal in three ways: (i) neutral quinone form; (ii) mono-negative semiquiononate radical form and (iii) dinegative catecholate form (scheme 3.1).[3]

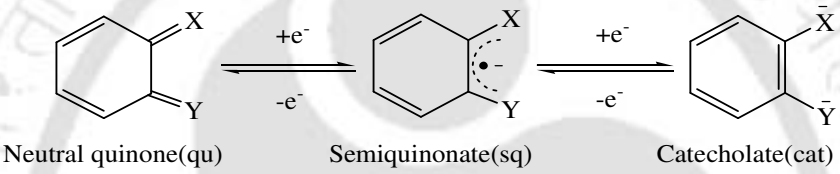

Scheme 3.1

However, in cases with considerable degree of covalency between a redox active metal center and coordinated redox active ligand, due to appreciable mixing of the metal and ligand orbitals, the assignment of the oxidation states to the metal or to the ligand leads to ambiguity.[4] In such cases, establishment of the native state valence configuration of the metal and ligand is a formidable challenge. In this direction, variety of mononuclear ruthenium quinonoid systems have been synthesized and studied over the last few years.[5] However, the ambiguities vary substantially depending on the nature of X and Y in the quinonoid (L) framework (Scheme 3.2) and the electronic nature of the ancillary ligands in the complex moieties.[6-8]

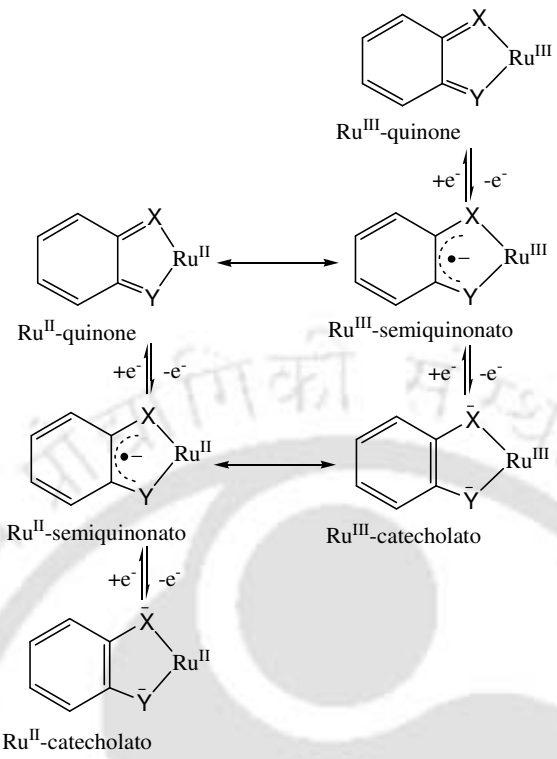

Scheme 3.2 Redox series of $Ru^{II/III}$ - dioxolene complexes.

For example, distinct localized {Ru^{II}Lcat} and {Ru^{II}Lsq} configurations are reported in case of $[(tap)_2RuL]$[9] [tap = 2-(*m*-tolylazo)pyridine] and $[(PPh_3)_2RuL_2]$,[8] respectively; however, the $[(bpy)_2RuL]^+$ (bpy = 2,2′-bipyridine) and $[(t\text{Bupy})_2RuL_2]$ complexes (L = X = Y = O, Scheme 3.1) are described as charge-delocalized systems.[4] On the other hand, the RuL valence state configurations in [(Cl/OAc)(trpy)RuL] (L = X = Y = O; trpy = 2,2′:6′,2″-terpyridine, Scheme 3.1) have been described as a resonance equilibrium between Ru^{II}Lsq and Ru^{III}Lcat.[10] Hence, continuous experimental and theoretical studies with newer molecules are necessary to understand the electronic distribution of metal quinonoids.[11] This, indeed, instigate us to study the valence-state distribution profile of {RuL} coordinated to not yet explored 2,6-*bis*(bezimidazol-2-yl)pyridine as ancillary ligand.

In this chapter, the valence state distribution pattern with iminoquinone, iminothioquinone complexes of ruthenium with bbp ancillary ligand will be explored.

All the complexes contain the general [Ru(bbp)(*o*-quinonoid)(S)] (bbp: 2,6-*bis*(benzimidazol-2-yl)pyridine; S = CH_3CN) unit and can posses one of the three valence state distributions: Ru^{II}-qu, Ru^{III}-sq or Ru^{IV}-cat (qu: neutral quinone; sq: semiquinonate radical and cat: catecholate form). Structural and spectral characterizations were used to assign the charges on the metal and ligand.

3.2 Results and Discussion

The complexes [Ru(bbp)(L)(CH_3CN)] (**3a**–**5a**) and [Ru(bbp)(L)(CH_3CN)](ClO_4) (**3b**-**5b**) [L = *o*-phenylenediamine, *o*-aminophenol and *o*-aminothiol in **3**(**a**,**b**), **4**(**a**,**b**) and **5**(**a**,**b**) respectively] have been synthesized by the reaction or [Ru(bbp)Cl_3] with the respective L, in presence of NEt_3 in refluxing ethanolic medium. Chromatographic purification on silica gel column using CH_2Cl_2/CH_3CN solvent mixture results into the pure products. The unsymmetrical nature of *o*-aminophenol, *o*-aminothiol is expected to give two isomeric products, **A** and **B**, in the present case (Scheme 3.3). However, in all cases, only

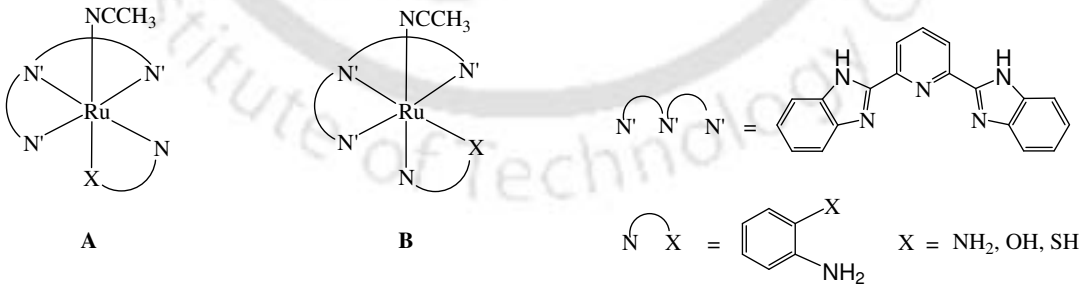

Scheme 3.3

isomer **A** was obtained preferentially.

The complexes, **3a**-**5a** are found to be neutral and nonconducting in acetonitrile whereas **3b**-**5b** behave as 1:1 electrolyte in the same solvent. All the complexes

exhibit satisfactory microanalysis (see Experimental Section).

3.2.1 Mass Spectroscopy

In the electrospray mass spectra, the (m+1) molecular ion peaks for complexes **3a, 4a, 5a, 3b**, **4b** and **5b** appear at 558.67, 560.09, 576.06, 658.05, 660.03 and 676.99, respectively, which again confirms the formation of the complexes (Figure 3.1a-f).

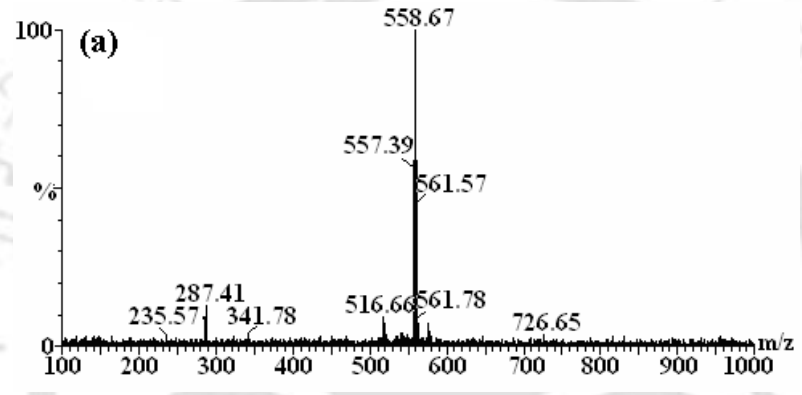

Figure 3.1a: ESI-Mass spectra for complex **3a** in CH_3CN/H_2O (50:50) with (0.1%) formic acid

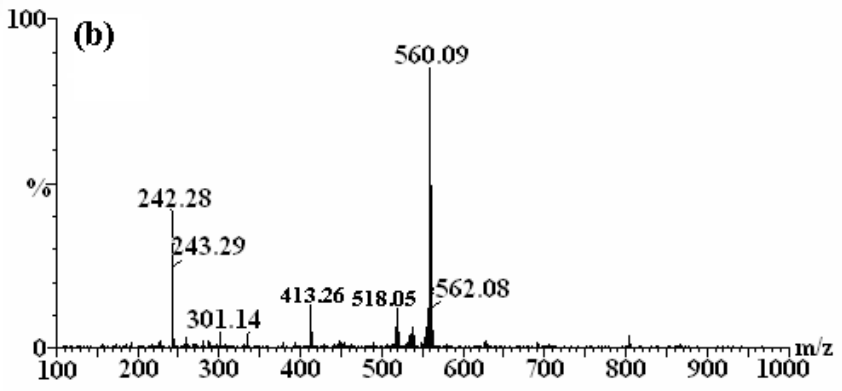

Figure 3.1b: ESI-Mass spectrum for **4a** in CH_3CN/H_2O (50:50) with (0.1%) formic acid

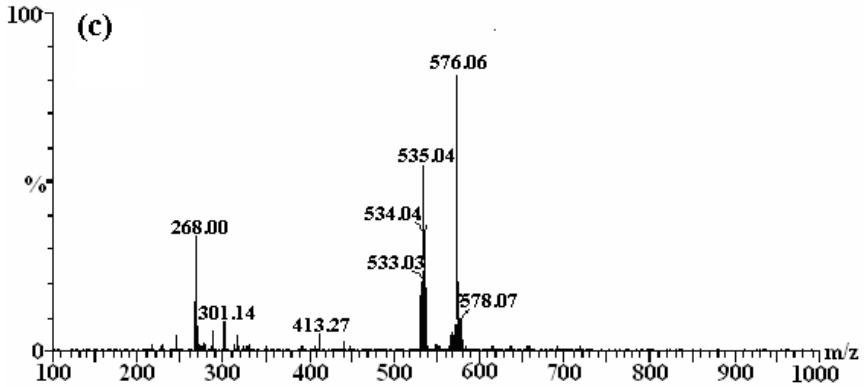

Figure 3.1c: ESI-Mass spectrum for **5a** in CH_3CN/H_2O (50:50) with (0.1%) formic acid

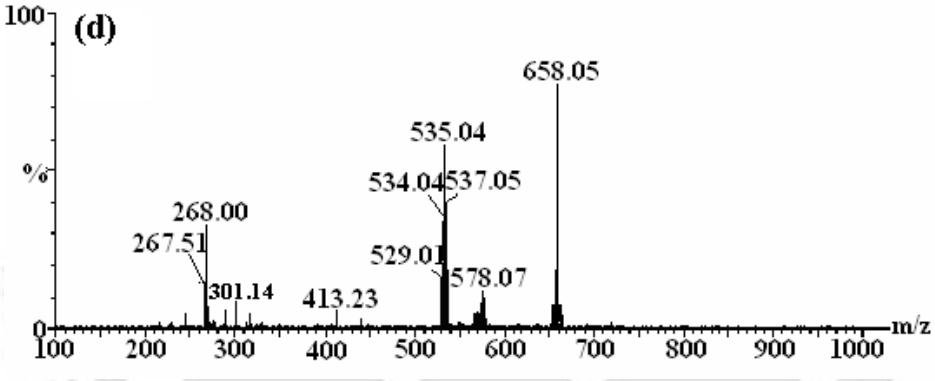

Figure 3.1d: ESI-Mass spectrum for complex **3b** in CH_3CN/H_2O (50:50) with (0.1%) formic acid

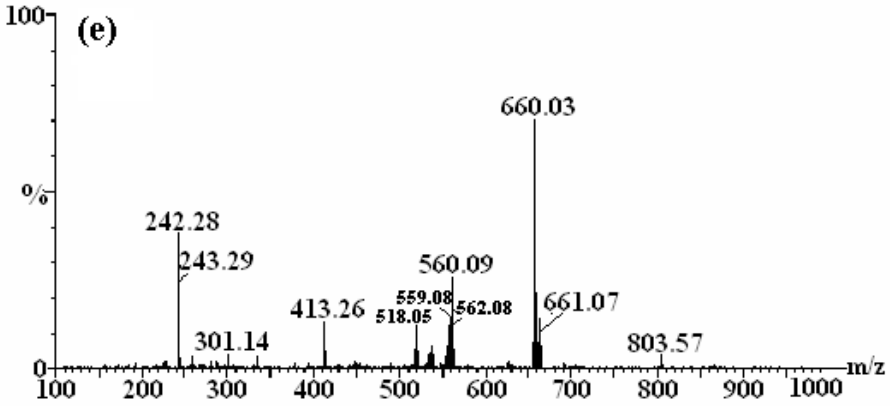

Figure 3.1e: ESI-Mass spectrum for complex **4b** in CH_3CN/H_2O (50:50) with (0.1%) formic acid

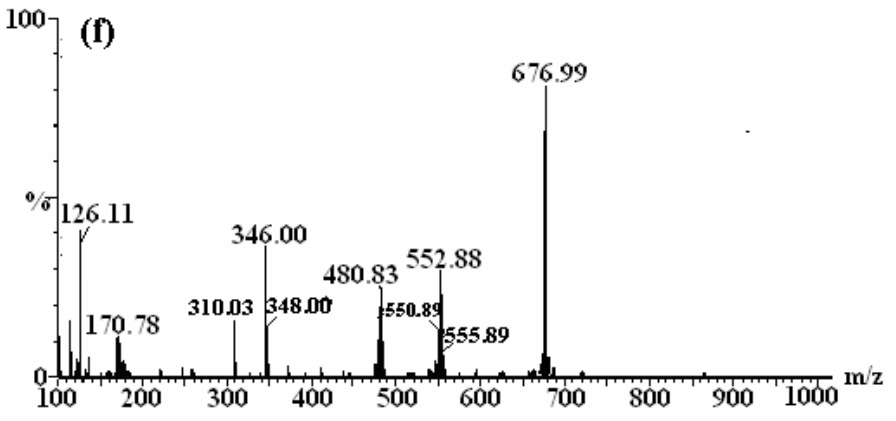

Figure 3.1f: ESI-Mass spectrum for complex **5b** in CH_3CN/H_2O (50:50) with (0.1%) formic acid.

The NH vibration was found to appear at near ~3300 cm^{-1} for all the cases. Room temperature magnetic moment measurements reveal the diamagnetic nature of the complexes **3a-5a**; whereas **3b-5b** show one electron paramagnetism. The X-band EPR spectral analysis at 77K indicates the presence of unpaired electron in the ligand framework. The observed diamagnetism of the complexes **3a**-**5a** can be attributed to the spin coupling of multiple paramagnetic centers present in the complex.[12] Hence, in the present case, the charge distribution on both the redox active ligand and metal have become of interest. The recent studies of the structural characteristics of complexes containing iminobenzoquinone, iminosemiquinone type ligands by Pierpont and Weighardt group have provided a sound basis to assign the charges on the ligand as well as metal ion.[13,14]

2.2.2 X-ray Crystallography

The structures of the complexes **3a** and **4a** are authenticated by their single crystal X-ray structures (Figures 3.2 and 3.5, respectively) and the crystallographic data are given in table 3.1. The important bond lengths and angles are listed in table 3.2 and 3.3, respectively. The geometrical constrains imposed due to the usual meridional

mode of binding of tridentate bbp ligand is reflected in the *trans* angles N(1)-(Ru(1)-N(3), 155.9(2)º; N(2)-Ru(1)-N(6), 177.28(16)º (Table 3.3) which are comparable to other ruthenium-terpyridne and ruthenium-bbp complexes N(1)-(Ru(1)-N(3), 158.6(3)º; N(2)-Ru(1)-N(5), 177.8(3); N(4)-(Ru(1)-N(6), 156.0(3)º; and N(1)-(Ru(1)-N(3), 159.5(3)º; N(2)-Ru(1)-N(5), 176.1(3)º; N(4)-(Ru(1)-N(6), 156.8(3)º [15] It has been found that in **3a** and **4a**, the bbp ligand binds in its bi-negative form.[16] The acetonitrile solvent is *trans* to the O-atom of the oxolene moiety in complex **4a**. 1.993(5) Å, Ru(1)-N(3), 2.055(4) Å; N(1)-Ru(1)-N(2), 78.2(2)º; N(2)-Ru(1)-N(3), 78.47(19)º match well with the reported related complexes.[15-17] The Ru-N(L) (L = *o*-quinonoid ligands) distances Ru(1)-N(6), 2.060(5) Å in **3a** and 2.087(5) Å in **4a** are appreciably shorter than the corresponding Ru-N(bbp) Ru(1)-N(3), 2.071(5) Å in **3a** and 2.055(4) Å in **4a** because of appreciable degree of mixing of dπ(Ru) and π^* of L in the respective LUMO.[18] It has been found from the reported structures of *o*-quinonoid molecules that the C-O and C-N bond lengths with localized semiquinone ligands are in the range of 1.30 Å and 1.35 Å, respectively; whereas, in case of quinone, they are 1.22 Å and 1.31 Å, respectively.[19]

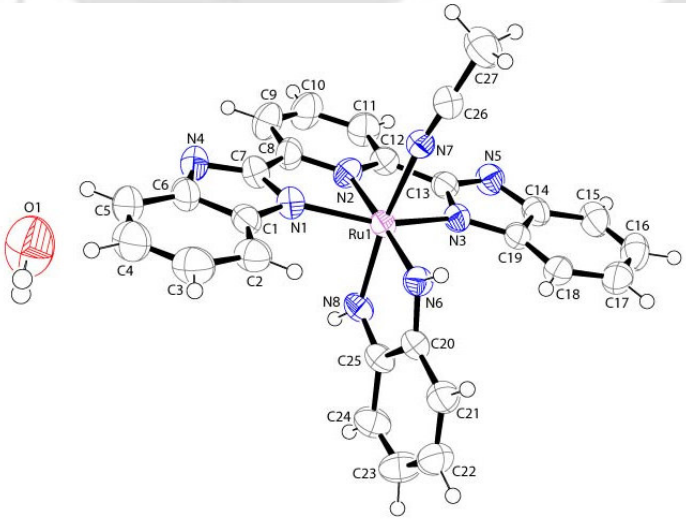

Figure 3.2: ORTEP diagram for complex **3a** (50% thermal ellipsoids plot).

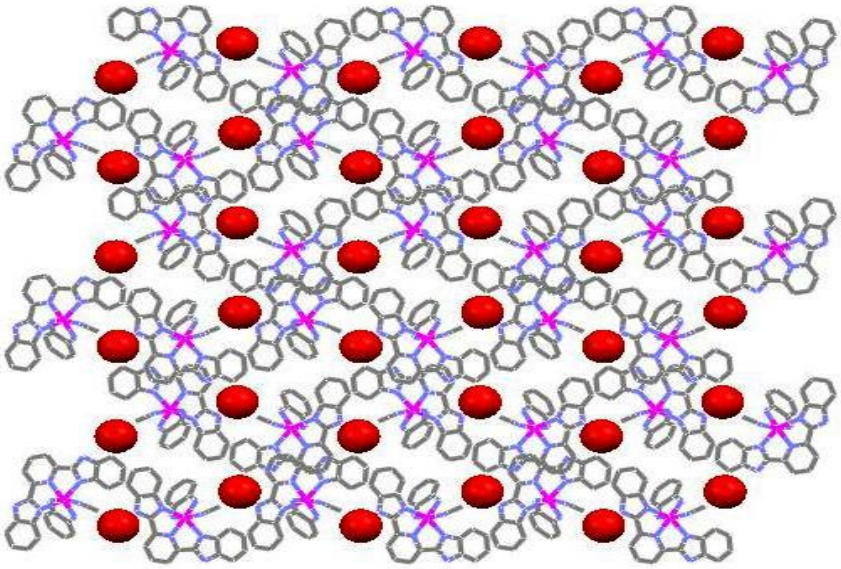

Figure 3.3: Packing diagram for complex **3a**.

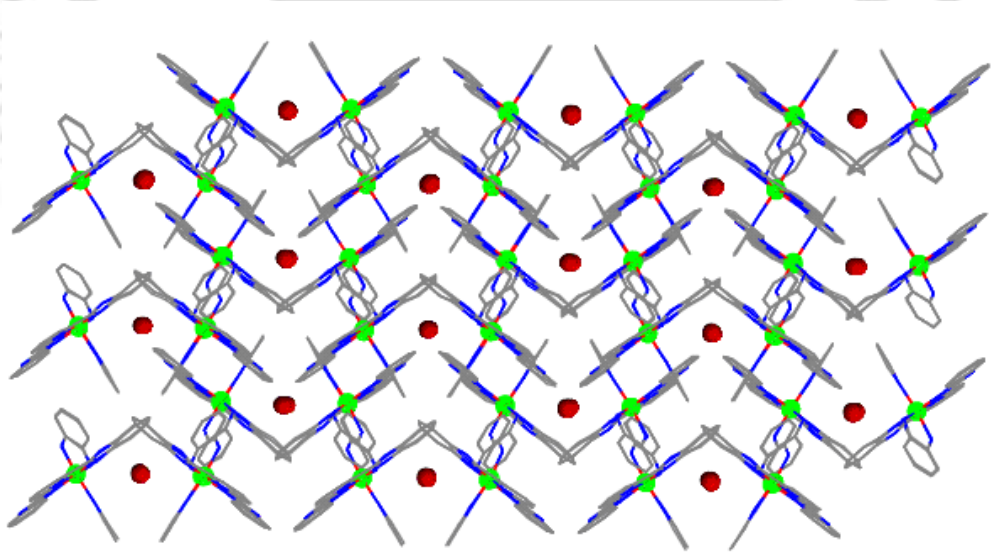

Figure 3.4: Packing diagram for complex **3a**.

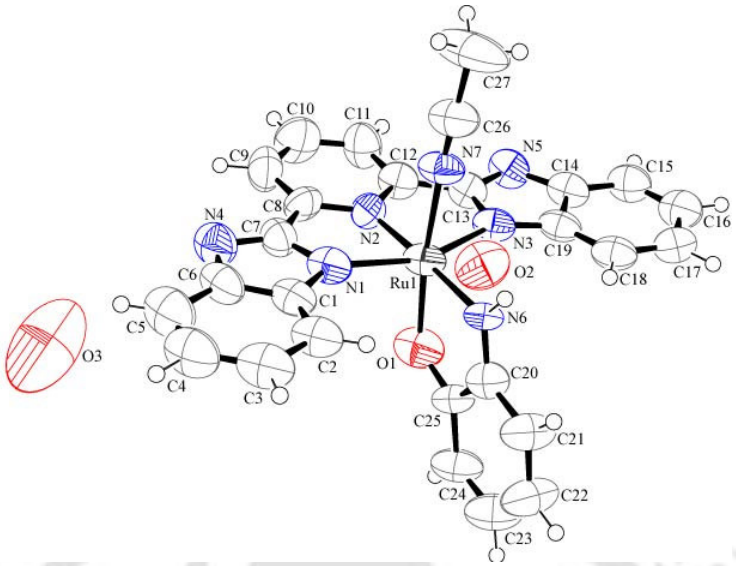

Figure 3.5: ORTEP diagram for complex **4a** (50% thermal ellipsoids plot).

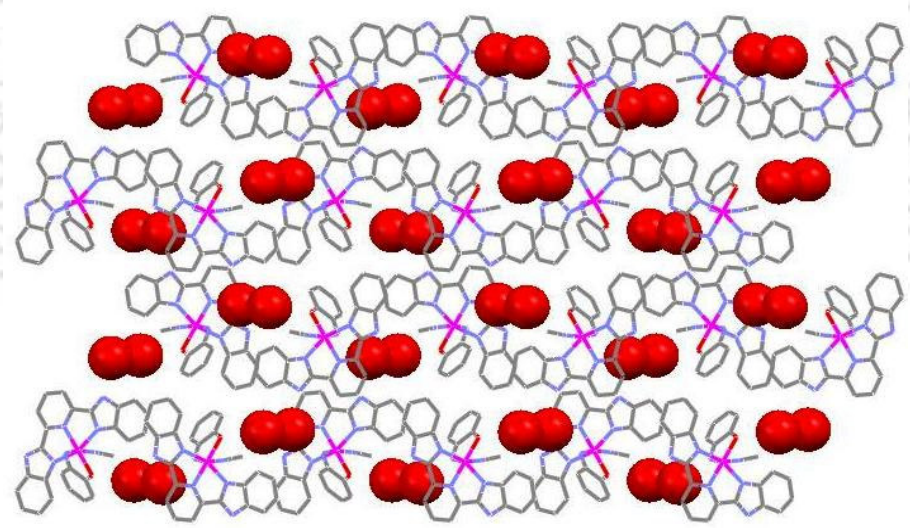

Figure 3.6: Packing diagram for complex **4a**.

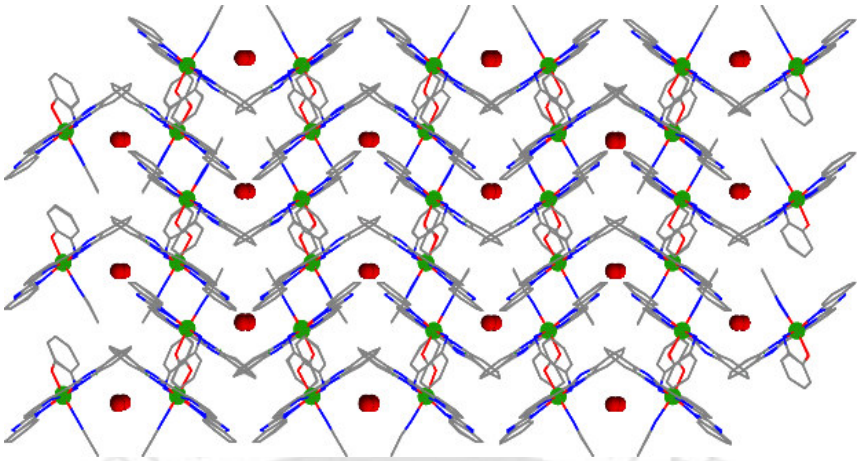

Figure 3.7: Packing diagram for complex **4a**.

In the present case, C(25)-N(8) and C(20)-N(6) distances are 1.325(9) Å and 1.321(8) Å respectively, in **3a** and C(25)-O(1) and C(20)-N(6) distances are 1.3510(8) Å and 1.286(7) Å, respectively, in **4a** (Table 3.2) which are clearly too low for the Ru^{IV}(amidophenolate); on the other hand, they are comparable for the average double bonds in iminoquinone charge distribution.[19] The assignment considering Ru(III) and an iminosequinonate form of oxolene moiety is also not consistent with the charge distribution observed in the earlier reported $Ru(PPh_3)_2$(PhenoxSQ)Cl_2 {PhenoxSQ = 1-hydroxy-2,4,6,8-tetra-tert-butyl phenoxazinyl radical} and $Ru(PPh_3)_2$(3,5-DBSQ)Cl_2.[20] {3,5-DBSQ = 3,5 di-*tert*-butyl semiquinone}. In addition, short intra-ring C-C distances of oxolene moiety for complex **3a,** C(20)-C(21), 1.427(9) Å; C(21)-C(22), 1.353(11) Å; C(22)-C(23), 1.409(12) Å; C(23)-C(24), 1.312(11) Å; C(24)-C(25), 1.417(9) Å and C(20)-C(25), 1.446(8) Å and for complex **4a,** C(20)-C(21), 1.414(8) Å; C(21)-C(22), 1.356(8) Å; C(22)-C(23), 1.413(10) Å; C(23)-C(24), 1.330(10) Å; C(24)-C(25), 1.418(7) Å; and C(20)-C(25), 1.417(8) Å also support the fact that **3a** and **4a** are primarily in Ru^{II}-iminoquinone state. The small deviation from the reported bond lengths might be because of a minor contribution from Ru^{III}-semiquinonate state.

Table 3.1: Crystallographic data for complexes **3a** and **4a**

	3a	**4a**
Formulae	$C_{27}H_{22}N_8ORu$	$C_{27}H_{13}N_7O_3Ru$
Mol. wt.	597.96	584.51
Crystal system	Monoclinic	Monoclinic
Space group	P2(1)/c	P2(1)/c
Temperature /K	298(2)	273(2)
Wavelength /Å	0.71073	0.71073
a /Å	9.0095(6)	8.9657(10)
b /Å	16.9233(12)	16.9661(16)
c /Å	16.3307(12)	17.367(2)
α/°	90.00	90.00
β/°	100.047(2)	99.356(7)
γ/°	90.00	90.00
V/ $Å^3$	2451.8(3)	2606.5(5)
Z	4	4
Density/Mgm^{-3}	1.564	1.490
Abs. Coeff. /mm^{-1}	0.681	0.643
F(000)	1196	1168
Total no. of reflections	21002	22310
Reflections, I > 2σ(I)	4624	3341
Max. 2θ/°	28.35	27.36
Ranges (h, k, l)	-11 <= h <=10 -19 <= k <=22 -21 <= l <= 21	-11 <= h <=11 -22 <= k <=21 -21 <= l <= 22
Complete to 2θ (%)	98.3	97.6
Refinement method	Full-matrix least-squares on F^2	Full-matrix least-squares on F^2
Data/ Restraints/Parameters	6013/0/335	5765/0/344
WR_2(all data)	0.2223	0.1825
Goof (F^2)	1.032	1.082
R indices [I > 2σ(I)]	0.0645	0.0695
R indices (all data)	0.0818	0.1168

Table 3.2: Selected bond lengths (Å) of complexes **3a** and **4a**

Bond length (Å)	**3a**	**4a**
Ru(1)-N(1)	2.073(5)	2.049(5)
Ru(1)-N(2)	2.055(5)	2.005(5)
Ru(1)-N(3)	2.071(5)	2.055(5)
Ru(1)-N(6)	2.060(5)	2.087(5)
Ru(1)-N(7)	1.968(5)	2.051(4)
Ru(1)-N(8)	1.980(5)	-
Ru(1)-O(1)	-	1.937(5)
N(1)-C(1)	1.373(8)	1.402(7)
N(1)-C(7)	1.361(8)	1.371(8)
N(2)-C(8)	1.337(8)	1.342(8)
N(2)-C(12)	1.346(8)	1.357(7)
N(3)-C(13)	1.357(8)	1.362(7)
N(3)-C(19)	1.375(8)	1.363(8)
N(4)-C(6)	1.381(10)	1.393(9)
N(4)-C(7)	1.337(9)	1.319(8)
N(5)-C(13)	1.341(8)	1.340(7)
N(5)-C(14)	1.375(9)	1.398(9)
N(7)-C(26)	1.137(8)	1.111(7)
N(6)-C(20)	1.325(8)	1.286(7)
N(8)-C(25)	1.321(9)	-
O(1)-C(25)	-	1.351(8)

Table 3.3: Selected bond angles (°) for complexes **3a** and **4a**

Bond angle (°)	**3a**	**4a**
N(1)-Ru(1)-N(3)	153.7(2)	155.8(2)
N(1)-Ru(1)-N(6)	92.5(2)	88.44(19)
N(1)-Ru(1)-N(7)	104.7(2)	101.61(19)
N(1)-Ru(1)-N(8)	104.7(2)	-
N(1)-Ru(1)-O(1)	-	94.43(19)
N(2)-Ru(1)-N(1)	76.2(2)	78.1(2)
N(2)-Ru(1)-N(3)	77.6(2)	78.5(2)
N(2)-Ru(1)-N(6)	93.5(2)	90.3(2)
N(2)-Ru(1)-N(8)	97.6(2)	-
N(2)-Ru(1)-O(1)	-	97.8(2)
N(3)-Ru(1)-N(7)	87.0(2)	102.07(19)
N(3)-Ru(1)-N(8)	92.8(2)	-
N(3)-Ru(1)-O(1)	-	94.54(17)
N(6)-Ru(1)-N(3)	87.0(2)	85.83(18)
N(6)-Ru(1)-N(7)	90.6(2)	92.02(18)
N(6)-Ru(1)-N(8)	168.6(2)	-
N(6)-Ru(1)-O(1)	-	171.8(2)
N(7)-Ru(1)-N(2)	175.7(2)	177.66(17)
N(7)-Ru(1)-N(3)	101.6(2)	102.07(19)
N(7)-Ru(1)-N(8)	78.3(2)	-
N(7)-Ru(1)-O(1)	-	79.87(19)

All the spectral features of complex **5a** are comparable to complex **3a** and **4a**. Hence, it is logical to assume that in **5a**, the charge distribution is mostly Ru^{II}-iminoquinone with a minor contribution from Ru^{III}-iminosemiquinonate form. In Ru^{III}-iminosemiquinonate form, the paramagnetic centers arising from Ru(III) and iminosemiquinonate radical couple antiferromagnetically to result into diamagnetism. Hence, all these complexes show sharp ^{1}H-NMR spectra with no residual low-level paramagnetic effect.

3.2.3 UV-visible Spectroscopy

UV-visible spectra of all the complexes, **3a-5a**, **3b–5b**, were recorded in acetonitrile solvent. All the complexes show strong MLCT transitions in the visible region and several intra-ligand transitions in the UV-visible region (Figures 3.8, 3.9). The λ_{max} and calculated ε values associated with the transitions are tabulated in table 3.4.

Table 3.4

Complexes	**$\lambda_{max/nm}$ (ε/dm^{3}mol^{-1}cm^{-1})**
3a	514(5898); 341(15119); 326(14827); 222(28595)
3b	518(5700), 338(13660), 327(13740), 219(24260)
4a	566(4060), 346(12540), 326(12770), 221(20600)
4b	571(4450), 343(13660), 327(13700)
5a	488(4540), 336(17520), 310(18070), 272(23940)
5b	527(4440), 324(13660)

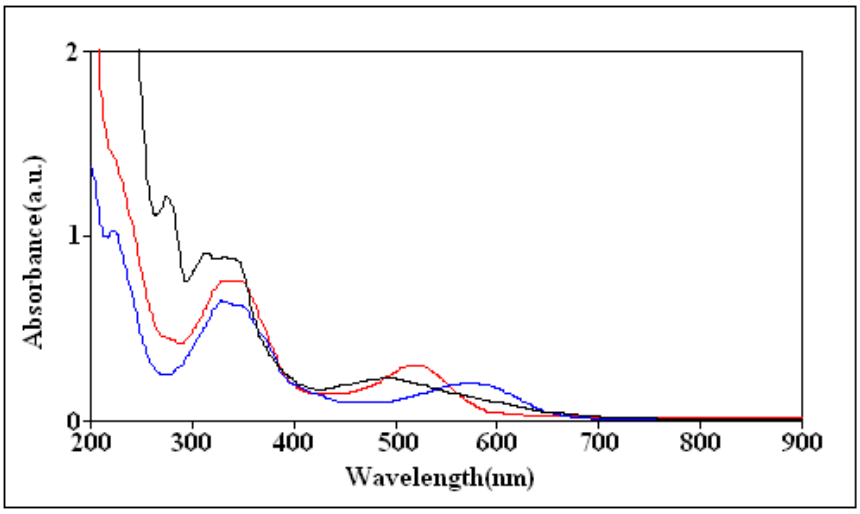

Figure 3.8: UV-visible of **3a** (red), **4a** (blue) and **5a** (green) spectra in acetonitrile solvent.

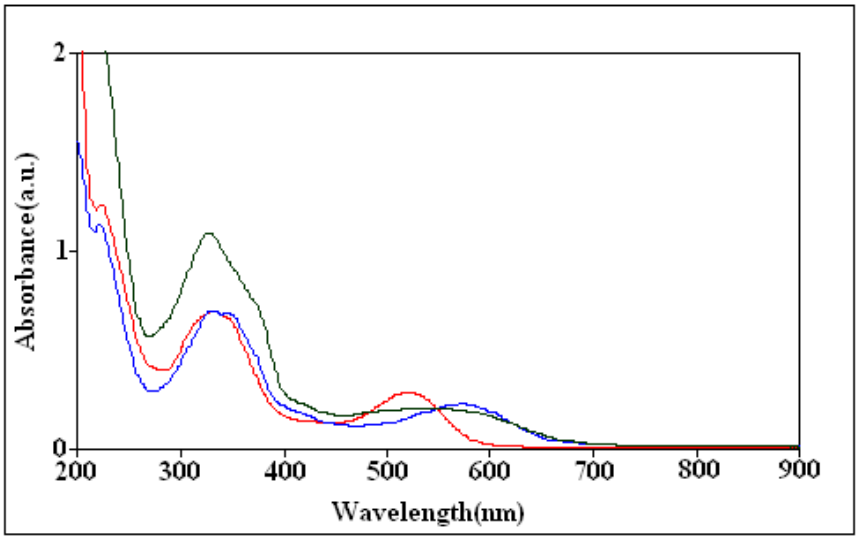

Figure 3.9: UV-visible of **3b** (red), **4b** (blue) and **5b** (green) spectra in acetonitrile solvent.

3.2.4 FT-IR Spectroscopy

The FT-IR spectra of all the complexes were recorded in KBr pellets. In case of complexes **3b**-**5b**, the characteristic perchlorate vibrations appear at ~1100 and ~625 cm^{-1} which are absent in case of **3a**-**5a**. A sharp band is observed at ~1725 cm^{-1} in all the complexes (Figure 3.10). It should be noted that this band is found to be absent in the corresponding [Ru(bbp)(L)Cl] {L = *o*-phenylenediamine} complex (see Chapter 6). This

band is attributed to the nitrile frequency of the coordinated acetonitrile in the complexes. It is interesting to note that this is appreciably lower than the expected ν(CN) for coordinated nitriles. This extremely low frequency might be an indication either of an unusual strong π-back bonding or the involvement of its η^2-bonding.[21] The later was observed in $[Mo(Cp)_2(CH_3CN)]$, which exhibits the ν(CN) at 1725 cm^{-1}.[22] However, in the present case, the crystal structure

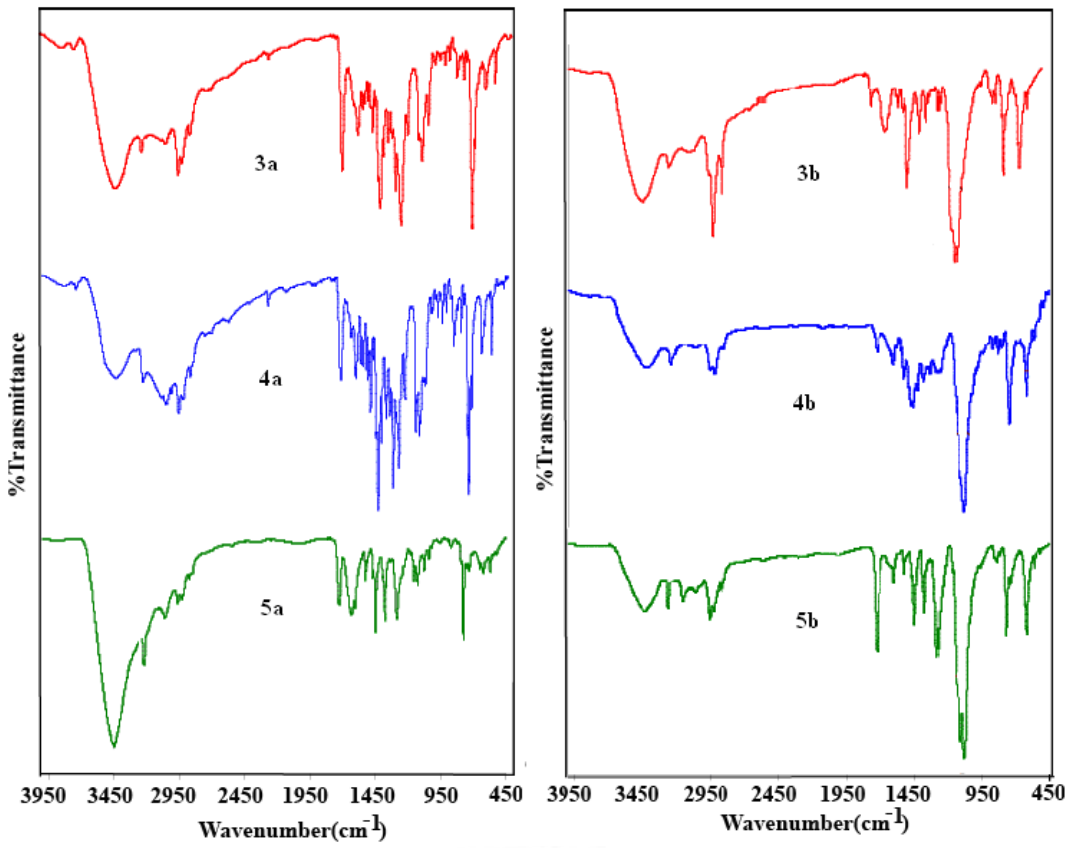

Figure 3.10: FT-IR spectra for complexes **3a-5b** in KBr pellets.

of complexes reveal that CH_3CN is bonded to the metal in normal η^1-fashion through N atom. On the other hand, the Ru-$N_{acetonitrile}$ and C-$N_{acetonitrile}$ bond distances, 2.059 Å and 1.137 Å, respectively. This C-$N_{acetonitrile}$ distance is longer than the normal C-N distance

(~1.115 Å) observed in case of coordinated acetonitrile.[23] Hence, this low ν(CN) can be attributed to the strong π-back bonding from the metal center to the acetonitrile.

3.2.5 ^{1}H-NMR Spectroscopy

The ^{1}H-NMR spectra of all the complexes were recorded in $(CD_3)_2SO$ solvent at room temperature. Complexes **3a-5a** exhibit well resolved spectra (Figure 3.11); whereas, the same for **3b**-**5b** are broad and unresolved because of the presence of inherent paramagnetism (Figure 3.12). The ^{1}H-NMR spectra of the complexes **3a-5a** show the calculated number of aromatic protons overlapping between 6.5–8.4 ppm; eleven from the bbp ligand and four from *o*-quinonoid moiety (see Experimental Section)(Figure 3.11). The NH- protons from *o*-quinonoid moiety appear at ~ 8.22 ppm for complex **4a** and ~ 11.80 ppm for complexes **3a** and **5a**, respectively; which are appreciably shifted towards downfield because of the coordination to the metal center. This NH-proton, as expected, disappeared on D_2O exchange.[24] In all the complexes, the three methyl protons of the coordinated acetonitrile appear as a sharp singlet at δ, 2.04 ppm. The similar signal for coordinated acetonitrile in [Ru(trpy)(PAP)(CH_3CN)] {trpy: 2,2′:6′,2″-terpyridine; PAP: phenylazopyridine} was found to appear at 1.87 ppm.[25]

3.2.6 EPR Spectroscopy

From FT-IR, NMR spectroscopic and conductivity studies, it is evident that the actual electronic structure of complexes **3b-5b** is either Ru^{II}-iminosemiquinonate or Ru^{III}-iminoquinone or somewhere between these two resonance forms. EPR spectral studies of frozen solutions is known as one of the most powerful technique to understand the electronic structure or charge distribution of transition metal dioxolene complexes.[25] As

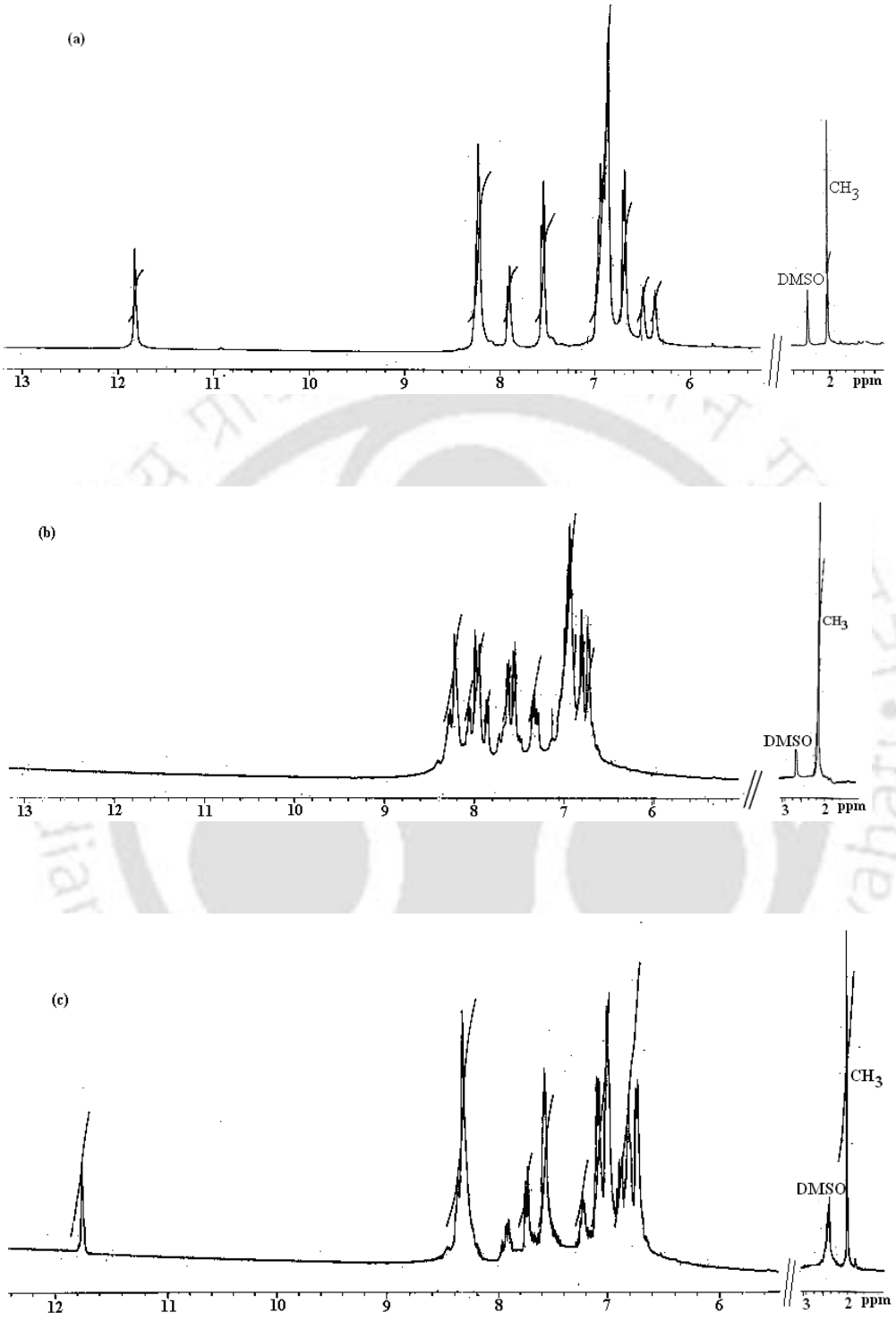

Figure 3.11: ^{1}H-NMR spectra of complexes (a) **3a**, (b) **4a** and (c) **5a** in $(CD_3)_2SO$ solvent.

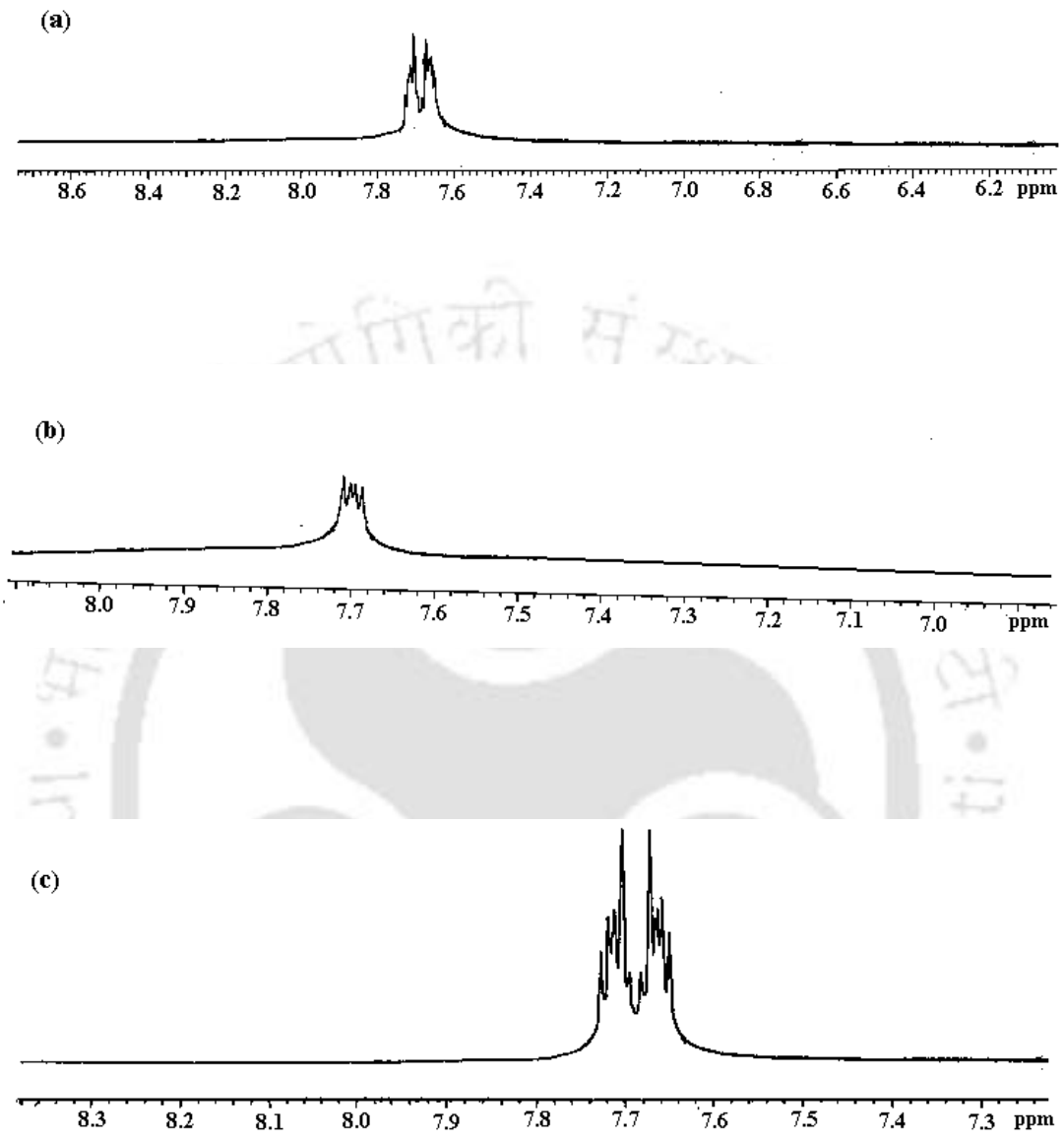

Figure 3.12: ^{1}H-NMR spectra of complexes (a) **3b**, (b) **4b** and (c) **5b** in $(CD_3)_2SO$ solvent.

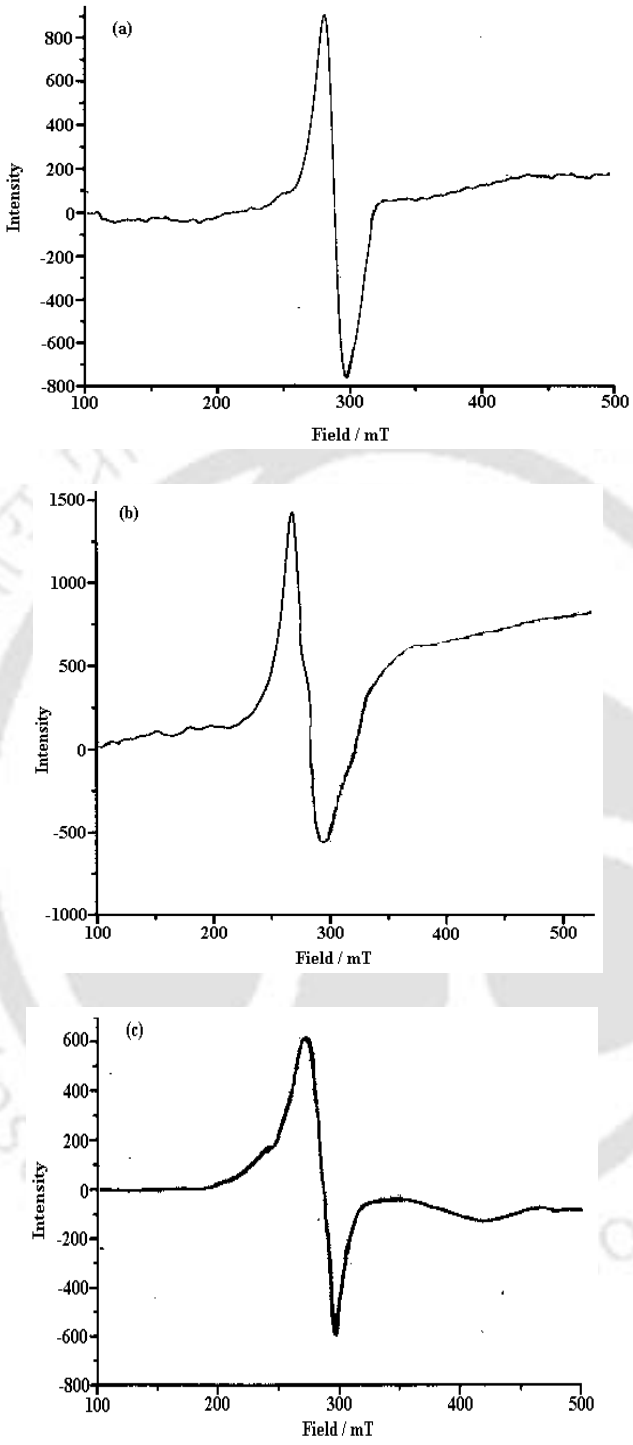

Figure 3.13: X-band EPR spectra of complexes (a) **3b**, (b) **4b** and (c) **5b** in acetonitrile:toluene (1:1; v/v) mixture at 77K.

the amount of spin on the metal can be estimated by the degree of anisotropy of the *g* tensor quantified as $\Delta g = g_1 - g_3$ and the isotropic g factor, $\langle g \rangle$ shows the deviation from its value for free electron (i.e. 2.0023) and for the semiquinone anion radicals (g = ~2.005).[8]

For all the three paramagnetic complexes, **3b**–**5b**, the EPR spectra were recorded in acetonitrile:toluene (1:1; v/v) at 77K. The observed spectra of complexes **3b-5b** are shown in figure 3.13. At 77K, the signals are isotropic in nature with the g values close to 2.023 which is larger than free semiquinone radical, but close. Hence, the charge distribution in complexes **3b-5b** is attributed mostly to Ru^{II}-iminosemiquinonate form. The absence of anisotropy in the spectrum precludes existence of the Ru^{III}-catecholate form.

3.2.7 Electrochemical studies

The complexes **3a**-**5a** show a one-electron quasi-reversible oxidation couple at 0.84 V, 0.94 V and 0.89 V *vs* SCE, respectively in cyclic voltammetric studies using glassy carbon working electrode (Figure 3.14). These potentials can be attributed to the Ru^{II}/Ru^{III} couple. The same couple were reported to appear at 0.95 V and 1.35 V in case of $[Ru(bpy)_2(NH_2\text{-}NH_2)]^{2+}$.[25] In the present case observed lower oxidation potential for Ru^{II}/Ru^{III} process is attributed to the better δ- donar ability of the bbp ligand in its deprotonated state. These couples have been followed by another one-electron quasi-reversible couple at 1.21 V, 1.18 V and 1.22 V *vs* SCE, for complexes **3a**-**5a**, respectively, which have been attributed to the semiquinone to quinone oxidation. In the negative side of the voltammogram, three distinct one-electron reversible couples have been observed in each case.

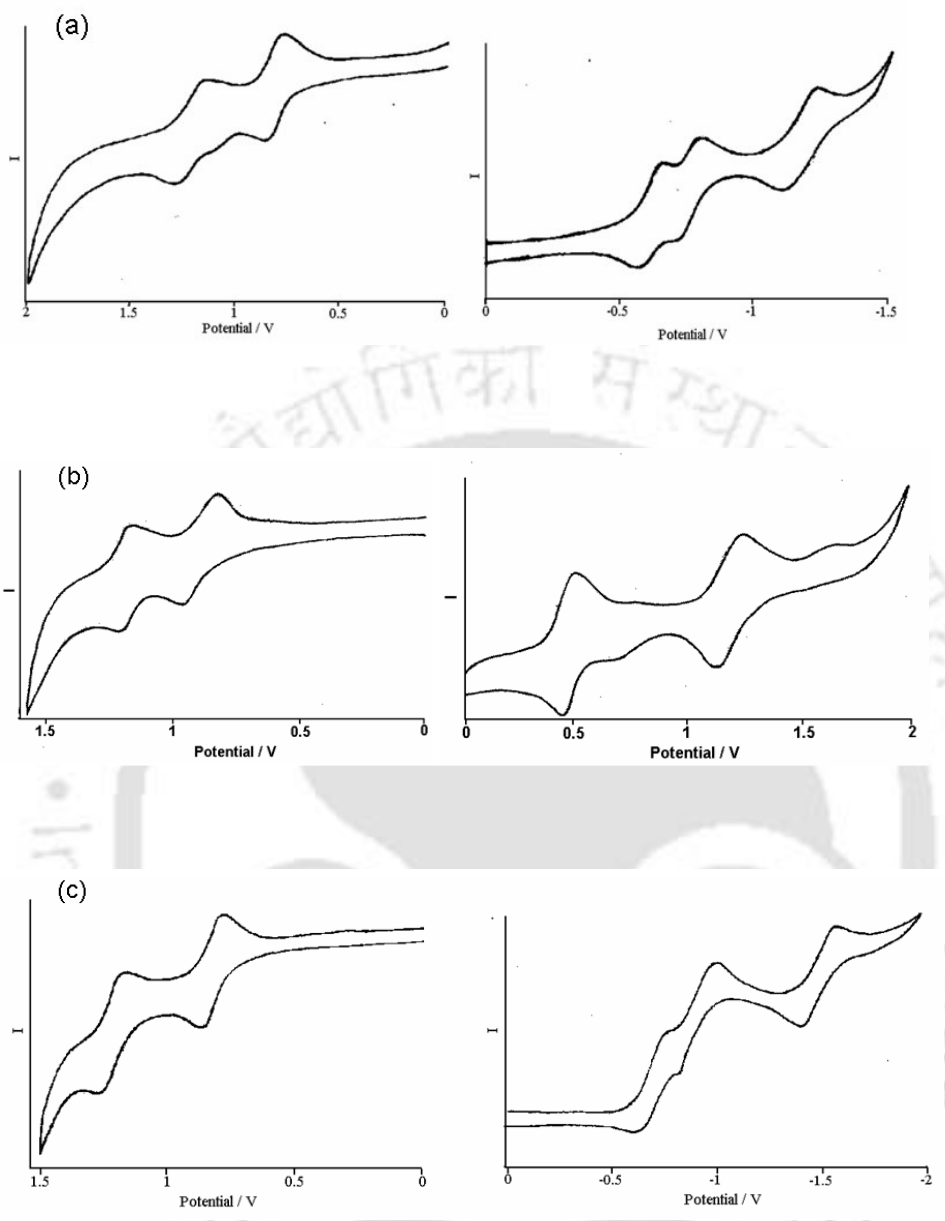

Figure 3.14: Cyclic voltammograms of complexes (a) **3a**, (b) **4a** and (c) **5a** in acetonitrile solvent at scan rate 50 mV/s (SCE: Reference electrode; Glassy Carbon: Working electrode; Supporting electrolyte: TBAP).

For complex **3a**, the couples appear at -0.61 V, -0.76 V and -1.18 V; for complex **4a**, the couples appear at -0.48 V, -1.20 V, 1.66 V and in case of **5a**, the same appear at -0.69 V, -0.91 V and -1.48 V *vs* SCE, respectively. The first couple is attributed to the

semiquinonato to catecholate reduction process whereas the other two are assigned for the bbp reduction.

On the other hand, complexes **3b-5b** display one quasi-reversible single-electron transfer process at 0.66 V, 0.80 V and 0.76 V *vs* SCE, respectively (Figure 3.15). In the negative side

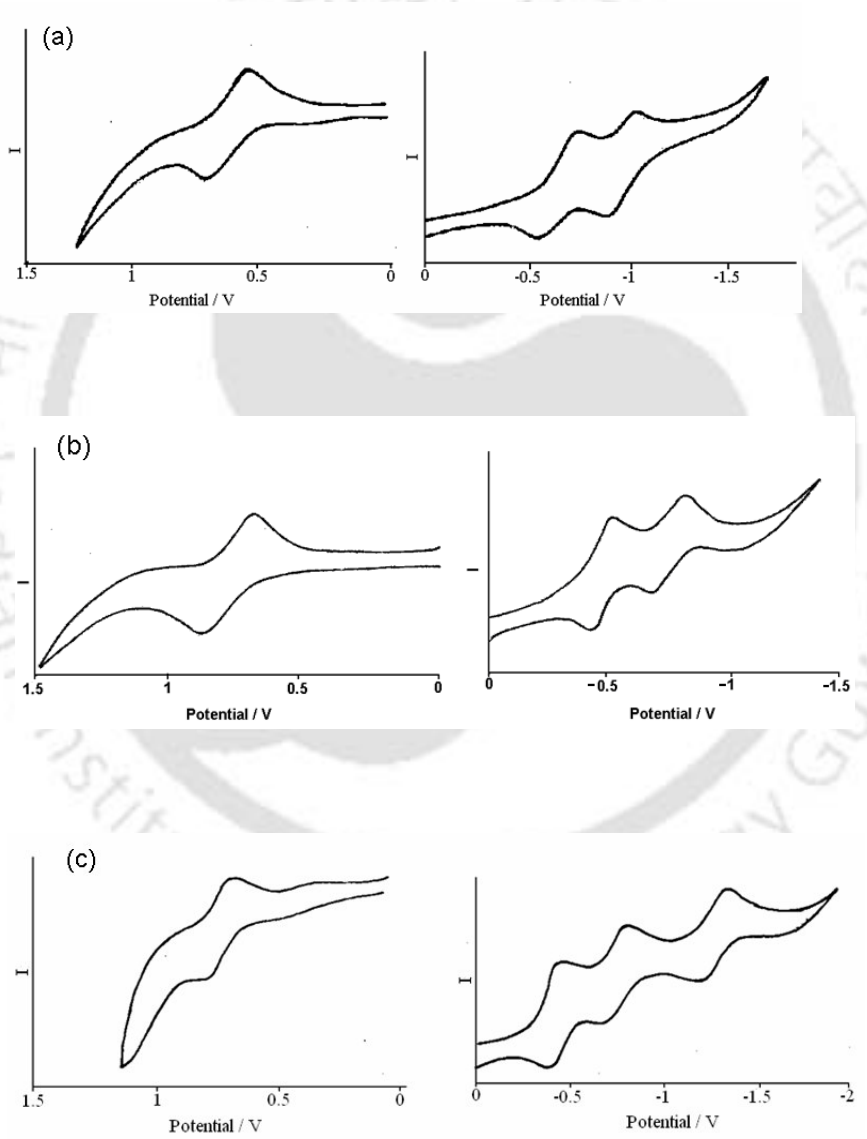

Figure 3.22: Cyclic voltammograms of complex (c) **5b** in acetonitrile solvent at scan rate 50 mV/s (SCE: Reference electrode; Glassy Carbon: Working electrode; Supporting electrolyte: TBAP).

of SCE, two one-electron transfer processes have been observed in all the three cases, **3b-5b**, which are attributed to the semiquinonate to catecholate and bbp reductions.

Thus from the all spectral features of complexes **3a-5a,** it is assume that the charge distribution is mostly Ru^{II}-iminoquinone with a minor contribution from Ru^{III}-iminosemiquinonate form. On the other hand, the paramagnetism of the complexes **3b-5b** can be attributed to: (i) Ru^{III}-catecholate; (ii) Ru^{III}-quinone or (iii) Ru^{II}-semiquinonate charge distribution as Ru^{I}-quinone is quite uncommon.[7] In magnetic moment studies, all the three complexes, **3b**-**5b**, exhibit moment corresponding to one unpaired electron (1.82-1.98 BM). The sharp isotropic signal in X-band EPR spectral studies at 77K indicates the presence of organic radical rather than Ru^{III} center in these complex moieties. The presence of characteristic perchlorate frequencies and 1:1 electrolytic nature of the complexes support the neutral bbp binding. Hence, the observed paramagnetism of the complexes **3b**-**5b** can be attributed to the Ru^{II}-iminosemiquinonate state. It would be worth mentioning here that in $[Ru^{II}(trpy)(DBQ)(CH_3CN)]ClO_4$ [trpy: 2,2′:6′,2″-terpyridine and DBQ = 3,5-di-tertiarybutylquinone] the Ru^{II}-semiquinonate valence state distribution was observed with the unpaired electron in the DBQ moiety.[7]

3.3 Conclusion

In conclusion, the present chapter described a set of ruthenium complexes of bbp ligand with oxolene ligands. This is an example where the mode of oxolene binding has been found to be controlled by the protonation and deprotonation of the bbp ligand. The di-negative binding of the bbp ligand (de-protonated form) stabilizes the Ru(II)-quinone distribution whereas the protonated form of bbp favors the Ru(II)-semiquinonate valence distribution.

3.4 Experimental Section

3.4.1 Materials

Reagent-grade chemicals were used in all experiments and solvents were purified using standard procedures. The anciallry ligand, 2,6-*bis*(benzimidazol-2-yl)pyridine (bbp)[26] and the staring complex, $Ru(bbp)Cl_3$[27] were synthesized using procedures reported previously. *o*-phenylenediamine, *o*-aminophenol, *o*-aminothiophenol were purchased from Loba Chemie, Mumbai, India and purified before use.

3.4.2 Physical Measurements

Elemental analyses (C, H, N) were carried out using a Perkin-Elmer 240C elemental analyzer. Electronic and FT-IR spectra were recorded on Perkin-Elmer Lambda 25 and Perkin-Elmer spectrophotometer, respectively. Magnetic susceptibility measurements were made using PAR 155 vibrating sample magnetometer interfaced with a walker L75FBAL magnet. ^{1}H-NMR spectra were obtained from a 400 MHz Varian FT Spectrometer. Solution electrical conductivity was checked using a Systronic 305 conductivity bridge. Electrochemical measurements were made using CH Instruments 660A potentiostat. A glassy carbon working electrode, Pt wire auxiliary electrode and an aqueous saturated calomel reference electrode were used in a three-electrode configuration. All electrochemical measurements were done at 298K under nitrogen atmosphere in acetonitrile solution containg TBAP as supporting electrolyte. The scan rate used was 50 mV/s. The half- wave potential E^0_{298} was set equal to $0.5(E_{pa} + E_{pc})$, where E_{pa} and E_{pc} are anodic and cathodic cyclic voltammetric peak potentials respectively. All the electrochemical data are uncorrected for junction potential.

3.4.3 X-ray Crystallography

X-ray quality crystals were grown by slow diffusion followed by slow evaporation technique. The intensity data were collected using a Bruker SMART APEX-II CCD diffractometer, equipped with a fine focus 1.75 kW sealed tube MoK_α radiation (λ = 0.71073 Å) at 273(3) K, with increasing ω (width of 0.3° per frame) at a scan speed of 3 s/frame. The SMART software was used for data acquisition. Data integration and reduction were undertaken with SAINT and XPREP[28] software. Multi-scan empirical absorption corrections were applied to the data using the program SADABS.[29] Structures were solved by direct methods using SHELXS-97 and refined with full-matrix least squares on F^2 using SHELXL-97.[30] All non-hydrogen atoms were refined anisotropically. The hydrogen atoms were located from the difference Fourier maps and refined. Structural illustrations have been drawn with ORTEP-3 for Windows.[31]

3.4.4 Synthesis of complexes 3a, 3b

The precursor complex $Ru(bbp)Cl_3$ (200 mg, 0.39 mmol) is taken in 20 ml of ethanol and added 1,2 phenylenediammine (42 mg, 0.39 mmol) and NEt_3 (0.4 ml) and heated to reflux for 4h. The initial dark brown color of the solution was changed gradually to dark red. Then the volume of reaction mixture was reduced to 5 ml and an excess saturated aqueous solution of $NaClO_4$ was added to it. It was kept in refrizerator for 5h and solid precipitate thus obtained was filtered off and washed with cold distilled water. The product was dried in vacuo over P_2O_5. It was then purified by using silica gel column. The complexes were collected by (4:1) CH_2Cl_2/CH_3CN mixture. Evaporation of the solvent under reduced pressure afforded a pure solid. Yield: Complex **3a**: 95 mg (50%); Complex **3b**: 40 mg (20%).

Complex **3a**: Anal. Calcd.(%)($C_{27}H_{20}N_8Ru$): C: 58.16; H: 3.62; N: 20.11. Found (%) C: 58.06; H: 3.58; N: 20.16. ESI-Mass: 558.67, ^{1}H-NMR[$(CD_3)_2SO$, δ, ppm]: 11.82(s, NH), 8.23(t, 1H), 7.92(d, 2H), 7.56(d, 2H), 6.91(m, 5H), 6.71(t, 2H), 6.49(s, 1H), 6.37(d, 2H), 2.04(s, 3H)

Complex **3b**: Anal. Calcd.(%)($C_{27}H_{22}N_8O_4ClRu$): C: 49.21; H: 3.36; N: 17.00. Found (%) C: 42.71; H: 2.90; N: 14.78. ESI-Mass: 658.05. Conductivity: 127.97 $\Omega^{-1}mol^{-1}cm^2$

3.4.5 Synthesis of complexes 4a, 4b

Both the complexes have been synthesized by the reaction of $Ru(bbp)Cl_3$ (200 mg, 0.39 mmol) and *o*-aminophenol (43 mg, 0.39 mmol) following the same procedure as above. Yield: Complex **4a**, 120 mg (60%); Complex **4b**, 40 mg (20%).

Complex **4a**: Anal. Calcd.(%)($C_{27}H_{20}N_8ORu$): C: 58.06; H: 3.43; N: 17.55. Found (%) C: 58.04; H: 3.42; N: 17.54. ESI-Mass: 560.09. ^{1}H-NMR[$(CD_3)_2SO$, δ_{ppm}]: 8.26(t, 1H), 8.20(d, 2H), 7.98(d, 2H), 7.85(t, 2H), 7.62(d, 2H), 7.55(d, 2H)7.32(m, 4H), 6.95(m, 1H), 6.90(t, 1H), 6.71(d, 1H), 2.01(s, 3H).

Complex **4b**: Anal. Calcd.(%): ($C_{27}H_{21}N_7O_9ClRu$): C: 49.13; H: 3.21; N: 14.86. Found (%) C: 49.14; H: 3.18; N: 14.85. ESI-Mass: 660.03, Conductivity: 149 $\Omega^{-1}mol^{-1}cm^2$.

3.4.6 Synthesis of complexes 5a, 5b

The complexes **5a** and **5b** have been synthesized by the reaction of $Ru(bbp)Cl_3$ (200 mg, 0.39 mmol) and *o*-aminothiophenol (49 mg, 0.39 mmol) following the same procedure as above Yield: Complex **5a**, 100 mg (50%); Complex **5b**, 75 mg (40%).

Complex **5a**: Anal. Calcd.(%)($C_{27}H_{19}N_7SRu$): C: 56.44; H: 3.33; N: 17.06. Found (%)C: 56.48; H: 3.31; N: 17.05. ESI-Mass: 576.06. ^{1}H-NMR[$(CD_3)_2SO$, δ_{ppm}]: 11.8(s, 1NH),

8.31(t, 3H), 7.74(d, 2H), 7.57(t, 2H), 7.09(d, 2H), 6.99(d, 2H), 6.84(m, 5H), 6.74(d, 2H), 1.99(s, 3H).

Complex **5b**: Anal. Calcd.(%)($C_{27}H_{21}N_7O_4ClSRu$): C: 47.97; H: 3.13; N: 14.50. Found (%) C: 47.96; H: 3.13; N: 14.49. ESI-Mass: 676.99; Conductivity: 135 $\Omega^{-1}mol^{-1}cm^2$.

3.5 References

1. Dodsworth, E. S.; Lever, A. B. P. *Chem. Phys. Letter*, **1990**, *172*, 151.

2. (a) Raymond, K. N.; Carrano, C. J. *Acc. Chem. Res.* **1979**, *12*, 183. (b) Pierpont, C. G; Buchanan, R. M. *Coord. Chem Rev.* **1981**, *38*, 45.

3. (a) Bhattacharya, S.; Gupta, P.; Basuli, F.; Pierpont, C. G. *Inorg. Chem.* **2002**, *41*, 5810. (b) Maji, S.; Patra, S.; Chakraborty, Janardanan, D.; Mobin, S. M.; Sunoj, R. B; Lahiri, G. K. *Eur. J. Inorg. Chem*, **2007**, *2*, 314.

4. (a) Pierpont, C. G.; Lange, C. W. *Prog. Inorg. Chem.* **1994**, *41*, 331. (b) Kar, S.; Sarkar, B.; Ghumaan, S.; Janardanan, D.; Slageren, Fiedlar, J. V.; Puranik, V. G.; Sunoj, R. B.; Kaim, W.; Lahiri, G. K. *Chem. Eur. J.* **2005**, *11*, 4901. (c) Vlcˇek Jr., A. *Comments Inorg. Chem.* **1994**, *16*, 207. (d) Salmonsen, R. B.; Abelleira, A.; Clarke, M. J. *Inorg. Chem.* **1984**, *23*, 387. (f) Haga, M.; Dodsworth, E. S.; Lever, A. B. P. *Inorg. Chem.* **1986**, *25*, 447. (g) Dei, A.; Gatteschi, D.; Pardi, L. *Inorg. Chem.* **1990**, *29*, 1443. (g) Pierpont, C. G.; Attia, A. S. *Collect. Czech. Chem. Commun.* **2001**, *66*, 33 (i) Pierpont, C. G. *Coord. Chem. Rev.* **2001**, *219–221*, 415. (j) Rall, J.; Wanner, M.; Albrecht, M.; Hornung, F. M.; Kaim, W. *Chem. Eur. J.* **1999**, *5*, 2802. (k) Speier, G.; Whalen, A.; Csihony, J.; Pierpont, C. G. *Inorg. Chem.* **1995**, *34*, 1355. (l) Kasack, V.; Kaim, W.; Binder, H.; Jordanov, J.; Roth, E. *Inorg. Chem.* **1995**, *34*, 1924. (m) Ebadi, M.; Lever, A. B. P. *Inorg. Chem.* **1999**, *38*, 467. (n) Verani, C. N.; Gallert, S.; Bill, E.; Weyhermüller, T.; Wieghardt, K.; Chaudhuri, P. *Chem. Commun.* **1999**, 1747. (o) Chaudhuri, P.; Verani, C. N.; Bill, E.; Bothe, E.; Weyhermüller, T.; Wieghardt, K. *J. Am. Chem. Soc.* **2001**, *123*, 2213. (p) Chun, H.; Bill, E.; Bothe, E.; Weyhermüller, T.; Wieghardt, K. *Inorg. Chem.* **2002**, *41*, 5091. (q) Ghosh, P.; Begum, A.; Herebian, D.; Bothe, E.; Hildenbrand, K.; Weyhermüller, T.; Wieghardt, K. *Angew. Chem. Int. Ed.* **2003**, *42*, 563. (r) Min, K. S.; Weyhermüller, T.; Wieghardt,

K. *Dalton Trans.* **2003**, 1126. (s) Patra, S.; Sarkar, B.; Ghumaan, S.; Fiedler, J.; Zalis, S.; Kaim, W.; Lahiri, G. K. *Dalton Trans.* **2004**, 750. (t) Gorelsky, S. I.; Lever, A. B. P. *J. Organomet. Chem.* **2001**, *635*, 187. (u) Gorelsky, S. I.; Dodsworth, E. S.; Lever, A. B. P.; Vlcek, A. A. *Coord. Chem. Rev.* **1998**, *174*, 469. (v) Lever, A. B. P.; Gorelsky, S. I. *Coord. Chem. Rev.* **2000**, *208*, 153. (w) Cunha, C. J.; Dodsworth, E. S.; Monteiro, M. A.; Lever, A. B. P. *Inorg. Chem.* **1999**, *38*, 5399. (x) Metcalfe, R. A.; Lever, A. B. P. *Inorg. Chem.* **1997**, *36*, 4762. (y) Boone, S. R.; Pierpont, C. G. *Inorg. Chem.* **1987**, *26*, 1769.

5. Bag, N.; Lahiri, G. K.; Basu, P.; Chakravorty, A. *J. Chem. Soc., Dalton Trans.* **1992**, 113.
6. Wada, T; Yamanaka, M.; Fujihara, T.; Miyazato, Y.; Tanaka, K. *Inorg. Chem.* **2006**, *45*, 8887.
7. Kurihara, M.; Daniele, S.; Tsuge, K.; Sugimoto, H.; Tanaka, K. *Bull. Chem. Soc. Jpn.* **1998**, *71*, 867.
8. Bhattacharya, S. *Polyhedron* **1994**, *13*, 451.
9. Elias, B.; De Masmaeker, A. K. *Coord. Chem. Rev*. **2006**, *250*, 1627.
10. (a) Ray, K.; Begum, A.; Weyhermüller, T.; Piligkos, S.; van Slageren, J.; Neese, F.; Wieghardt, K. *J. Am. Chem. Soc.* **2005**, *127*, 4403.
11. (a) Bachler, V.; Olbrich, G.; Neese, F.; Wieghardt, K. *Inorg. Chem.* **2002**, *41*, 4179. (b) Tao, J.; Maruyama, H.; Sato, O. *J. Am. Chem. Soc.* **2006**, *128*, 1790.
12. (a) Bhattacharya, S.; Gupta, P.; Basuli, F.; Pierpont, C. G. *Inorg. Chem.* **2002**, *41*, 5810. (b) Pierpont, C. G.; Atta, A. S. *Collect. Czech. Chem. Commun.* **2001**, *66*, 33.
13. (a) DeLearie, L. A.; Haltiwanger, R. C.; Pierpont, C. G. *Inorg. Chem.* **1989**, *28*, 644. (b) Karsanov, I. V.; Ivakhnenko, Y. P.; Khandkarova, V. S.; Prokofev, A. I.; Rubezhov, A. Z.; Kabachnik, M. I. *J. Organomet. Chem.* **1989**, 379, 1. (c) Bhattacharya, S.; Pierpont , C. G.; *Inorg. Chem*. **1992**, *31*, 2020. (d) Bhattacharya, S.;

Pierpont, C. G. *Inorg. Chem.* **1994**, *33*, 6038. (e) Whalen, A. M.; Bhattacharya, S.; Pierpont, C. G. *Inorg. Chem.* **1994**, *33*, 347. (f) Speier, G.; Whalen, A. M.; Csihony, J.; Pierpont, C. G. *Inorg. Chem.* **1995**, *34*, 1355. (g) Speier, G.; Whalen, A. M.; Csihony, J.; Pierpont, C. G. *Inorg. Chim. Acta* **1996**, *245*, 1.

14. (a) Verani, C. N.; Gallert, S.; Bill, E.; Weyhermuller, T.; Weighardt, K.; Chaudhuri, P. *Chem. Commun*. **1999**, 1747. (b) Chaudhuri, P.; Verani, C. N.; Bill, E.; Weyhermuller, T.; Weighardt, K. *J. Am. Chem. Soc.* **2001**, *123*, 2213. (c) Chun, H.; Verani, C. N.; Chaudhuri, P.; Bothe, E.; Bill, E.; Weyhermuller, T.; Weighardt, K. *Inorg. Chem.* **2001**, *40*, 4157. (d) Chun, H.; Weyhermuller, T.; Bill, E.; Weighardt, K. *Angew. Chem., Int. Ed. Engl.* **2001**, *40*, 2489. (e) Chun, H.; Chaudhuri, P; Weyhermuller, T.; Weighardt, K. *Inorg. Chem.* **2002**, *41*, 790. (f) Sun, X.; Chun, H.; Hildenbrand, K.; Bothe, E.; Weyhermuller, T.; Weighardt, K. *Inorg. Chem.* **2002**, *41*, 4295.

15. (a) Chanda, N.; Mobin, S. M.; Puranik, V. G.; Dutta, A.; Niemeyer, M.; Lahiri, G. K. *Inorg. Chem.* **2004**, *43*, 1056. (b) Mondal, B.; Puranik, V. G. ; Lahiri, G. K. *Inorg. Chem.* **2002**, *41*, 5831. (c) Chanda, N.; Mondal, B.; Puranik, V. G.; Lahiri, G. K. *Polyhedron* **2002**, *21*, 2033. (d) Mondal, B.; Paul, H.; Puranik, V. G. ; Lahiri, G. K. *J. Chem. Soc., Dalton Trans.* **2001**, 481. (e) Mondal, B.; Walawalkar, M. G.; Lahiri, G. K. *J. Chem. Soc., Dalton Trans.* **2000**, 4209. (f) Sarkar, S.; Sarkar, B.; Chanda, N.; Kar, S.; Mobin, S. M.; Fiedler, J.; Kaim, W.; Lahiri, G. K. *Inorg. Chem.* **2005**, *44*, 6092. (g) Chanda, N.; Paul, D.; Kar, S.; Mobin, S. M.; Dutta, A.; Puranik, V. G.; Rao, K. K.; Lahiri, G. K. *Inorg. Chem.* **2005**, *44*, 3499. (h) Patra, S.; Sarkar, B.; Ghumaan, S.; Patil, M. P.; Mobin, S. M.; Sunoj, R. B.; Kaim, W.; Lahiri, G. K. *Dalton Trans.* **2005**, 1188.

16. Singh, A.; Pramanik, A.; Das, G.; Mondal, B. *Organometaliics* **2008**, *27*, 6403 and unpublished work.

17. (a) Sans, C.; Rodriguez, M.; Romero, I.; Llobet, A. *Inorg. Chem.* **2003**, *42*, 8385. (b) Hartshorn, C. M.; Maxwell, K. A.; White, P. S.; DeSimone, J. M.; Meyer, T. J. *Inorg. Chem.* **2001**, *40*, 601. (c) Claustro, I.; Abate, G.; Sanchez, E.; Acquaye, J. H. *Inorg. Chim. Acta* **2003**, *342*, 29. (d) Ziessel, R.; Grosshenny, V.; Hissler, M.; Stroh, C. *Inorg. Chem.* **2004**, *43*, 4262. (e) Kobayashi, K.; Ohtsu, H.; Wada, T.; Kato, T.; Tanaka, K. *J. Am. Chem. Soc.* **2003**, *125*, 6729. (f) Bonnefous, C.; Chouai, A.; Thummel, R. P. *Inorg. Chem.* **2001**, *40*, 5851. (g) Rack, J. J.; Winkler, J. R.; Gray, H. B. *J. Am. Chem. Soc.* **2001**, *123*, 2432. (h) Hadadzadeh, H.; DeRosa, M. C.; Yap, G. P. A.; Rezvani, A. R.; Crutchley, R. J. *Inorg. Chem.* **2002**, *41*, 6521. (i) Gerli, A.; Reedijk, J.; Lakin, M. T.; Spek, A. L. *Inorg. Chem.* **1995**, *34*, 1836.

18. Gorelsky, S. I.; Lever, A. B. P.; Ebadi, M. *Coord. Chem. Rev.* **2002**, *230*, 97.

19. (a) Wright, T. C.; Wilkinson, G.; Motevalli, M.; hursthouse, M. B.; *J. Chem. Soc., Dalton Trans.* **1986**, 2017 (b) McGilligan, B. S.; Wright, T. C.; Wilkinson, G.; Motevalli, M.; Hursthouse, M. B. *J. chem. Soc., Dalton Trans.* **1988**, 1737.

20. (a) Bhattacharya, S.; Pierpont, C. G. *Inorg. Chem.* **1991**, *30*, 1511. (b) Bhattacharya, S.; Pierpont, C. G. *Inorg. Chem.* **1992**, *31*, 2020.

21. Nakamoto, K. *Infrared and Raman Spectra of Inorganic and Coordination Compounds*, *Part B*, 5th Ed. John Wiley and sons, Inc. **1997**, p113-116.

22. Wright, T. C.;Wilkinson, G.; Motevalli, M.; Hursthouse, M. B. *J. Chem. Soc., Dalton Trans.* **1986**, 2017.

23. Ghuman, S.; Kar, S.; Mobin, S. M.; Harish, B.; Puranik, V. D.; Lahiri, G. K. *Inorg. Chem.* **2006**, *45*, 2413.

24. (a) Mastone, J.; Armor, J. N. *Inorg. Nucl. Chem.* **1975**, *37*, 473. (b) Gomes, M. G.; Draranzo, C. V.; Silws, S. C.; Lopez, L. G. F.; Santos, P. S.; Franco, D. W.; *J. Chem. Soc., Dalton Trans*. **1998**, 601.

25. Ebadi, M.; Lever, A. B. P. *Inorg. Chem.* 1**999**, *38*, 467.

26. Addison, A. W.; Burke, P. J. *J. Heterocycl. Chem*. **1981**, *12*, 4455.

27. Haga, M.; Kato, N.; Monjushiro, H.; Wang, K.; Hossain, M. D. *Supramol. Sci.* **1998**, *5*, 337.

28. SMART, SAINT and XPREP, Siemens Analytical X-ray Instruments Inc., Madison, Wisconsin, USA, **1995**.

29. Sheldrick, G. M. SADABS: software for Empirical Absorption Correction, University of Gottingen, Institut fur Anorganische Chemieder Universitat, Tammanstrasse 4, D-3400 Gottingen, Germany, **1999–2003**.

30. Sheldrick, G. M. SHELXS-97, University of Gottingen, Germany, **1997**.

31. Farrugia, L. J. *J. Appl. Crystallogr.* **1997**, *30*, 565.

Abstract

Ruthenium complexes [Ru^{II}(bbp)(L_1)(CH_3CN)] (**6**) and [Ru^{III}(bbp)(L_2)(CH_3CN)] (**7**) [bbp: 2,6-*bis*(benzimidazol-2-yl)pyridine; L_1: semiquinonate form of 1,2-dihydroquinone; L_2: acetylacetonate] have been synthesized by the reaction of Ru(bbp)Cl_3 with catechol and acetylacetone. Both the complexes have been characterized by Mass, UV-visible, FT-IR, NMR and EPR spectroscopic techniques as well as elemental analysis, solution conductivity and cyclic voltammetry. It has been observed from the spectral studies that complex **6** is having Ru^{II}-sq valence state configuration with mono-anionic bbp whereas in complex **7**, it exists as Ru^{III}-acac with di-anionic bbp ligand.

4.1 Introduction

Redox-active ligands, sometimes termed as "non-innocent", can bind the transition metal ions in different formal oxidation states.[1,2] Transition metal complexes with redox-active ligands are found to be important in many redox processes, in particular when the transfer of more than one electron is required, for example in certain metalloenzymes.[3] In principle, the redox-active ligands (L) may exist in three oxidation states, neutral quinone (L), anionic semiquinonate ($L^{\bullet-}$), and dianionic catecholate (L^{2-}). The possible change in ligand oxidation state makes it difficult to assign unambiguous "physical" oxidation numbers to the metal center.[4] In open-shell cases, EPR spectroscopy has often been used to estimate the spin distribution from experimental data, and to subsequently assign oxidation numbers. It has been reported that the ruthenium complexes with monoanionic catecholate(cat) and acetylacetonate(acac), the formulation with an oxidation state Ru^{II} or Ru^{III} is most appropriate.[5] Tanaka et al. reported the experimental and theoretical studies on the electronic structures of a series of ruthenium complexes [Ru(OAc)-(dioxolene)(trpy)] (OAc = acetate) having various substituents on the dioxolene.[6,7] Meyer et al. and Pierpont et al. have extensively studied ruthenium-dioxolene complexes.[8,9]

This chapter presents the valence state distribution in [Ru(bbp)(L_1)(CH_3CN)] (**6**) and [Ru(bbp)(L_2)(CH_3CN)] (**7**) and a comparison of their spectral and electrochemical properties.

4.2 Results and Discussion

A set of two complexes, [Ru(bbp)(L_1)(CH_3CN)] (**6**) and [Ru(bbp)(L_2)(CH_3CN)] (**7**) [L_1 = semiquinone form of catechol; L_2 = acetylacetonate] have been synthesized to study the variation of their physicochemical properties depending on the ancillary ligands. The complexes **6** and **7** were prepared by the reaction of Ru(bbp)Cl_3 with the

respective ligands (catechol and acetylacetone in case of complexes **6** and **7**, respectively) in ethanolic medium (Scheme 4.1) followed by chromatographic separation using silica gel column and CH_3CN/CH_3OH (4:1) solvent mixture.

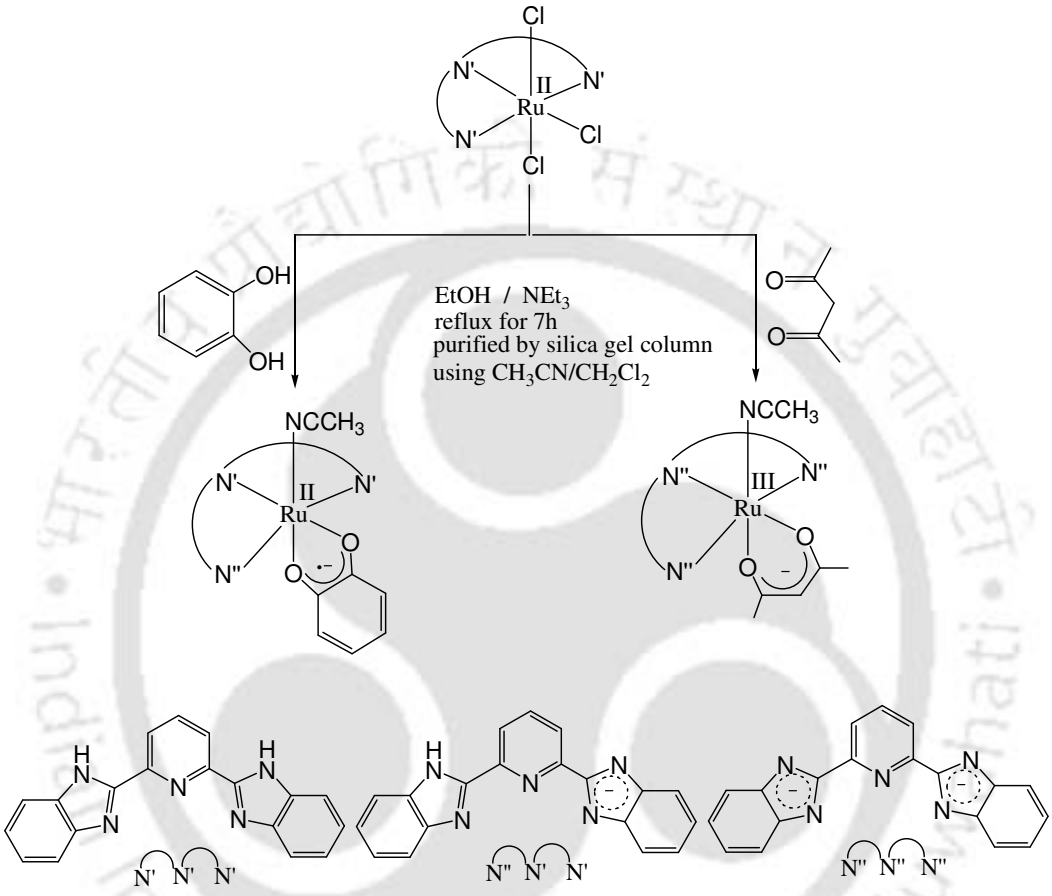

Scheme 4.1

Both the complexes were isolated as neutral molecules. They exhibit satisfactory microanalysis (see Experimental Section).

4.2.1 Mass Spectroscopy

In the electrospray mass spectra, the (m+1) molecular ion peaks for complexes **6** and **7** appear at 560.98 and 540.08, respectively (Figures 4.1), which support the formation of the complexes.

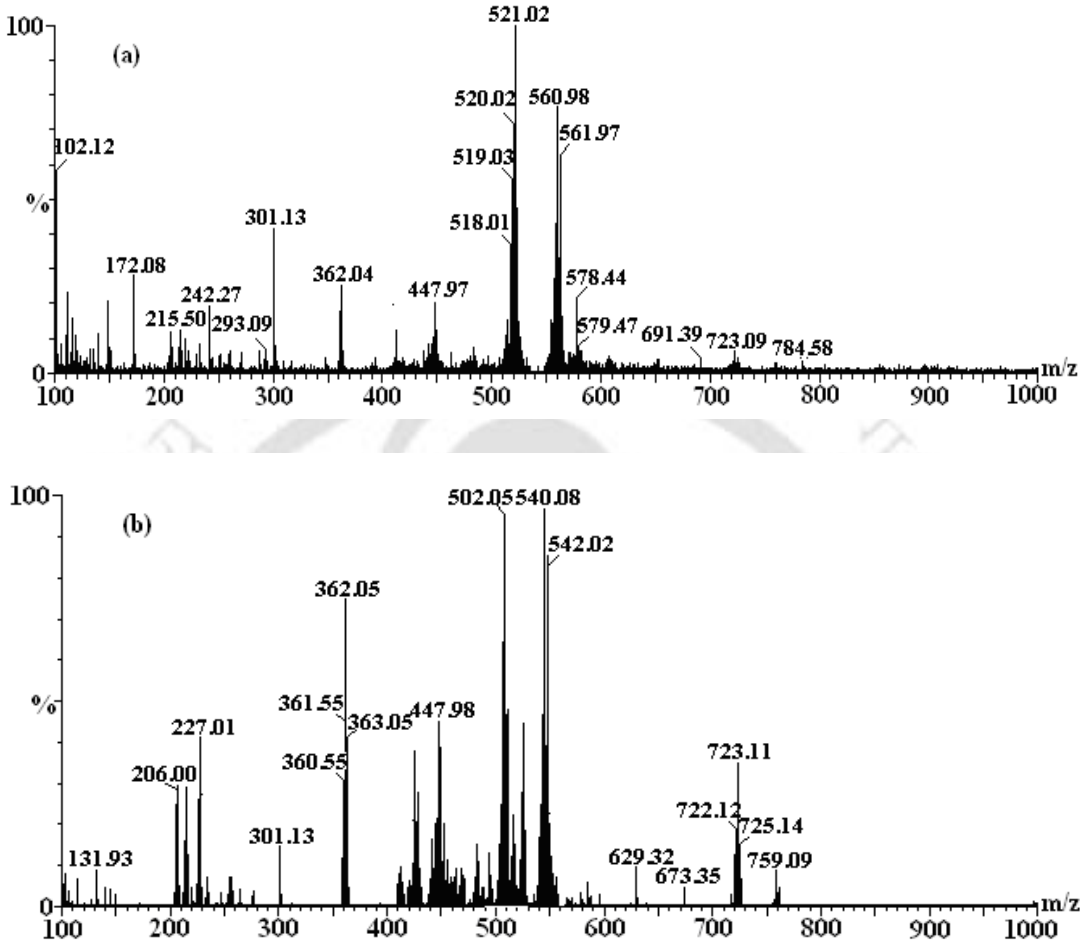

Figure 4.1: ESI-mass spectra of complexes (a) **6** and (b) **7** in acetonitrile with 0.1% formic acid.

Though the actual valence state configuration in complex **7** is quite straight forward, in complex **6**, it could be either Ru^{II}(*sq*) or Ru^{III}(*cat*) or lies between these two resonance forms (Scheme 4.2). The EPR and cyclic voltammetric studies have been used to assign the actual valence state in complex **6**.

Scheme 4.2

4.2.2 ^{1}H-NMR Spectroscopy

Both the complexes exhibit broad and unresolved signals in ^{1}H-NMR spectra. This is because of the presence of paramagnetic centres in both complexes **6** and **7**.

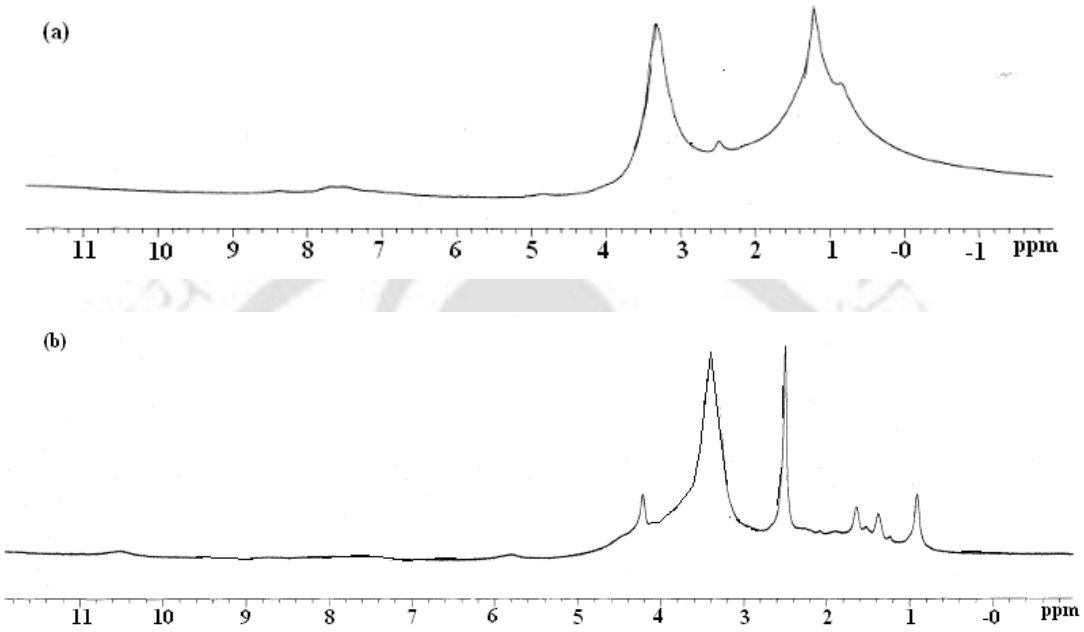

Figure 4.2: ^{1}H-NMR spectra of complexes (a) **6** and (b) **7** in $(CD_3)_2SO$ solvent

In magnetic moment measurement, both the complexes display magnetic susceptibility corresponding to one unpaired electron.

4.2.3 EPR Spectroscopy

One of the most powerful techniques to investigate the electronic structure of the transition metal dioxolene complexes is EPR spectroscopic study of the frozen solution. The amount of spin on the metal can be determined by the anisotropy of the g tensor ($\Delta g = g_1 - g_3$) whereas the isotropic g factor indicates the deviation from the value for the free electron ($g = 2.0023$) as well as for the free semiquinonate radicals ($g = 2.005$). The X-band EPR spectrum of the frozen solution of complex **6** shows an

isotropic signal with g = 2.103 at 77K (Figure 4.3). The higher g value from the free semiquinonato anion radical indicates the partial mixing of the metal *d*-orbital with the molecular orbitals from catechol moiety which are of comparable energy. Hence for complex **6**, one could think of a Ru^{II}-sq charge distribution. The complex **7** exhibits a broad signal at g = 2.284 with a degree of anisotropic character (Figure 4.4).

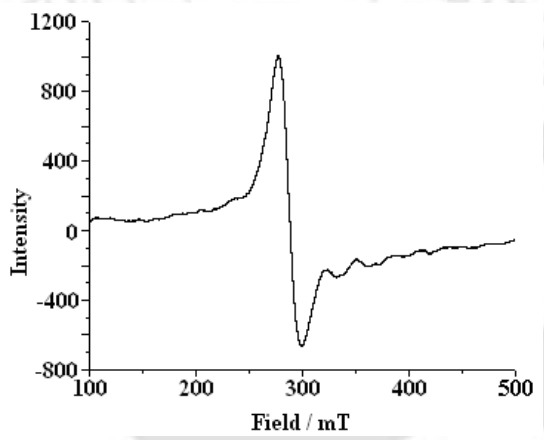

Figure 4.3: X-band EPR spectrum for complex **6** in acetonitrile/toluene at 77K.

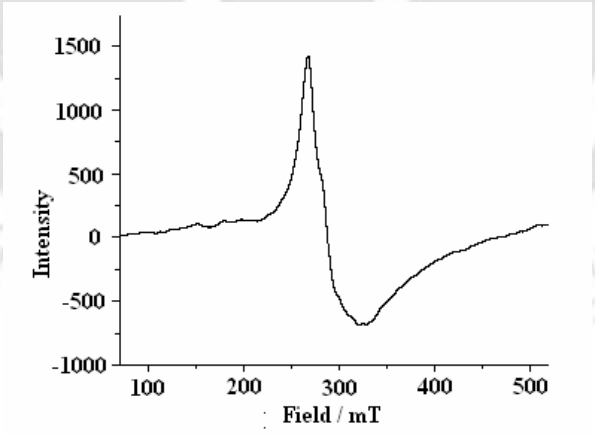

Figure 4.4: X-band EPR spectrum for complex **7** in acetonitrile/toluene at 77K.

This unresolved anisotropic signal indicates the presence of the unpaired electron on the metal center. Hence in complex **7**, the Ru(III)-acetylacetonato charge distribution is more probable.

4.3.4 UV-visible Spectroscopy

UV-visible spectra of both the complexes **6** and **7** were recorded in acetonitrile solvent and figure 4.5 exhibits the respective spectra. Complex **6** exhibits strong electronic absorptions at $\lambda_{max/nm}(\varepsilon/dm^3mol^{-1}cm^{-1})$: 312(17360), 343(18770), 445(4640) and 890(3780) nm. The 890 nm band is attributed to the charge transfer transition within the Ru-dioxolene framework which is comparable to the 850 nm band of $[Ru(^tBu_2Sq)(bpy)_2]^+$ {$^tBu_2Sq$: 3,5-di-*tert*-butylbenzosemiquinone}and 883 nm band of $[Ru(OAc)(3,5\text{-}^tBu_2C_6H_2O_2)(trpy)]$.[6] {$3,5\text{-}^tBu_2C_6H_2O_2$: 3,5-di-*tert*-butylcatechol). This band has been assigned as the MLCT transition band by Lever and co-workers.[10] Wada et al reported that this charge transfer transition is related to the bonding π-orbital [dπ(Ru) + π^*(sq), singly occupied molecular orbital] and antibonding π^* orbital [dπ(Ru) - π^*(sq), lowest unoccupied molecular orbital (LUMO)] and hence the intensity of the band depends on the degree of mixing between dπ(Ru) and π^*(sq) in the ground and excited states.[6] Complex **7**, exhibits a number of intense transitions at $\lambda_{max/nm}(\varepsilon/dm^3mol^{-1}cm^{-1})$: 309(22327), 334(24745), 349(29218) and 476(5803) nm. These transitions are because of the presence of different acceptor levels of the bbp and acetylacetonato ligand. The lowest energy band at 476 nm can be assigned as the ligand to metal charge transfer transitions involving bbp and acac based acceptor levels to Ru(III). In both the cases, the strong transitions in the UV region are believed to originate from the intra ligand $\pi \rightarrow \pi^*$ transitions.

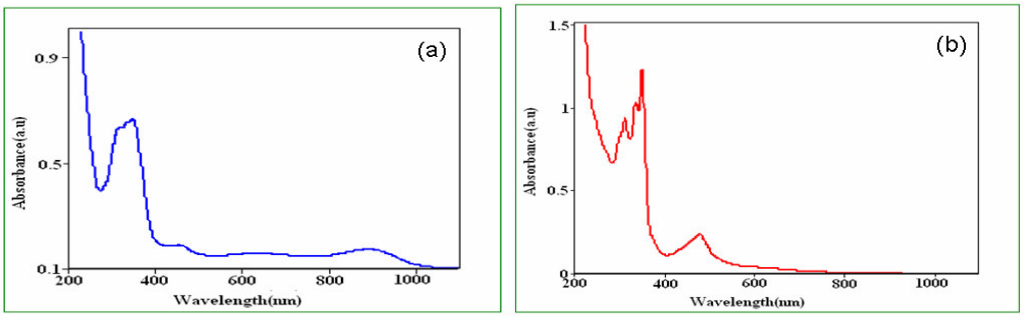

Figure 4.5: UV-visible spectra of complexes (a) **6** and (b) **7** in acetonitrile solvent.

4.2.5 Electrochemical studies

The redox properties of the complexes **6** and **7** have been studied by cyclic voltammetry in acetonitrile solvent. The cyclic voltammogram of complex **6** exhibits the two quasi-reversible couples in both the positive and negative side of SCE (Figure 4.6). One electron nature of all the couples were established by constant potential coulometric study. The couple I at 0.91 V *vs* SCE is assigned to the Ru^{II}/ Ru^{III} process. The same couple appears at 0.94 V *vs* SCE in case of [Ru(trpy)(oxolene)Cl] complex.[11] Couple II at 1.13 V has been assigned for the *sq/q* oxidation. This assignment is in well agreement with the earlier reported *sq/q* oxidation processes in ruthenium complexes with various ancillary ligands.[11,12]

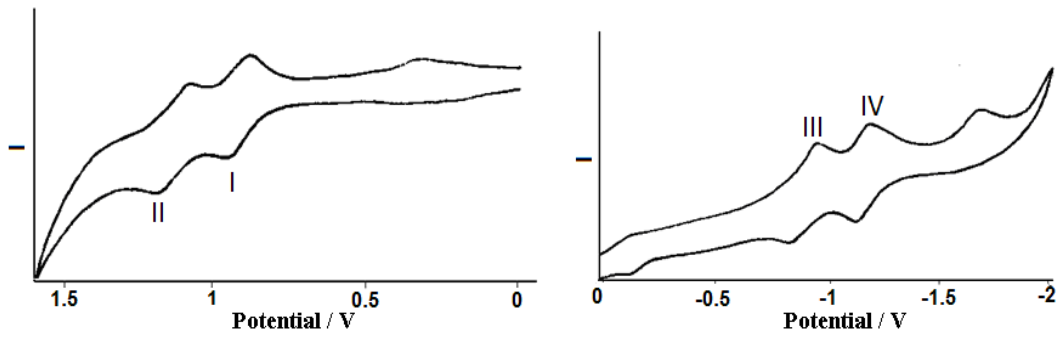

Figure 4.6: Cyclic voltammograms for complex **6** *vs* SCE (0.1M TBAP) at 50 mv/s in acetonitrile solvent (SCE: Reference electrode; Glassy Carbon: Working electrode).

Couples III and IV in the negative side of SCE are attributed to the *sq/cat* and bbp-based reductions, respectively. In case of complex **7**, the couple appears at 0.82 V *vs* SCE is assigned to the Ru^{III}/Ru^{IV} process and the Ru^{III}/Ru^{II} reduction appears at -0.71 V (Figure 4.7). The low potential for both the couple in case of complex **7** can be attributed to the better σ-donor ability of the dianionic bbp and acetylacetonate ligand. The low reduction potential value of the Ru^{III}/Ru^{II} couple suggests the higher stability of the Ru^{III}-acac state in complex **7**. The couple at -1.71 V is assigned to the bbp ligand based reduction.

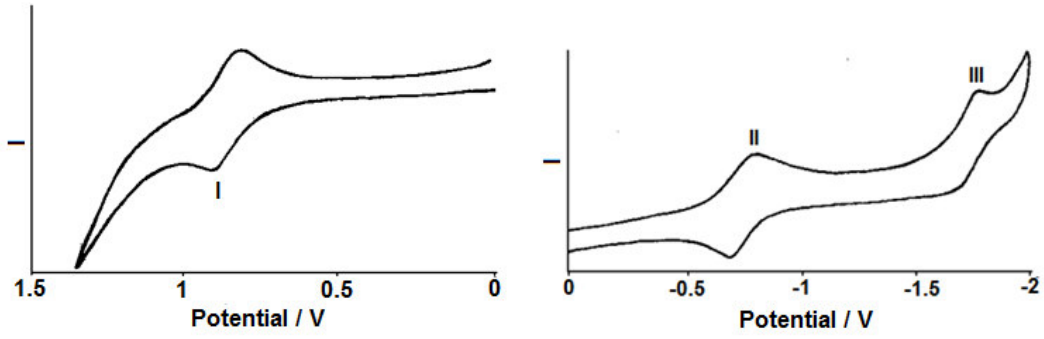

Figure 4.7: Cyclic voltammograms for complex **7** *vs* SCE (0.1M TBAP) at 50 mv/s in acetonitrile solvent (SCE: Reference electrode Glassy Carbon: Working electrode).

4.2.6 FT-IR Spectroscopy

The FT-IR spectra have been recorded in KBr pellets. A sharp band has been observed at ~1725 cm^{-1} in both complexes. This band is attributed to the nitrile frequency of the metal coordinated acetonitrile in the complexes. It is interesting to note that this is appreciably lower than the expected ν(CN) for coordinated nitriles. This low frequency might be an indication either of an unusual strong π-back bonding or the involvement of its η^2-bonding.[13] The later was observed in $[Mo(Cp)_2(CH_3CN)]$, which exhibits the ν(CN) at 1725 cm^{-1}.[14]

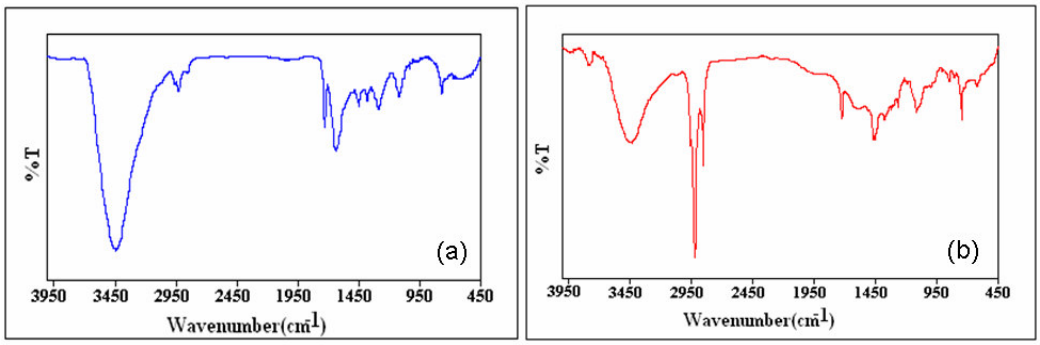

Figure 4.8: FT-IR spectra of complexes **6** and **7** in KBr pellets.

4.3 Conclusion

In conclusion, the present chapter demonstrated the synthesis and spectral characterization of two ruthenium-bbp complexes, **6** and **7,** with catecholate and acetylacetonate ligand, respectively. The complex **6** shows isotropic signal (g = 2.103) in X-band EPR spectra at 77K and complex **7** shows an unresolved broad signal with an appreciable degree of anisotropic character indicating the presence of paramagnetic center on the metal center. In case of complex **6**, Ru^{II}-sq valence state distribution is assigned based on EPR spectroscopy and cyclic voltammetric studies; whereas, in complex **7**, the metal is present in Ru^{III} state.

4.4 Experimental Section

4.4.1 General

All reagents and solvents were purchased from commercial sources and were of reagent grade. Acetonitrile was distilled from calcium hydride. UV-visible spectra were recorded on a Perkin Elmer Lambda-25 spectrophotometer. FT-IR spectra were taken on a Perkin Elmer spectrophotometer with samples prepared as KBr pellets. Solution electrical conductivity was checked using a Systronic 305 conductivity bridge. ^{1}H-NMR spectra were obtained with a 400 MHz Varian FT spectrometer. Chemical shifts (ppm) were

referenced to the residual solvent peaks. Elemental analyses were obtained from a Perkin Elmer Series II Analyzer. The X-Band Electron Paramagnetic Resonance (EPR) spectra of the complex **6** and 7 were recorded on a JES-FA 200 ESR spectrometer, at 77K.

4.4.2 Synthesis of complex 6

The $Ru(bbp)Cl_3$ (300 mg, 0.59 mmol) and 1,2-dihydroxyquinone (64 mg, 0.39 mmol) is taken in 20 ml of ethanol and added NEt_3 (0.4 ml) and heated to reflux for 5h. Then the volume of reaction mixture was reduced to 5 ml and it was kept in freezer for overnight. The solid precipitate thus obtained was filtered off and washed with cold water. The product was dried in vacuo over P_2O_5. It was then purified by using silica gel column by using (1:1) CH_3CN/CH_3OH as eluent. Evaporation of the solvent under reduced pressure afforded a pure solid. Yield 210 mg (70%) Anal. Calcd.(%): $C_{27}H_{18}N_6O_2Ru$: C: 57.75; H: 3.59; N: 14.97. Found (%) C: 57.79; H: 3.58; N: 14.98. ESI-mass (m/z): 560.98.

4.4.3 Synthesis of complex 7

The $Ru(bbp)Cl_3$ (300 mg, 0.59 mmol) and acetylacetone (39 mg, 0.59 mmol) were taken in 20 ml of ethanol and added NEt_3 (0.4 ml) and heated to reflux for 9h. The volume of reaction mixture was then reduced to 5 ml and the solution was kept in freezer for overnight to get solid precipitate which was then filtered off and washed with cold distilled water. The product was dried in vacuo over P_2O_5. It was then purified by using silica gel column by using (1:1) CH_3CN/CH_3OH as eluent. Removal of the solvent under reduced pressure afforded a pure solid. Yield 225 mg (85%) Anal. Calcd.(%): $C_{25}H_{20}N_6O_2Ru$: C: 55.86; H: 3.75; N: 15.63. Found (%) C: 55.84; H: 3.76; N: 15.67. Mass spectral data, (m/z): 540.08.

4.5 References

1. Jo¨rgensen, C. K. *Oxidation Numbers and Oxidation States*; Springer: Heidelberg, Germany, **1969**.

2. Ward, M. D.; McCleverty, J. A. *J. Chem. Soc., Dalton Trans.* **2002**, 275.

3. Kaim, W.; Schwederski, B. *Pure Appl. Chem.* **2004**, *76*, 351 and references therein.

4. For a discussion on the distinction between formal and physical oxidation numbers in complexes with "non-innocent" ligands: Chaudhuri, P.; Verani, C. N.; Bill, E.; Bothe, E.; Weyhermu¨ller, T.; Wieghardt, K. *J. Am. Chem. Soc.* **2001**, *123*, 2213 and references therein

5. (a) Patra, S.; Sarkar, B.; Mobin, S. M.; Kaim, W.; Lahiri, G. K. *Inorg. Chem.* **2003**, *42*, 6469. (b) Masui, H.; Lever, A. B. P.; Auburn, P. A. *Inorg. Chem.* **1991**, *30*, 2402. (c) Das, C.; Kamar, K. K.; Ghosh, A. K.; Majumdar, P.; Hung, C.-H.; Goswami, S. *New J. Chem.* **2002**, *26*, 1409.

6. Wada, T.; Yamanaka, M.; Fujihara, T.; Miyazato, Y.; Tanaka, K. *Inorg. Chem.* **2006**, *45*, 8887.

7. Sugimoto, H.; Tanaka, K. *J. organomett. Chem.* **2001**, *622*, 280.

8. (a) Haga, M; Dodsworth, E. S; Lever, A. B. P. *Inorg. Chem.* **1986**, *25*, 447. (b) Masui, H.; Lever, A. B. P.; Auburn, P. R. *Inorg. Chem.* **1991**, *30*, 2402. (c) da Cunha, C. J.; Fielder, S. S.; Stynes, D. V.; Masui, H.; Auburn, P. R.; Lever, A. B. P. *Inorg. Chim. Acta* **1996**, *242*, 293.

9. (a) Bhattacharya, S.; Boone, S. R.; Fox, G. A.; Pierpont, C. G. *J. Am. Chem. Soc.* **1990**, *112*, 1088. (b) Haga, M.; Isobe, K.; Boone, S. R.; Pierpont, C. G. *Inorg. Chem.* **1990**, *29*, 3795. (c) Boone, S. R.; Pierpont, C. G. *Inorg. Chem.* **1987**, *26*, 1769.

10. Ebadi, M.; Lever, A. B. P. *Inorg. Chem.* **1999**, *38*, 467.

11. Maji, S.; Patra, S.; Chakraborty, Janardanan, D. ; Mobin, S. M. ; Sunoj, R. B; Lahiri, G. K. *Eur. J. Inorg. Chem*, **2007**, *2*, 314.

12. Masui, H.; Lever, A. B. P.; Dodsworth, E. S. *Inorg. Chem.* **1993**, *32*, 258.

13. Nakamoto, K. *Infrared and Raman Spectra of Inorganic and Coordination Compounds*, *Part B*, 5th Ed. John Wiley and sons, Inc. **1997**, p113-116.

14. (a) Wright, T. C.; Wilkinson, G.; Motevalli, M.; hursthouse, M. B.; *J. Chem. Soc., Dalton Trans.* **1986**, 2017. (b) McGilligan, B. S.; Wright, T. C.; Wilkinson, G.; Motevalli, M.; Hursthouse, M. B. *J. Chem. Soc., Dalton Trans.* **1988**, 1737.

Abstract

A ruthenium complex, [Ru^{II}(bbp)(L)(CH_3CN)] (**3a**) [L: *o*-phenylenediamine], has been synthesized and characterized by various spectroscopic and analytical techniques as well as by single crystal X-ray structure. The coordinated acetonitrile is found to be reduced to ethylamine in the presence of *p*-phenylenediamine or hydroquinone. The reduced product, complex **8**, has been characterized by spectroscopic studies and single crystal X-ray structure determination.

5a.1 Introduction

The reduction of the coordinated acetonitrile (-$N_\alpha \equiv C_\beta - CH_3$) to acetimidoyl [$\eta^2$-N(H)=C–$CH_3$; bonded through N_α and C_β], ethylidenimido [η^2-N=CH–CH_3],[1] azavinylidenyl [-N=CH–CH_3],[2] imino [-NH=CH–CH_3],[2-3] ethylimido [≡N–CH_2–CH_3],[4] ethylamido [-NH–CH_2–CH_3][2] and aza-allylic [η^3-CH_2–CH–NH_2][5] ligands are well documented in the literature. In all cases, the reductions are carried out either by hydrogen[6] or by hydride[7] sources (e.g. NaH, $NaBH_4$, $LiAlH_4$, $LiHBEt_3$ etc.).[8] There is also precedence for the protonation of acetonitrile complexes by HCl or $HBF_4.Et_2O$. This protonation leads to the oxidation of electron rich metal center to form ethylimido[9] or imino complexes.[5] In some cases, hydride formation also takes place.[10] Meyer et al. have reported an example of reversible $2e^-/2H^+$ reduction of coordinated acetonitrile to the corresponding imine in Os^{III}-sulfilimido complexes.[11]

This chapter demonstrates the reduction of coordinated acetonitrile to ethylamine in [Ru^{II}(bbp)(L)(CH_3CN)] (**3a**) [L : *o*-phenylenediamine] in presence of *p*-phenylenediamine or hydroquinone (**Scheme 5a.1**).

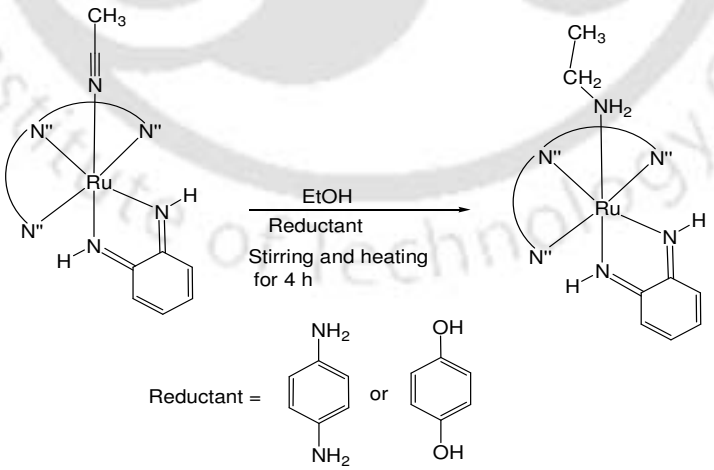

Scheme 5a.1

5a.2 Results and Discussion

Complex **3a** has been prepared by refluxing an ethanolic solution of [Ru(bbp)Cl_3] in presence of equivalent amount of *o*-phenylenediamine followed by chromatographic separation with acetonitrile:dichloromethane solvent mixture (see Chapter 3). The neutral, nonconducting complex **3a** shows the (m + 1) molecular ion peak at 558.67 in the positive ion ESI-mass spectrum. The complex **3a**, on refluxing with three equivalent of *p*-phenylenediamine in ethanol solvent for 4h, afforded a dark color solution. The solvent was then dried and the dark colored solid mass, on chromatographic purification using silica gel column, yields the complex **8** (yield ~ 70%) (Scheme 5a.1). In the positive ion ESI mass spectrum, the (m+1) molecular ion peak appears at 562.74 which indicates the reduction of coordinated acetonitrile to ethylamine (Figure 5a.1).

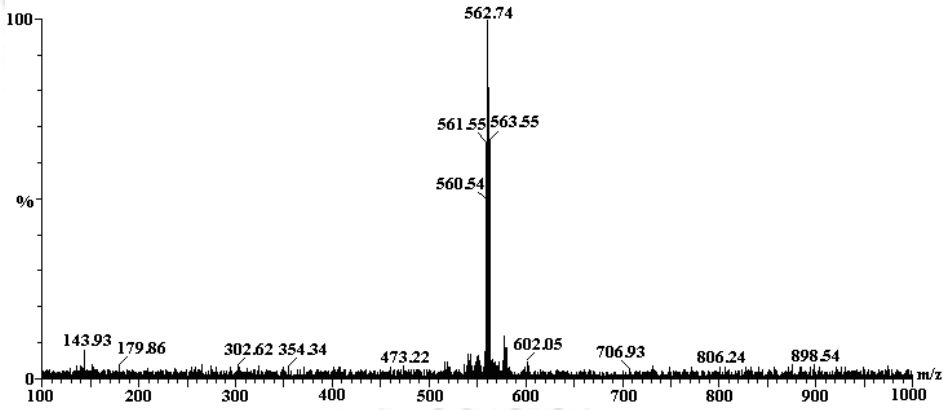

Figure 5a.1: ESI-mass spectrum of complex **8** in CH_3CN:H_2O(50:50) with 0.1% formic acid.

5a.2.1 X-ray Crystallography

The single crystal X-ray structure of complex **3a** has been discussed in chapter 3. The formation of the complex **8** has been confirmed from the single crystal X-ray structure determination (Figure 5a.2). The crystal structure reveals that the bbp ligand is

bonded to the metal in di-anionic form and the ancillary ligand, *o*-phenylenediamine is present in neutral iminoquinone form. The bond distances are comparable with that of reported quinone form of *o*-phenylenediamine ligand [Ru(1)-N(7), 1.967(5) Å; Ru(1)-N(6), 1.980(5) Å; N(6)-C(20), 1.323(8) Å; N(7)-C(25), 1.326(7) Å; C(21)-C(22), 1.310(11) Å; C(22)-C(23), 1.414(11) Å; C(23)-C(24), 1.350(10) Å; C(24)-C(25), 1.425(9) Å; C(250-C(20), 1.450(8)Å].[12] The crystal data, important bond distances and angles are given in table 5a.1 and 5a.2, respectively. In complex **8**, the Ru-amine(N8) bond has been found to be elongated to 2.173(4) Å in comparision to Ru-nitrile bond {2.059(5)Å} in complex **3a**.

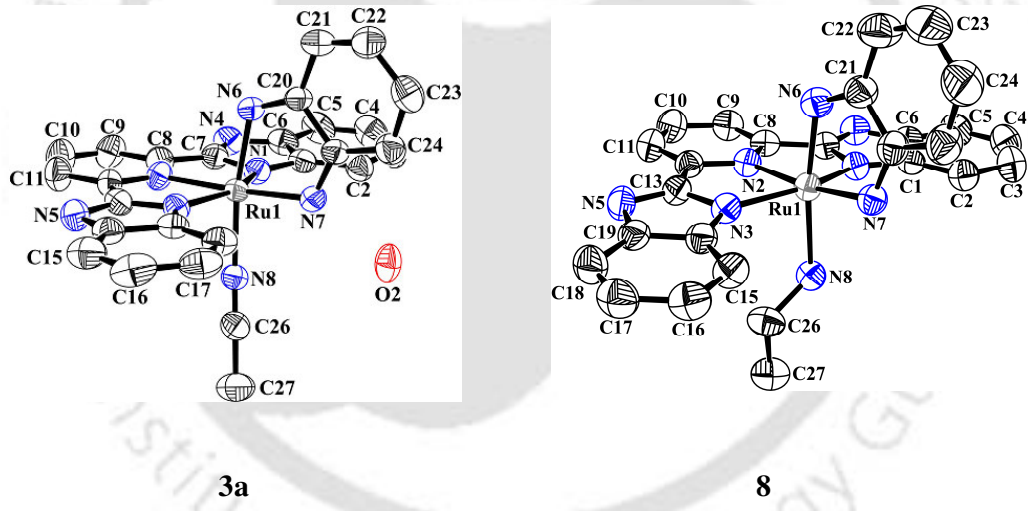

3a **8**

Figure 5a.2: ORTEP diagram of complexes **3a** and **8** (H atoms are removed for clarity)(50% thermal ellipsoids plot).

Table 5a.1: Crystallographic data for complex **8**

	8
Formulae	C_{27} H_{24} N_8 Ru
Mol. wt.	561.61
Crystal system	Monoclinic
Space group	C2/c
Temperature /K	296
Wavelength /Å	0.71073
a /Å	24.113(3)
b /Å	10.6297(11)
c /Å	23.011(2)
α/°	90.00
β/°	121.60
γ/°	90.00
V/ $Å^3$	5023.6(9)
Z	8
Density/Mgm^{-3}	1.485
Abs. Coeff. /mm^{-1}	0.656
F(000)	2288
Total no. of reflections	33440
Reflections, I > 2σ(I)	2149
Max. 2θ/°	26.63
Ranges (h, k, l)	-30 <= h <=30 -13 <= k <=13 -28 <= l <= 28
Complete to 2θ (%)	98.2
Refinement method	Full-matrix least-squares on F2
Data/ Restraints/Parameters	5203 / 0 / 334
WR2(all data)	0.0966
Goof (F2)	1.035
R indices [I > 2σ(I)]	0.0405
R indices (all data)	0.0662

Table 5a.2: Selected bond lengths (Å) and angles (º) of complex **8**

Bond lengths (Å)		**Bond angles (º)**	
Ru(1)-N(2)	2.027(4)	N(1)- Ru(1)-N(3)	153.77(15)
Ru(1)-N(3)	2.068(3)	N(1)- Ru(1)-N(8)	85.30(14)
Ru(1)-N(6)	1.993(4)	N(2)- Ru(1)-N(1)	77.25(14)
Ru(1)-N(7)	1.997(4)	N(2)- Ru(1)-N(3)	77.39(14)
Ru(1)-N(8)	2.173(4)	N(2)- Ru(1)-N(8)	92.70(14)
N(1)-C(1)	1.378(5)	N(3)- Ru(1)-N(1)	77.37(10)
N(1)-C(7)	1.362(6)	N(3)- Ru(1)-N(8)	92.67(13)
N(2)-C(8)	1.360(6)	N(6)- Ru(1)-N(1)	91.20(15)
N(2)-C(12)	1.368(5)	N(6)- Ru(1)-N(2)	93.27(15)
N(3)-C(13)	1.354(6)	N(6)- Ru(1)-N(3)	96.84(14)
N(3)-C(14)	1.378(6)	N(6)- Ru(1)-N(7)	78.33(15)
N(4)-C(6)	1.369(6)	N(6)- Ru(1)-N(8)	178.25(14)
N(4)-C(7)	1.327(5)	N(7)- Ru(1)-N(1)	102.02(14)
N(5)-C(13)	1.337(5)	N(7)- Ru(1)-N(2)	171.60(15)
N(5)-C(19)	1.368(6)	N(7)- Ru(1)-N(3)	103.05(14)
N(6)-C(21)	1.330(6)	N(7)- Ru(1)-N(8)	97.75(14)

5a.2.3 UV-visible Spectroscopy

UV-visible spectra of both complexes **3a** and **8** were recorded in acetonitrile solvent. The UV-visible spectrum of complex **3a** has been discussed in chapter 3. The complex **8** shows strong MLCT transition in the visible region and intra-ligand transitions in the UV region (Figure 5a.3). Complex **8**, $\lambda_{max/nm}(\varepsilon/dm^3mol^{-1}cm^{-1})$: 509(4350); 340(10191); 324(9813); 248(39429).

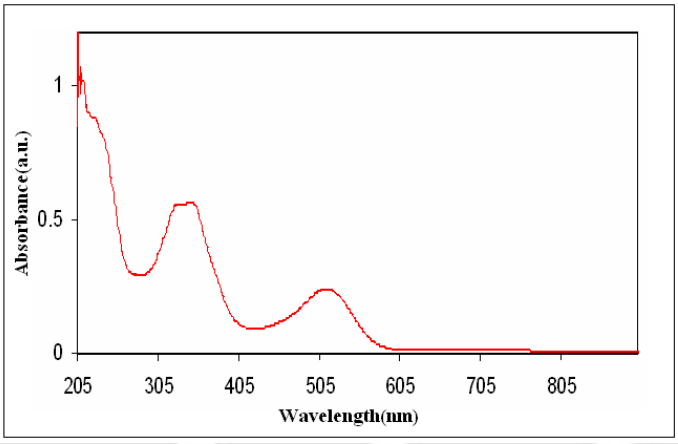

Figure 5a.3: UV-visible spectrum for complex **8** in acetonitrile solvent.

5a.2.3 FT-IR Spectroscopy

The reduction of the coordinated acetonitrile to ethylamine is supported by the FT-IR studies, also. The FT-IR spectra of the complexes were recorded in KBr pellets. The strong sharp band at 1725 cm^{-1} of complex **3a** is found to disappear in complex **8** (Figure 5a.4). This band is attributed to the nitrile frequency of the coordinated acetonitrile in complex **3a**. It is interesting to note that this is appreciably lower than the expected ν(CN) for coordinated nitriles. This extremely low frequency might be an indication either of an unusual strong π-back bonding or the involvement of its η^2-bonding.[14] The later was observed in [Mo(*Cp*)$_2$(CH_3CN)] , which exhibits the ν(CN) at 1725 cm^{-1}.[15] However, in the present case, the crystal structure of complex **3a** reveals that CH_3CN is bonded to the

metal in normal η^1-fashion through N atom, Ru(1)-N(8)-C(26), 172.45°. On the other hand, the Ru-$N_{acetonitrile}$ and C-$N_{acetonitrile}$ bond distances, 2.059 Å and 1.137Å, respectively. This C-$N_{acetonitrile}$ distance is longer than the normal C-N distance (~1.115Å) observed in case of coordinated acetonitrile.[16]

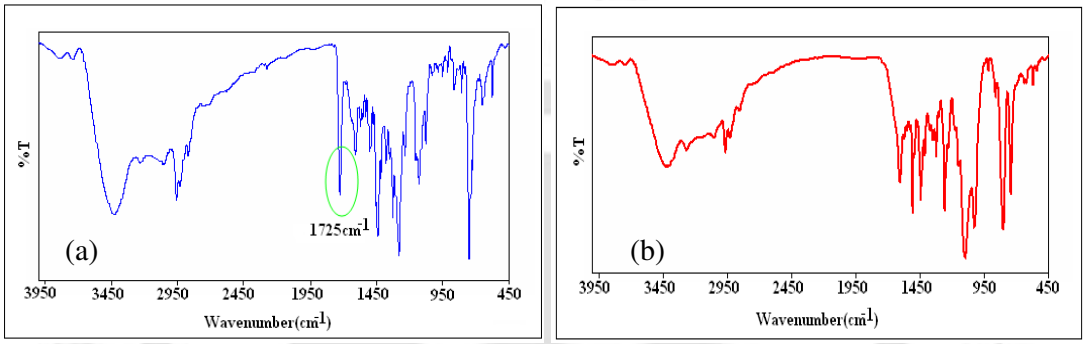

Figure 5a.4: FT- IR spectra of complexes (a) **3a** and (b) **8** in KBr pellets.

Hence this low ν(CN) can be attributed to the strong π-back bonding from the metal center to the acetonitrile. This π-back bonding ability is probably enhanced by the presence of the strong σ-donor ligands.

5a.2.4 ^{1}H-NMR Spectroscopy

The reduction of the coordinated acetonitrile to ethylamine is also confirmed by the ^{1}H-NMR studies. The ^{1}H-NMR spectra of complexes **3a** (see Chapter 3) and **8** in $(CD_3)_2SO$ display the calculated number of fifteen aromatic protons overlapping between 6.7 – 8.2 ppm {eleven from the bbp ligand and four from iminoquinone moiety}(Figure 5a.5). In both the complexes, the NH-protons from iminoquinone moiety appears at ~11.7 ppm; which is appreciably shifted downfield because of coordination to the metal center. These NH-protons, as expected, disappeared on D_2O exchange.[14] In complex **3a**, the three methyl protons of the coordinated acetonitrile appears as a sharp singlet at 2.04 ppm (see

Chapter 3); whereas, in complex **8**, the CH_3 and CH_2 protons of the coordinated ethyl amine appear at 1.5 ppm as a triplet and 2.4 ppm as a multiplet, respectively.

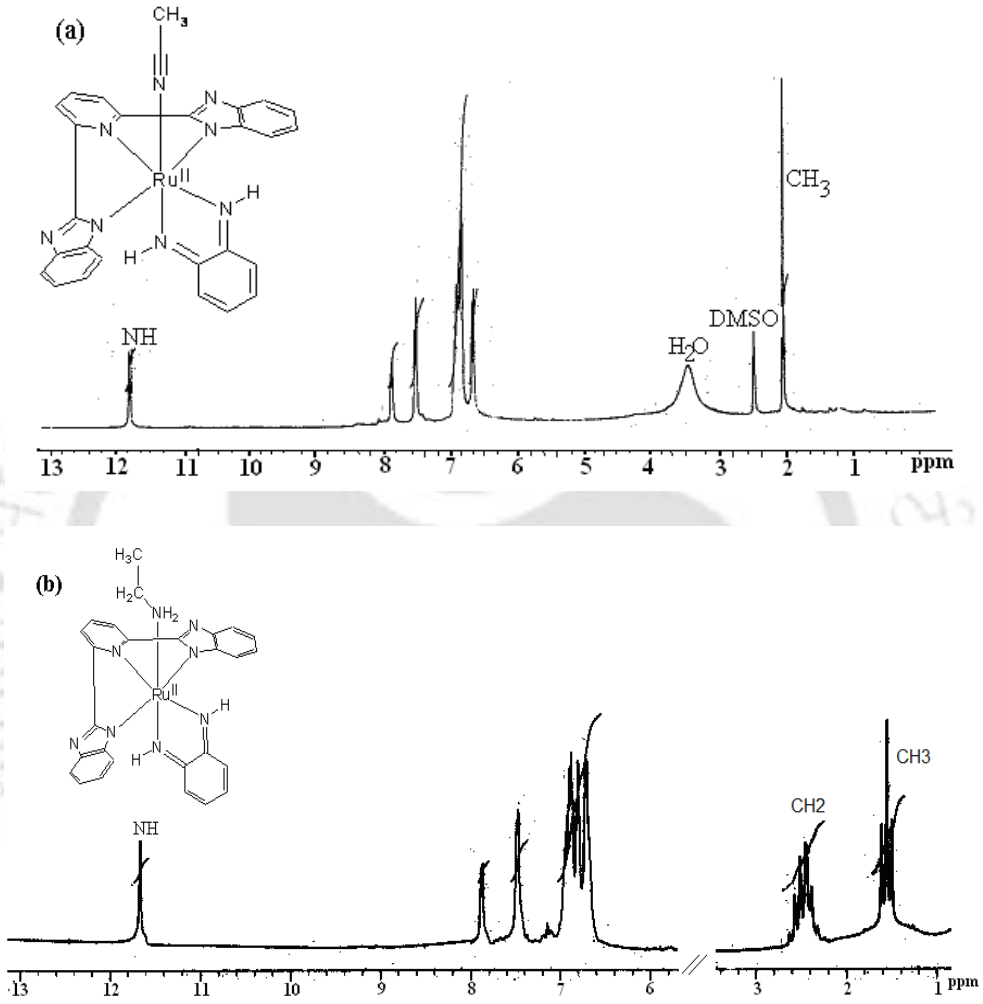

Figure 5a.5: ^{1}H-NMR spectra of complexes (a) **3a** and (b) **8** in $(CD_3)_2SO$ solvent.

The reduction of the acetonitrile to ethylamine is evidently a $4e^-/4H^+$ process; hence, it results into the oxidation of two equivalent of *p*-phenylenediamine to corresponding aminoquinone (in case of hydroquinone, to corresponding quinone) (quantitatively determined by isolated product analysis). The ESI-Mass spectra confirmed the oxidation of *p*-phenylenediamine and hydroquinone (Figure 5a.6 and 5a.7).

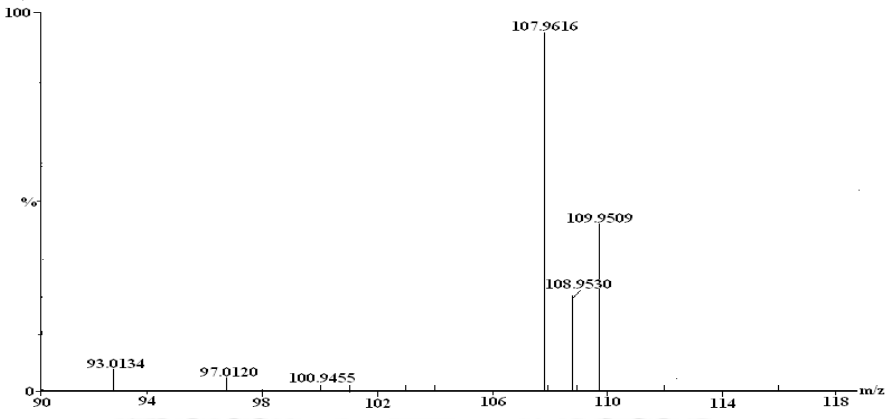

Figure 5a.6: ESI-mass spectrum of iminoquinone in CH_3CN:H_2O (50:50) with 0.1% formic acid.

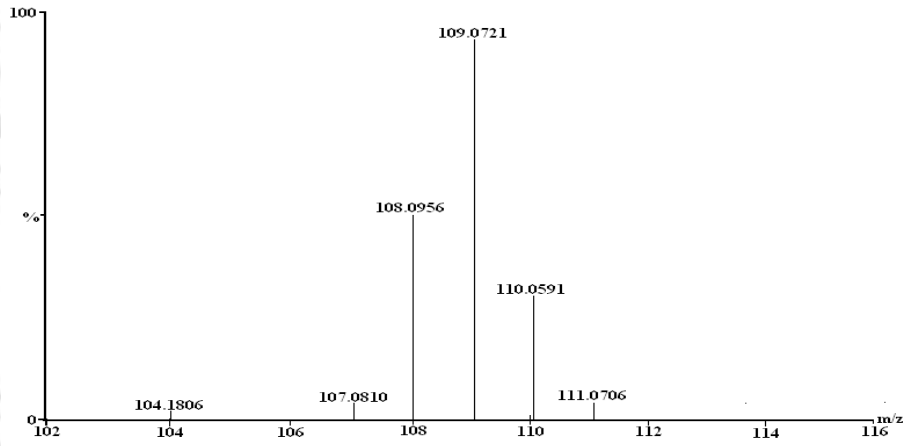

Figure 5a.7: ESI-mass spectrum of quinone in CH_3CN:H_2O (50:50) with 0.1% formic acid.

In contrast, Meyer et al. have recently reported that [(trpy)(Cl)(NSAr)Os^{III}-N≡CCH_3], in $2e^-/2H^+$ reduction gives [(trpy)(Cl)(NSAr)Os^{III}-N(H)=$CHCH_3$] [trpy = 2,2′:6,2″-terpyridine; Ar = C_6H_5, 4-MeC_6H_4, 3,5-$Me_2C_6H_3$].[11] This [(trpy)(Cl)($NSC_6H_3Me_2$)Os^{III}-N(H)=$CHCH_3$] complex can do reductions of various substrates like PhCHO, CH_3CN, 1,4-quinone etc. and itself comes back to the parent acetonitrile coordinated complex. Venanzi et al. reported the conversion of acetonitrile to ethylamine in $[(triars)Ru(NCMe)_3]^{2+}$ with $NaBH_4$ in methanolic solution.[15] It is proposed that the ruthenium center first polarizes the nitrile and activates the β-carbon toward hydride attack followed by the addition of proton to the

nitrogen and this finally results into the amine.[16] However, it is not clear that whether the hydrides are introduced directly to the β-carbon or through a 1,3-metal hydride shift from the ruthenium to β-carbon. The azavinylidene and imine complexes are the proposed intermediates for this conversion.[17]

5a.3 Conclusion

Thus, the present chapter illustrated an example of reduction of coordinated acetonitrile to ethylamine by *p*-phenylenediamine or hydroquinone. This results into the oxidation of the reductant to corresponding iminoquinone or quinone derivatives. The reduced product is characterized by microanalysis, UV-visible spectra, ^{1}H-NMR, Mass spectroscopy and finally by crystal structure determination. The oxidation products are determined quantitatively by GC-Mass as well as isolated yield analysis.

5a.4 Experimental Section

5a.4.1 General

All reagents and solvents were purchased from commercial sources and were of reagent grade. Acetonitrile was distilled from calcium hydride. *p*-phenylenediamine and hydroquinone were recrystallized from hexane before use. UV-visible spectra were recorded on a Perkin Elmer Lambda-25 spectrophotometer. FT-IR spectra were taken on a Perkin Elmer spectrophotometer with samples prepared as KBr pellets. Solution electrical conductivity was checked using a Systronic 305 conductivity bridge. ^{1}H- NMR spectra were obtained with a 400 MHz Varian FT spectrometer. Chemical shifts (ppm) were referenced to the residual solvent peaks. Elemental analyses were obtained from a Perkin Elmer Series II Analyzer. Single crystals were grown by slow diffusion followed by slow evaporation technique. The intensity data were collected using a Bruker SMART

APEX-II CCD diffractometer, equipped with a fine focus 1.75 kW sealed tube MoK_α radiation (λ = 0.71073 Å) at 273(3) K, with increasing ω (width of 0.3° per frame) at a scan speed of 3 s/frame. The SMART software was used for data acquisition. Data integration and reduction were undertaken with SAINT and XPREP software. Multi-scan empirical absorption corrections were applied to the data using the program SADABS. Structures were solved by direct methods using SHELXS-97 and refined with full-matrix least squares on F^2 using SHELXL-97. All non-hydrogen atoms were refined anisotropically. The hydrogen atoms were located from the difference Fourier maps and refined. Structural illustrations have been drawn with ORTEP-3 for Windows.

5a.4.2 Synthesis of complex 3a

The synthesis of complex **3a** has been discussed in chapter 3.

5a.4.3 Synthesis of complex 8

The complex **3a** (100 mg, 0.18 mmol) was taken in 5 ml ethanol and added three equivalent of *p*-phenylenediammine (58.5 mg, 0.54 mmol). It was refluxed for 4h and the solvent was removed under reduced pressure. The solid mass was then purified using silica gel column. The oxidized iminoquinone was eluted first as light yellow fraction with pure CH_2Cl_2 (yield: 40 mg, 70%) and complex **8** was then eluted with 1:4 CH_2Cl_2/CH_3CN mixture. Yield: 70 mg, ~70%.

The complex **8** has also been synthesized by the reaction of complex **3a** (100 mg, 0.18 mmol) and hydroquinone (59 mg, 0.53 mmol) following the same procedure as above Yield: Complex **8**, 75 mg (75%).

Characterization of complex 8

Anal. Calcd. (%): C: 57.75; H: 4.28; N: 19.96. Found (%) C: 57.79; H: 4.29; N: 19.97. UV-visible (in acetonitrile solvent): $\lambda_{max}(\varepsilon/dm^3mol^{-1}cm^{-1})$: 248(39429); 324(9813); 340(10191); 509(4350). Mass spectral data (m/z): 562.74

Characterization of iminoquinone

Anal. Calcd (%): C: 67.92; H: 5.66; N: 26.41. Found (%) C: 67.91; H: 5.67; N: 26.42. Mass spectral data (m/z): 107.96

Characterization of quinone

Anal. Calcd (%): C: 66.67; H: 3.73. Found (%) C: 66.69; H: 3.71. Mass spectral data (m/z): 109.07

5a.5 References

1. (a) Andrews, M. A.; Kaesz, H. D. *J. Am. Chem. Soc*. **1979**, *101*, 7238. (b) Andrews, M. A.; Kaesz, H. D. *J. Am. Chem. Soc*. **1979**, *101*, 7255. (c) Andrews, M. A.; Vanbuskirk, G.; Knobler, C. B.; Kaesz, H. D. *J. Am. Chem. Soc*. **1979**, *101*, 7245. (d) Andrews, M. A.; Kaesz, H. D. *J. Am. Chem. Soc*. **1979**, *101*, 7260.
2. Feng, S. G.; Templeton, J. L. *J. Am. Chem. Soc*. **1989**, *111*, 6477.
3. Yeh, W. Y.; Ting, C. S.; Peng, S. M.; Lee, G. H. *Organometallics* **1995**, *14*, 1417 and references therein.
4. (a) Anderson, S. J.; Wells, F. J.; Wilkinson, G.; Hussain, B. Hursthouse, M. B. *Polyhedron* **1988**, *7*, 2615. (b) Barron, A. R.; Salt, J. E.; Wilikinson, G.; Motevalli, M.; Hursthouse, M. B. *J. Chem. Soc. Dalton Trans*. **1987**, 2947. (c) Bakir, M.; Fanwick, P. E.; Walton, R. A. *Inorg. Chem*. **1988**, *27*, 2016.
5. McGilligan, B. S.; Wright, T. C.; Wilkinson, G.; Motevalli, M.; Hursthouse, M. B. *J. Chem. Soc. Dalton Trans*. **1988**, 1737.
6. (a) Sutyagina, A. A.; Kulchitskaya, T. V.; Vovchenko, G. D. *Sov. Electrochem*. **1975**, *11*, 1335. (b) Sutyagina, A. A.; Kulchitskaya, T. V.; Balabontseva, T. L.; Vovchenko, G. D. *Vestn. Mosk. Univ. Ser. 2: Khim*. **1976**, *17*, 332.
7. Rhodes, L. F.; Venanzi, L. M. *Inorg. Chem*. **1987**, *26*, 2692.
8. March, J. *Advanced Organic Chemistry*, 3rd ed., Wiley Interscience, New York, 1985, p. 809 and p. 815.
9. Seino, H.; Tanabe, Y.; Ishii, Y.; Hidai, M. *Inorg. Chim. Acta* **1998**, *280*, 163.
10. (a) Dasilva, J. J. R. F.; Dasilva, M. F. C. G.; Henderson, R. A.; Pombeiro, A. J. L.; Richards, R. L. *J. Organomet. Chem*. **1993**, *461*, 141. (b) Pombeiro, A. J. L.; Hughes, D. L.; Richards, R. L. *J. Chem. Soc. Chem. Commun*. **1988**, 1052. (c) Pombeiro, A. J.

L. *Inorg. Chim. Acta* **1992**, *200*, 179. (d) Pombeiro, A. J. L. *New J. Chem*. **1994**, *18*, 163.

11. Huynh, M. H. V.; Baker, R. T.; Morris, D. E.; White, P. S.; Meyer, T. J. *Angew. Chem. Int. Ed*. **2002**, *41*, 3870.
12. (a) deLearie, L. A.; Haltiwanger; R. C.; Pierpont, C. G. *Inorg. Chem*. **1989**, *28*, 644. (b) Bhattacharya, S.; Pierpont, C. G. *Inorg. Chem*. **1994**, *33*, 6038. (c) Whalen; A. M.; Bhattacharya, S.; Pierpont, C. G. *Inorg. Chem*. **1994**, *33*, 347. (d) Speier, G.; Whalen, A. M.; Csihony, J.; Pierpont, C. G. *Inorg. Chem*. **1995**, *34*, 1355. (e) Verani, C. N.; Gallert, S.; Bill, E.; Weyhermuller, T.; Weighardt, K.; Chaudhuri, P. *Chem. Commun*. **1999**, 1747. (f) Chaudhuri, P.; Verani, C. N.; Bill, E.; Weyhermuller, T.; Weighardt, K. *J. Am. Chem. Soc*. **2001**, *123*, 2213. (g) Chun, H.; Verani, C. N.; Chaudhuri, P.; Bothe, E.; Bill, E.; Weyhermuller, T.; Weighardt, K. *Inorg. Chem*. **2001**, *40*, 4157. (h) Chun, H.; Weyhermuller, T.; Bill, E.; Weighardt, K. *Angew. Chem., Int. Ed. Engl*. **2001**, *40*, 2489. (i) Sun, X.; Chun, H.; Hildenbrand, K.; Bothe, E.; Weyhermuller, T.; Weighardt, K. *Inorg. Chem*. **2002**, *41*, 4295.
13. Pramanik, N. C.; Pramanik, K.; Ghosh, P.; Bhattacharya, S. *Polyhedron* **1998**, *17*, 1525.
14. Singh, A.; Chetia, B.; Mobin, S. M.; Das, G.; Iyer, P. K.; Mondal, B. *Polyhedron* **2008**, *27*, 1983.
15. Rhodes, L. F.; Venanzi, L. M. *Inorg. Chem*. **1987**, *26*, 2692.
16. Creaser, I. I.; Sargeson, A. M. *J. Chem. Soc., Chem. Commun*. **1975**, 974.
17. Rylander, P. N. *Catalytic Hydrogenation in Organic Synthesis*; Academic; New York, **1979**; p. 138 and references therein.

Abstract

[Ru(bbp)(L){NH=CO(CH_3)CH_3}] (**9**) has been synthesized by the reaction of [Ru(bbp)(L)(CH_3CN)] {bbp = 2,6-*bis*(benzimidazol-2-yl)pyridine, L = *o*-phenylenediamine} with $NaOCH_3$ in methanol solution. It has been characterized by various spectroscopic techniques and elemental analysis. The spectroscopic studies revealed the formation of the imido-type complex rather than amido-type complex.

5b.1 Introduction

Nucleophilic addition to metal-activated RC≡N species is one of the frontier areas of current research on organonitriles and this topic has been the subject of comprehensive reviews including recent surveys.[1-6] In general, the interest in conversions of nitrile at metal centers stems from the following possibilities: first, to use nitriles as synthons for the preparation of compounds with a broad spectrum of applications (e.g., phthalocyanines);[7] second, to provide environmental friendly metal-catalyzed hydrolytic transformations of RCN species to amides (e.g., of industrial and pharmacological significance);[4] and third, to synthesize, via the nucleophilic addition, diverse imino complexes (e.g., exhibiting antitumor properties).[8] Thus the formation of C-O bond due to metal-mediated nitrile-nucleophile coupling have been developed upto date.[1-6] Nagao et al. reported the reaction of acetonitrile coordinated to nitrosyl-ruthenium complex *cis*-$[Ru(NO)(CH_3CN)(bpy)_2]^{3+}$ (bpy = 2,2′-bipyridine) with H_2O or CH_3OH under mild condition and they have found the nitrosyl-ruthenium complexes containing the N-bound methylcarboxyimido complex, *cis*-$[Ru(NO)(NH{=}C(O)CH_3(bpy)_2]^{3+}$ and methylcarboxy-imido acid complex, *cis*-$[Ru(NO)(NH{=}C(OH)CH_3(bpy)_2]^{3+}$.[9]

There are two possible resonance structures (imido-type) and (amidato-type)(Scheme 5b.1):

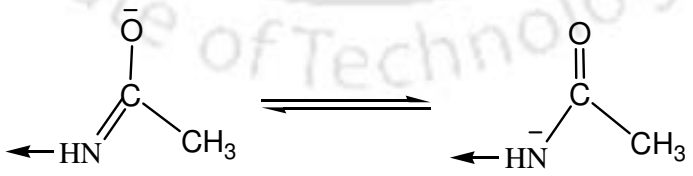

Imido-type Amidato-type

Scheme 5b.1

This chapter deals with an example where the metal coordinated acetonitrile transforms into the corresponding imido derivative by nucleophillic addition reaction of $NaOCH_3$ on coordinated acetonitrile site.

5b.2 Results and Discussion

$[Ru^{II}(bbp)(L)\{NH=C(OCH_3)CH_3\}]$ (**9**) has been synthesized by the reactions of complex $[Ru^{II}(bbp)(L)(CH_3CN)]$ (**3a**) with $NaOCH_3$ in methanol solvent, followed by chromatographic separation with methanol:dichloromethane solvent mixture (Scheme 5b.2). The complex is found to be neutral and nonconducting in acetonitrile as complex **3a**. The complex exhibits satisfactory microanalysis (see Experimental Section).

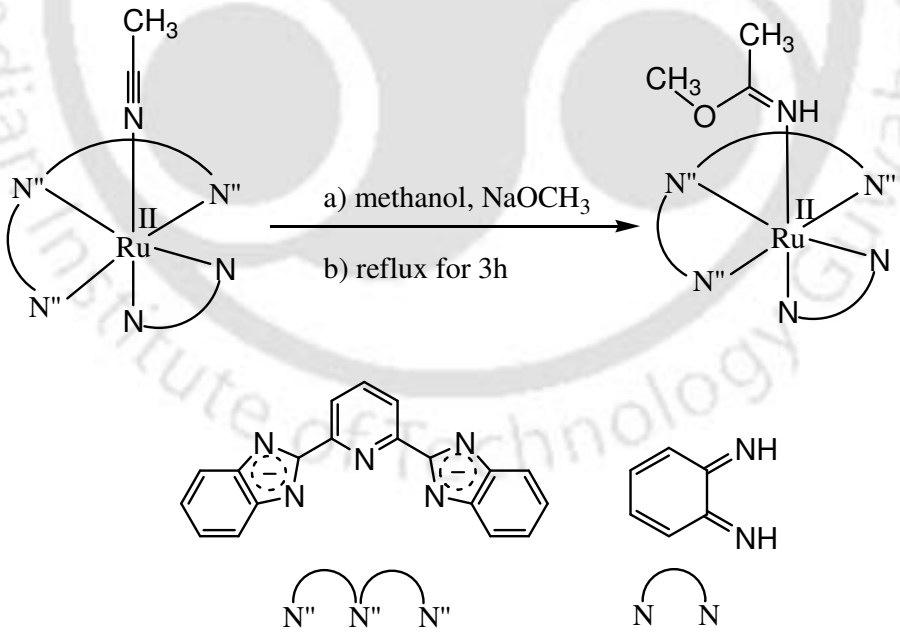

Scheme 5b.2

The ESI-mass has been recorded in methanol solvent. In the positive ion ESI mass spectrum, the (m+1) molecular ion peak appears at 590.47 which indicates the formation of complex **9** (Figure 5b.1).

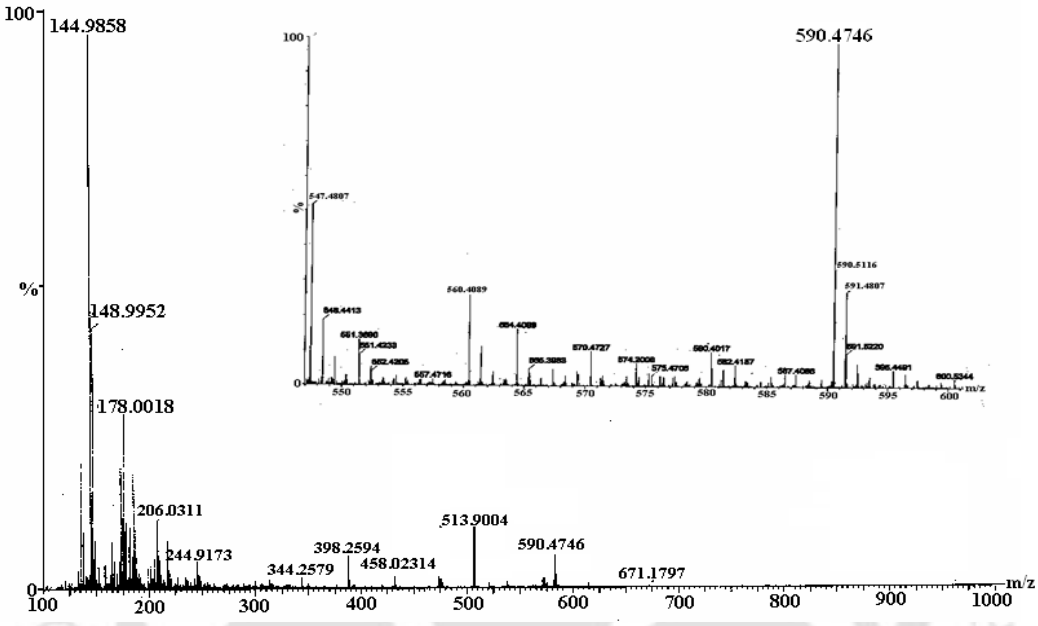

Figure 5b.1: ESI-Mass spectrum for complex **9** in methanol solvent with (0.1%) formic acid.

5b.2.1 UV-visible Spectroscopy

The UV-visible spectra of complexes have been recorded in methanol solvent. The UV-visible spectrum of complex **3a** has been discussed in chapter 3. The complex **9** show the MLCT band, $\lambda_{max}(\varepsilon/dm^3mol^{-1}cm^{-1})$ at 504(4287) with ligand based $\pi\rightarrow\pi^*$ transitions at 341(14987) nm and 322(15300) nm (Figure 5b.2).

5b.2.2 FT-IR Spectroscopy

The FT-IR spectrum of the complex **9** was recorded in KBr pellet. The band at 3250 cm^{-1} is assigned to the N-H stretching vibration.

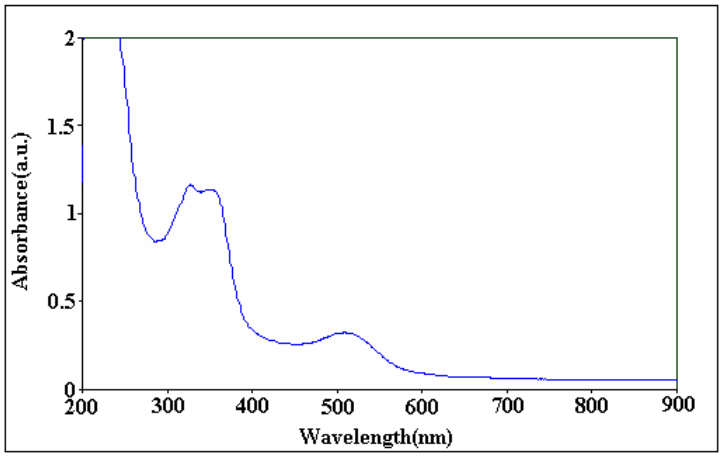

Figure 5b.2: UV-visible spectrum for complex **9** in methanol solvent.

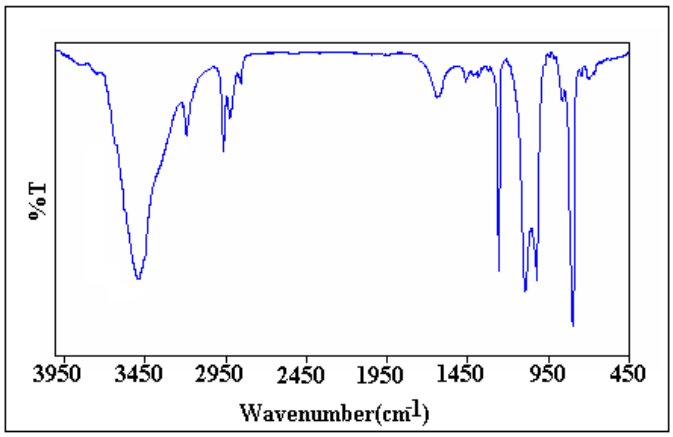

Figure 5b.3: FT-IR spectrum of the complex **9** in KBr pellet.

The complex **3a** exhibits the nitrile stretching frequency at 1725 cm^{-1}(see Chapter 5a) which is absent in complex **9** with the formation of a new band at 1658 cm^{-1} assigned to $\nu_{C=N.}$[11]

5b.2.3 ^{1}H- and ^{13}C-NMR Spectroscopy

The ^{1}H- and ^{13}C-NMR spectra for both the complexes have been recorded in the $(CD_3)_2SO$ solvent. In ^{1}H-NMR study, the complex **3a** exhibits the calculated number of fifteen aromatic protons overlapping between δ, 6.7 – 8.2 ppm; eleven from the bbp ligand and four from iminoquinone moiety (see Chapter 3). The NH-proton from iminoquinone moiety appears at ~11.7 ppm; which is appreciably shifted downfield because of coordination to the metal center. This NH-proton, as expected, disappeared on D_2O exchange.[10] The three methyl protons of the coordinated acetonitrile appear as a sharp singlet at 2.04 ppm in case of complex **3a**. Complex **9** also shows the expected number of aromatic protons in the region δ, 6-8 ppm. In addition, compared to complex **3a**, it exhibits two three proton singlets at δ, 1.34 and 3.11 ppm corresponding –CH_3 and -OCH_3 protons, respectively, of the imido derivative (Figure 5b.4). The NH-protons have been found to appear at δ, 11.8 ppm. In the ^{13}C-NMR study, two signals appear at δ, 30.16 ppm and 40.17 ppm for CH_3 and – OCH_3 along with the aromatic carbon signals in the region δ, 110-190 ppm (Figure 5b.5).

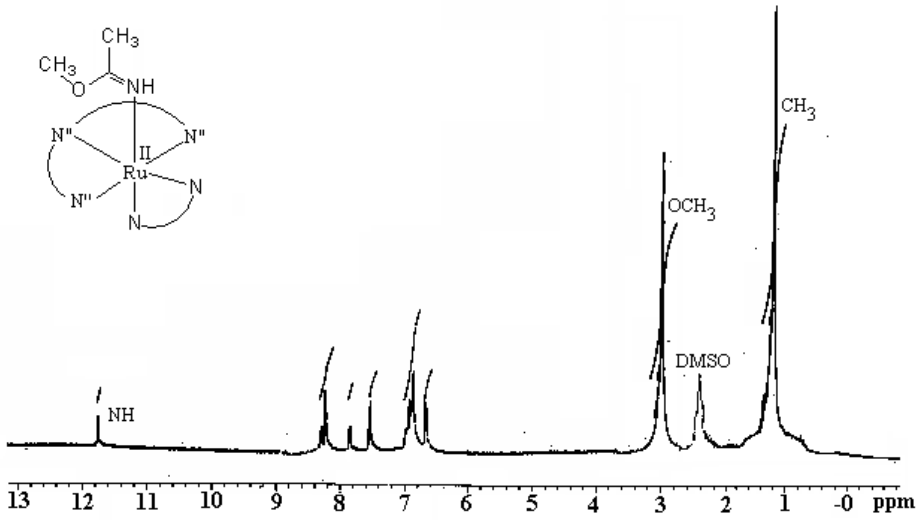

Figure 5b.4: ^{1}H-NMR spectrum for complex **9** in $(CD_3)_2SO$ solvent.

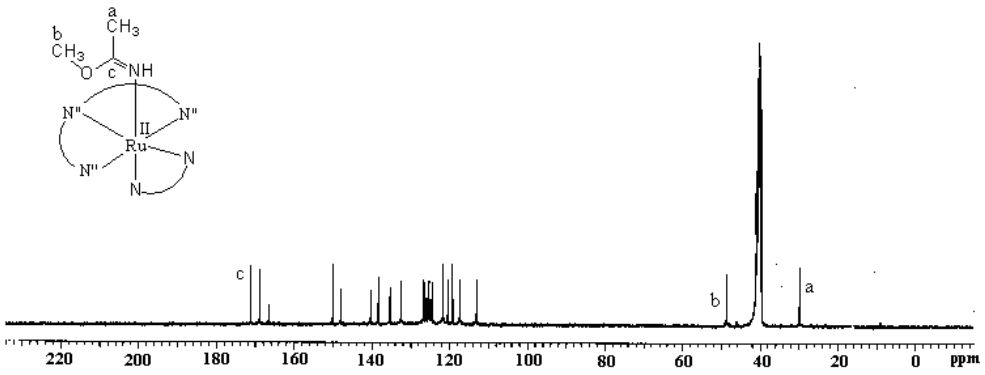

Figure 5b.5: ^{13}C-NMR spectrum for complex **9** in $(CD_3)_2SO$ solvent.

The signal at δ, 173.41 ppm is assigned to the -C=NH. This signals is reported to appear at δ, 175.6 and 177.0 ppm in case of *trans*-$[PtCl_2\{NH=C(Et)ON(H)CMe_2(Ph)=NOH\}_2]$ and $[Ph_3PCH_2Ph][PtCl_2\{NH=C(Et)ON=C(CH_2Ph)_2\}]$, repectively.[11]

5b.3 Conclusion

The nucleophilic addition of $NaOCH_3$ to the metal coordinated acetonitrile has been studied. The reaction resulted into the formation of metal coordinated imido derivative. The formation of the imido-complex has been confirmed by various spectroscopic techniques.

5.4b Experimental Section

5b.4.1 General

All reagents and solvents were purchased from commercial sources and were of reagent grade. Sodium methoxide used was prepared in laboratory using known procedure. UV-visible spectra were recorded on a Perkin Elmer Lambda-25 spectrophotometer. FT-IR spectra were taken on a Perkin Elmer spectrophotometer with samples prepared as KBr pellets. Solution electrical conductivity was checked using a Systronic 305 conductivity

bridge. ^{1}H and ^{13}C-NMR spectra were obtained with a 400 MHz Varian FT spectrometer. Chemical shifts (ppm) were referenced to the residual solvent peaks. Elemental analyses were obtained from a Perkin Elmer Series II Analyzer.

5b.4.2 Synthesis of complex $[Ru^{II}(bbp)(L)\{NH=C(OCH_3)CH_3\}]$, 9

The $[Ru^{II}(bbp)(L)(CH_3CN)])$ (50 mg, 0.095 mmol) is taken in 10 ml of methanol and added $NaOCH_3$ in excess and heated to reflux for 3h. The crude solution was then evaporated to dryness. The solid mass thus obtained was subjected to column chromatographic purification using silica gel column and using dichloromethane/ methanol as eluent. Removal of the solvent under reduced pressure afforded the complex **9** as dark colored solid. Yield 35 mg (70%). Anal. Calcd.(%): C: 57.04; H: 4.10; N: 19.00. Found (%) C: 57.09; H: 4.12; N: 18.97.

5b.5 References

1. Kukushkin, V. Yu.; Pombeiro, A. J. L. *Chem. Rev.* **2002**, *102*, 1771.

2. Pombeiro, A. J. L.; Kukushkin, V. Yu. *Reactions of Coordinated Nitriles*. *In Comprehensive Coordination Chemistry*, 2nd ed.; Lever, A. B. P., Ed.; Elsevier: New York, 2004; Vol. 1, Chapter 1.34, pp 639-660.

3. Michelin, R. A.; Mozzon, M.; Bertani, R. *Coord. Chem. Rev.* **1996**, *147*, 299.

4. Kukushkin, V. Yu.; Pombeiro, A. J. L. *Inorg. Chim. Acta* **2005**, *358*, 1.

5. Bokach, N. A.; Kukushkin, V. Yu. *Uspekhi Khimii* (*Russ. Chem. Rev.*), **2005**, *74*, 164.

6. Kuznetsov, M. L. *Uspekhi Khimii* (*Russ. Chem. Rev.*), **2002**, *71*, 307.

7. McKeown, N. B. *Phthalocyanines*. In *Comprehensive Coordination Chemistry*, 2nd ed.; Lever, A. B. P., Ed.; Elsevier: New York, 2004, Vol. 1, Chapter 1.24, pp 507-514 and references therein.

8. (a) Natile, G.; Coluccia, M. *Coord. Chem. Rev.* **2001**, *216-217*, 383. (b) Liu, Y.; Pacifico, C.; Natile, G.; Sletten, E. *Angew. Chem., Int. Ed.* **2001**, *40*, 1226. (c) Gonzalez, A. M.; Cini, R.; Intini, F. P.; Pacifico, C.; Natile, G. *Inorg. Chem.* **2002**, *41*, 470. (d) Cini, R.; Caputo, P. A.; Intini, F. P.; Natile, G. *Inorg. Chem.* **1995**, *34*, 1130.

9. Nagao, H.; Hirano, T.; Tsuboya, N.; Shiota, S.; Mukaida, M. *Inorg. Chem.* **2002**, *41*, 6267.

10. Singh, A.; Chetia, B.; Mobin, S. M.; Das, G.; Iyer, P. K.; Mondal, B. *Polyhedron* **2008**, *27*, 1983.

11. Luzyanin, K.V.; kukushkin, V. Y.; Kuznetsov, M. L.; Ryabov, A. D.; Galanski, M.; Haukka, M.; Pombeiro, J. L. *Inorg. Chem.* **2006**, *45*, 2296.

Abstract

The ruthenium complexes [Ru^{II}(bbp)(L)(Cl)] (**10**), [Ru^{II}(bbp)(L)(H_2O)] (**11**) and [Ru^{II}(bbp)(L)(DMSO)] (**12**) {bbp = 2,6-*bis*(benzimidazol-2-yl)pyridine, L = *o*-phenylenediamine} have been synthesized in a stepwise manner starting from [Ru^{III}(bbp)Cl_3]. The single crystal X-ray structures, except for the complex **11**, have been determined. All the complexes were characterized by UV-visible, FT-IR, ^{1}H-NMR, Mass spectroscopic techniques and cyclic voltammetry. The Ru^{III}/Ru^{II} couple for complexes **10**, **11** and **12** appears at 0.49 V, 0.55 V and 0.63 V, respectively *vs* SCE. It is observed that complex **11**, on refluxing in acetonitrile, results into [Ru^{II}(bbp)(L)(CH_3CN)], **3a** which has been prepared earlier in a different method (see chapter 3). The structural, spectral and electrochemical properties of complexes **10**, **11** and **12** were compared to those of earlier reported complex **3a**, [Ru^{II}(bbp)(L)(CH_3CN)].

6.1 Introduction

Over the past two decades ruthenium(II) polypyridyl chemistry has become an area of extensive research in inorganic chemistry.[1-3] The development of a new class of photo-redox active ruthenium polypyridyl complexes has been the subject matter of continuous research activity.[4] Strong metal to ligand charge transfer transitions, facile electron transfer properties and long lived ^{3}MLCT excited states of this class of complexes make them more effective for designing photochemical and electrochemical devices.[5] A large volume of articles involving polypyridyl complexes of ruthenium(II) have been published in last few years.[6,7]

In this direction mononuclear ruthenium chemistry with bbp [bbp = 2,6-*bis*(benzimidazol-2-yl)pyridine] ligand in combination with ancillary ligands are not much explored though it's chemistry with some transition metals like copper, iron, zinc and cadmium have been studied well.[8] The factors that make the bbp ligand as a potential substitute for trpy are: (i) similar chelating unit like trpy; (ii) due to extensive π-delocalization, its rigidity and planarity give well defined structure for metal complexes.[9]

The present chapter originates from the interest to use the 2,6-*bis*(benzimidazol-2-yl)pyridine (bbp) as tridentate ligand for synthesizing various ruthenium complexes with ancillary ligands.

This chapter deals with the synthetic, structural and electrochemical properties of a new set [Ru-bbp] complexes with *o*-phenylenediamine (L) as ancillary and these complexes can be used for designing the effective photo- and electrochemical devices.

6.2 Results and Discussion

The complex [Ru^{II}(bbp)(L)Cl] (**10**) has been synthesized by the reaction of [Ru(bbp)Cl_3] and L {L = *o*-phenylenediamine) in the presence of NEt_3 in refluxing ethanolic medium

(Scheme 6.1). The chromatographic purification of the crude product using alumina column and CH_2Cl_2:CH_3OH (9:1) solvent mixture affords the pure complex **10**.

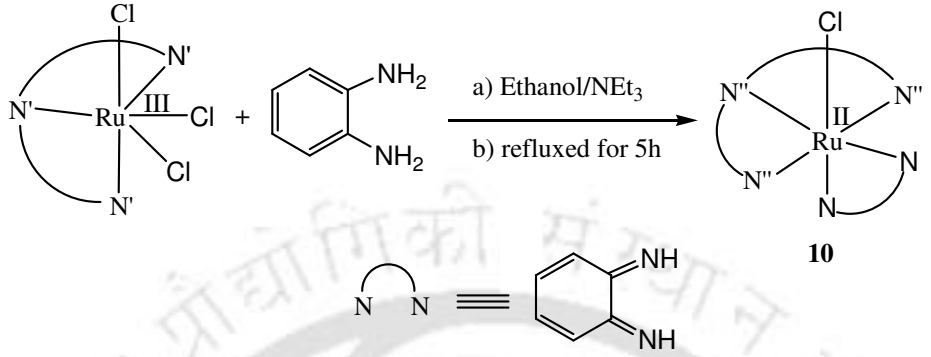

Scheme 6.1

Complex **10**, thus obtained, on heating with aqueous $AgNO_3$ solution in ethanol:water(1:4) mixture resulted into the formation of $[Ru^{II}(bbp)(L)(H_2O)]$ (**11**). Chromatographic purification using CH_2Cl_2:CH_3OH (5:1) as eluent affords pure product.

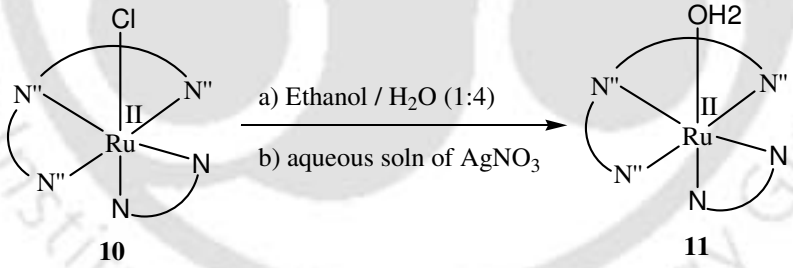

Scheme 6.2

This aqua derivative, **11**, when heated to reflux for 5h in acetonitrile solvent afforded a dark colored complex whose spectral properties match well with the earlier synthesized $[Ru^{II}(bbp)(L)(CH_3CN)]$ (**3a)** in a slightly different method in chapter 3. Hence it is assumed that this reaction leads to the solvent substitution resulting into the formation of complex **3a**. The mass spectral data supports the formation of complex **3a**, in this case.

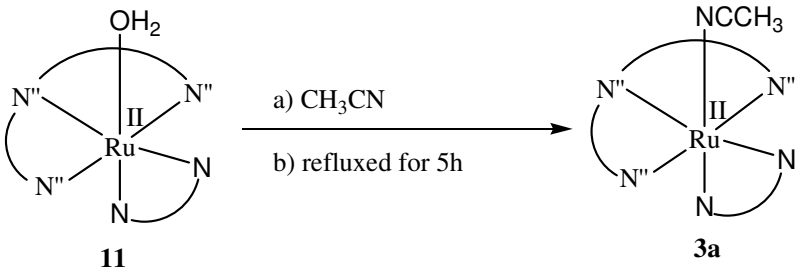

11 **3a**

Scheme 6.3

On the other hand, complex **11**, on heating with DMSO, followed by chromatographic purification using silica gel column and CH_2Cl_2:CH_3OH mixture leads to complex **12** as the pure solid product.

All the complexes, **10**, **11** and **12** are found to be neutral and nonconducting in methanol. Elemental analyses for all the complexes are in well agreement with the calculated values (see Experimental Section). Room temperature magnetic moment measurements reveals the diamagnetic nature of all complexes.

6.2.1 Mass Spectroscopy

The electrospray mass spectra for all the complexes were recorded in CH_3OH/H_2O (50:50) with (0.1%) formic acid. The (m+1) molecular ion peaks for complexes **10, 11** and **12** appear at 553.67, 535.42 and 596.07 respectively (Figure 6.1). The mass spectrum of complex **3a** has been discussed in chapter 3 (Figure 3.1).

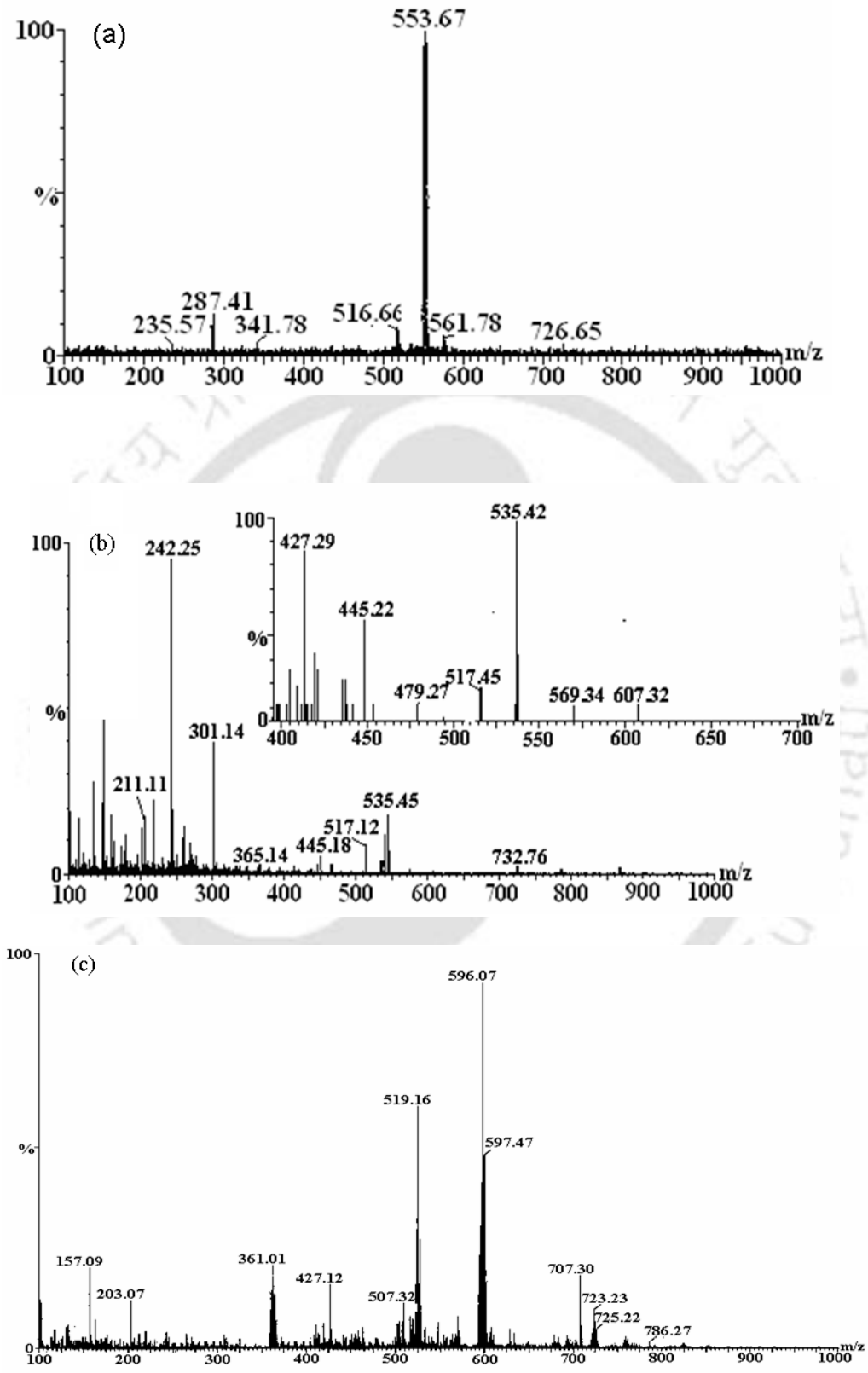

Figure 6.1: ESI-Mass spectra for complexes (a) **10**, (b) **11** and (c) **12** in CH_3OH/H_2O (50:50) with (0.1%) formic acid.

6.2.2 X-ray Crystallography

The single crystal X-ray structures of the complexes **10** and **12** are shown in figure 6.2 and 6.3, respectively. The single crystal X-ray structure of complex **3a** has already been discussed in chapter 3.[10] We have tried to grow the crystals of complex **11** from water but unfortunately we failed get X-ray quality crystals. Selected bond distances and bond angles are given in table 6.2 and 6.3, respectively. The RuN_5Cl and RuN_5O coordination spheres in **10** and **12**, respectively, are distorted octahedral as can be seen from the angles subtended at the metal ions (Table 6.3). bbp ligand is coordinated in the expected meridional fashion with the ligand L in *cis* orientation.[10] Similar binding fashion has been observed also in case of $[Ru^{II}(bbp)(L)(CH_3CN)]$, **3a** (Chapter 3). The chloride, DMSO and acetonitrile molecule in **10**, **12** and **3a**, respectively, are found to be in *trans* to the N6 nitrogen of L. The single crystal of **10** contains water of crystallization in the ratio [Ru(bbp)(L)Cl] : H_2O = 1:2; whereas **12** contains one molecule of water and ethanol as solvent of crystallization.

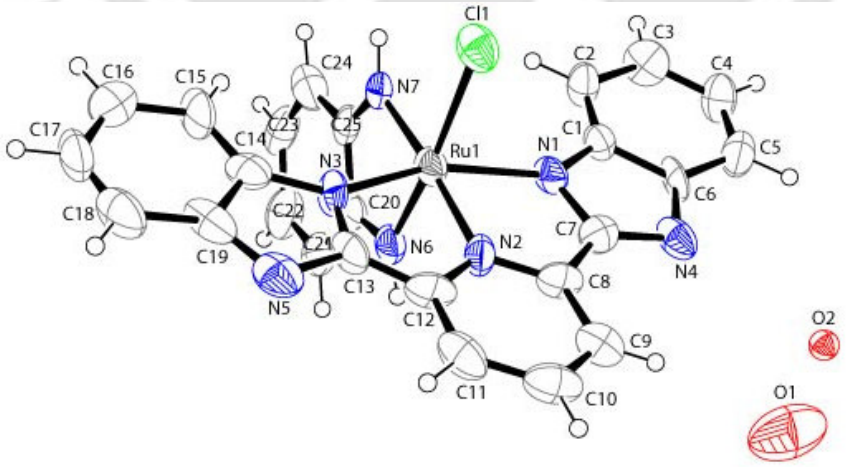

Figure 6.2: ORTEP diagram for complex **10** $[Ru^{II}(bbp)(L)(Cl)](H_2O)_2$ (50% thermal ellipsoids plot).

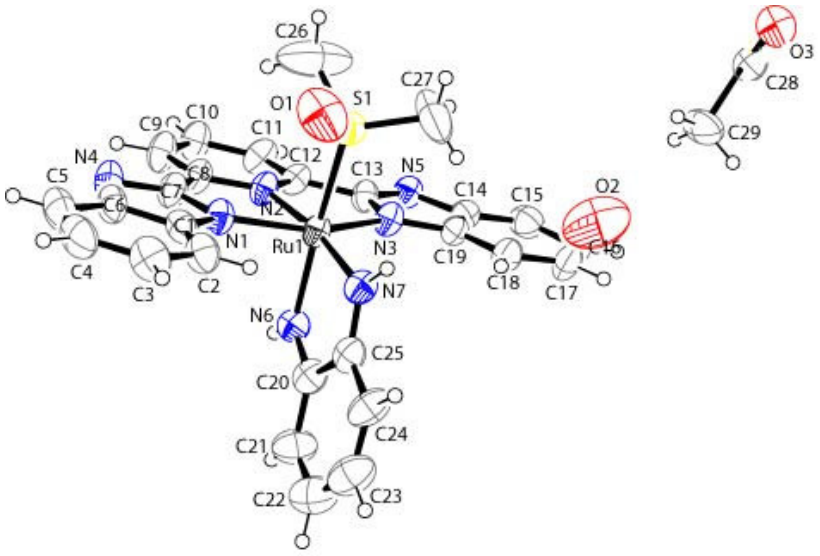

Figure 6.3: ORTEP diagram of complex **12** [Ru(bbp)(L){$(CH_3)_2SO$}]$(H_2O)(C_2H_5OH)$ (50% thermal ellipsoids plot).

The geometrical constrains imposed due to the usual meridional mode of binding of tridentate bbp ligand is reflected in the *trans* angles N(1)-Ru(1)-N(3), 153.67(3)º; N(2)-Ru(1)-N(7), 169.23(3)º (Table 6.3) which are comparable to other ruthenium-terpyridine and ruthenium-bbp complexes N(1)-Ru(1)-N(3), 158.6(3)º; N(2)-Ru(1)-N(5), 177.8(3); N(4)-Ru(1)-N(6), 156.0(3)º; and N(1)-Ru(1)-N(3), 159.5(3)º; N(2)-Ru(1)-N(5), 176.1(3)º; N(4)-Ru(1)-N(6), 156.8(3)º.[11] The Ru^{II}–Cl distance, 2.433(1) Å, in **10** is comparable to that observed in {Ru(trpy)(PAP)Cl]ClO_4 [PAP: phenylazopyridine; trpy: 2,2′:6′,2″-terpyridine], 2.408 Å;[12] and is little longer than that observed in [Ru(trpy)(oxazole)Cl]ClO_4 [oxazole = 2,6-bis(benzoxazol-2-yl)pyridine, 2.3815(7) Å][13] and [Ru(trpy)(biq)Cl]PF_6 (biq = 2,20-bisquinoline), 2.378(2) Å.[14-17] The Ru-S and S-O bond distances in complex **12** are 2.2564(6) Å and 1.478(2) Å, respectively, and are within the accepted limits.[18-20]

The ancillary ligand L is found to bind in neutral iminoquinone form in all the complexes. The N(6)-C(20) and N(7)-C(25) bond distances are 1.331(17)Å, 1.313(19) Å in case of complex **10** whereas both of them are observed to be 1.308(10) Å in complex **12**. In case of complex **3a**, these distances are found to be 1.325(8) Å and 1.321(9) Å.[10] By comparing

these distances with the other reported structural studies of the ruthenium oxolene complexes by Pierpont and Weigardt et al., it is evident that L is preferentially bonded to the ruthenium centre in its neutral iminoquinone form.[21,22]

It is clear from the crystal structures that in complex **10**, the bbp ligand binds the metal in its mono-anionic form whereas it binds the metal center as di-anion in case of **12**.

Table 6.1: Crystallographic data for complexes **10** and **12**

	10	**12**
Formulae	$C_{27}H_{18}N_7ClRu.2H_2O$	$C_{28}H_{23}N_7O_3RuS.H_2O.C_2H_5OH$
Mol. wt.	571.43	638.66
Crystal system	Triclinic	Triclinic
Space group	P-1	P-1
Temperature /K	298(2)	298(2)
Wavelength /Å	0.71073	0.71073
a /Å	13.6072(3)	13.3261(10)
b /Å	18.1572(4)	14.2750(11)
c /Å	24.3993(5)	15.5425(14)
α/°	90.011(1)	69.694(5)
β/°	117.9610(10)	83.739(4)
γ/°	89.995(1)	80.537(4)
V/ $Å^3$	5324.6(2)	2781.93(17)
Z	4	4
Density/Mgm^{-3}	1.430	1.525
Abs. Coeff. /mm^{-1}	0.724	0.682
F(000)	2236	1296
Total no. of reflections	9890	12713

Reflections, I > 2σ(I)	3748	6274
Max. 2θ/°	20.03	23.50
Ranges (h, k, l)	-13<h>13 -16<k>17 -23<l>23	-12<h>15 -16<k>16 -17<l>17
Complete to 2θ (%)	99.8	95.1
Refinement method	Full-matrix least-squares on F^2	Full-matrix least-squares on F^2
Data/ Restraints/Parameters	4980/0/694	7825/0/725
WR_2(all data)	0.2179	0.2050
Goof (F^2)	7.522	1.090
R indices [I > 2σ(I)]	0.0872	0.0678
R indices (all data)	0.1209	0.0815

Table 6.2: Selected bond lengths (Å) of complexes **10** and **12**

Bond length (Å)	**10**	**12**
Ru(1)-N(1)	2.055(12)	2.076(6)
Ru(1)-N(2)	1.995(13)	2.055(6)
Ru(1)-N(3)	2.045(13)	2.077(7)
Ru(1)-N(6)	1.948(11)	2.017(7)
Ru(1)-N(7)	1.986(12)	1.991(7)
Ru(1)-Cl1)	2.441(4)	-
Ru(1)-S(1)	-	2.297(2)
N(6)-C(20)	1.331(17)	1.308(10)
N(7)-C(25)	1.313(19)	1.308(10)
C(20)-C(21)	1.476(2)	1.449(13)
C(20)-C(25)	1.423(19)	1.443(12)
C(21)-C(22)	1.335(2)	1.348(14)
C(22)-C(23)	1.430(19)	1.419(13)
C(23)-C(24)	1.341(2)	1.363(16)
C(24)-C(25)	1.394(2)	1.449(12)
S(1)-O(1)	-	1.485(7)

Table 6.3: Selected bond angles (°) for complexes **10** and **12**

Bond angle (°)	**10**	**12**
N(1)-Ru(1)-N(2)	78.23(6)	77.39(3)
N(1)-Ru(1)-N(3)	153.03(7)	153.92(3)
N(1)-Ru(1)-N(6)	92.64(5)	91.88(3)
N(1)-Ru(1)-N(7)	102.75(5)	100.12(3)
N(1)-Ru(1)-Cl(1)	88.38(3)	-
N(1)-Ru(1)-S(1)	-	87.04(19)
N(2)-Ru(1)-N(3)	75.97(7)	76.80(3)
N(2)-Ru(1)-N(6)	92.29(5)	93.01(2)
N(2)-Ru(1)-N(7)	174.41(2)	170.66(3)
N(2)-Ru(1)-Cl(1)	92.46(5)	-
N(2)-Ru(1)-S(1)	-	95.62(19)
N(3)-Ru(1)-N(6)	92.67(5)	93.22(20
N(3)-Ru(1)-N(7)	103.22(6)	105.96(2)
N(3)-Ru(1)-Cl(1)	89.74(4)	-
N(3)-Ru(1)-S(1)	-	91.71(19)
N(6)-Ru(1)-N(7)	78.48(2)	77.31(3)
N(6)-Ru(1)-Cl(1)	172.23(4)	-
N(6)-Ru(1)-S(1)	-	170.81(2)

6.2.3 UV-visible Spectroscopy

The UV-visible spectra have been recorded in methanol solvent. The spectrum of complex **3a** is discussed in chapter 3. Electronic spectral data of the complexes **10**–**12** in methanol solvent are listed in table 6.4. The complexes display multiple transitions in the UV-visible region (Figure 6.4). The lowest energy bands near 500 nm are assigned to $(d\pi)Ru^{II} \rightarrow \pi^*$(ligand) metal to ligand charge transfer (MLCT) transitions.[23] Absorption bands in the UV region are believed to be originated from the ligand based charge-transfer transitions. Multiple charge transfer transitions may arise from the lower symmetry splitting of metal level, the presence of different acceptor orbitals and from the mixing of singlet and triplet configurations in the excited state through the spin-orbit coupling.[23] The MLCT band energy follows the order: **10** < **11** ≈ **12** (Table 6.4, Figure 6.4). This red shift in λ_{max} is due to the relative destabilization of the $(d\pi)$Ru electrons while moving from H_2O or DMSO to Cl complexes, making the $(d\pi) \rightarrow \pi^*$ transition occur at relatively lower energy.[24] It would be worth mentioning that in case of complex **3a**, the MLCT transition appears at 514 nm (chapter 3).

Table 6.4

Complexes	$\lambda_{max/nm}$ (ε/dm^{3}mol^{-1}cm^{-1})
10	324 (11240), 340 (11365), 513 (5400)
11	323 (9770), 345 (10670), 505 (5540)
12	327 (9750), 340 (9400), 517 (5125)

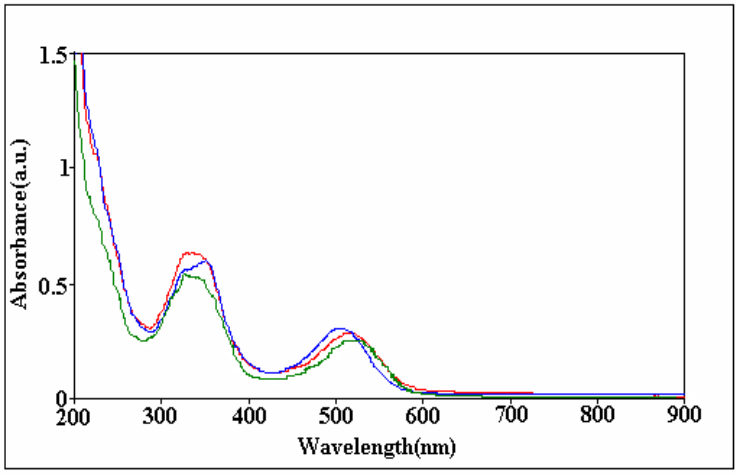

Figure 6.4: UV-visible spectra for complexes **10** (red), **11**(blue) and **12** (green) in methanol solvent.

6.2.4 FT-IR Spectroscopy

The FT-IR spectra of the complexes were recorded in KBr pellets. A strong sharp band has been observed at ~1725 cm^{-1} in complex **3a** (Chapter 3). This band is attributed to the nitrile frequency of the coordinated acetonitrile in the complex. This band is found to be absent in $[Ru^{II}(bbp)(L)(Cl)]$ (**10**), $[Ru^{II}(bbp)(L)(H_2O)]$ (**11**) and $[Ru^{II}(bbp)(L)(DMSO)]$ (**12**), resepectively, (Figure 6.5).

6.2.5 ^{1}H-NMR Spectroscopy

The ^{1}H-NMR spectra of all the complexes were recorded in $(CD_3)_2SO$ solvent at room temperature. The ^{1}H-NMR spectrum of **3a** has already been discussed earlier (Chapter 3) and reported.[10] Like complex **3a**, ^{1}H-NMR spectra of the complexes **10**, **11** and **12** show calculated number of aromatic protons overlapping between 6.5 – 8.4 ppm; eleven from the bbp ligand and four from *o*-quinonoid moiety (Figure 6.6).

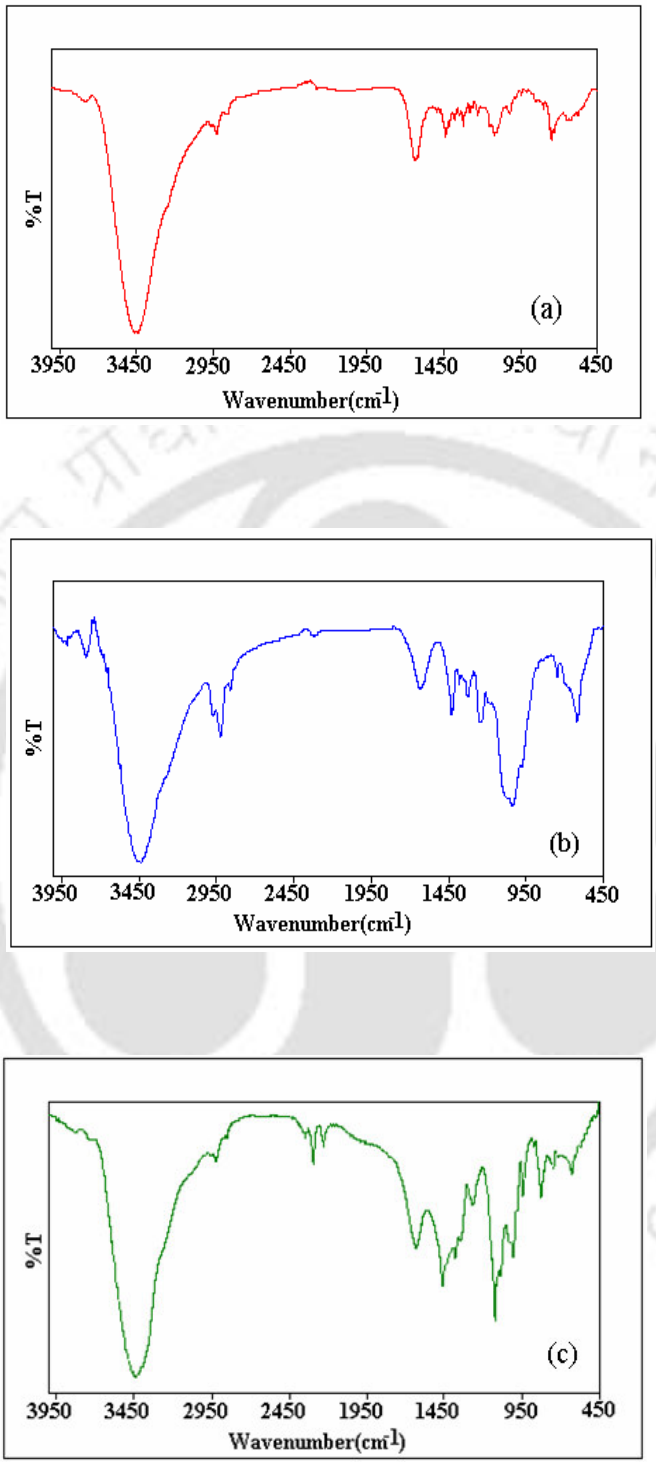

Figure 6.5: FT-IR spectra for complexes (a) **10**, (b) **11** and (c) **12** in KBr pellets.

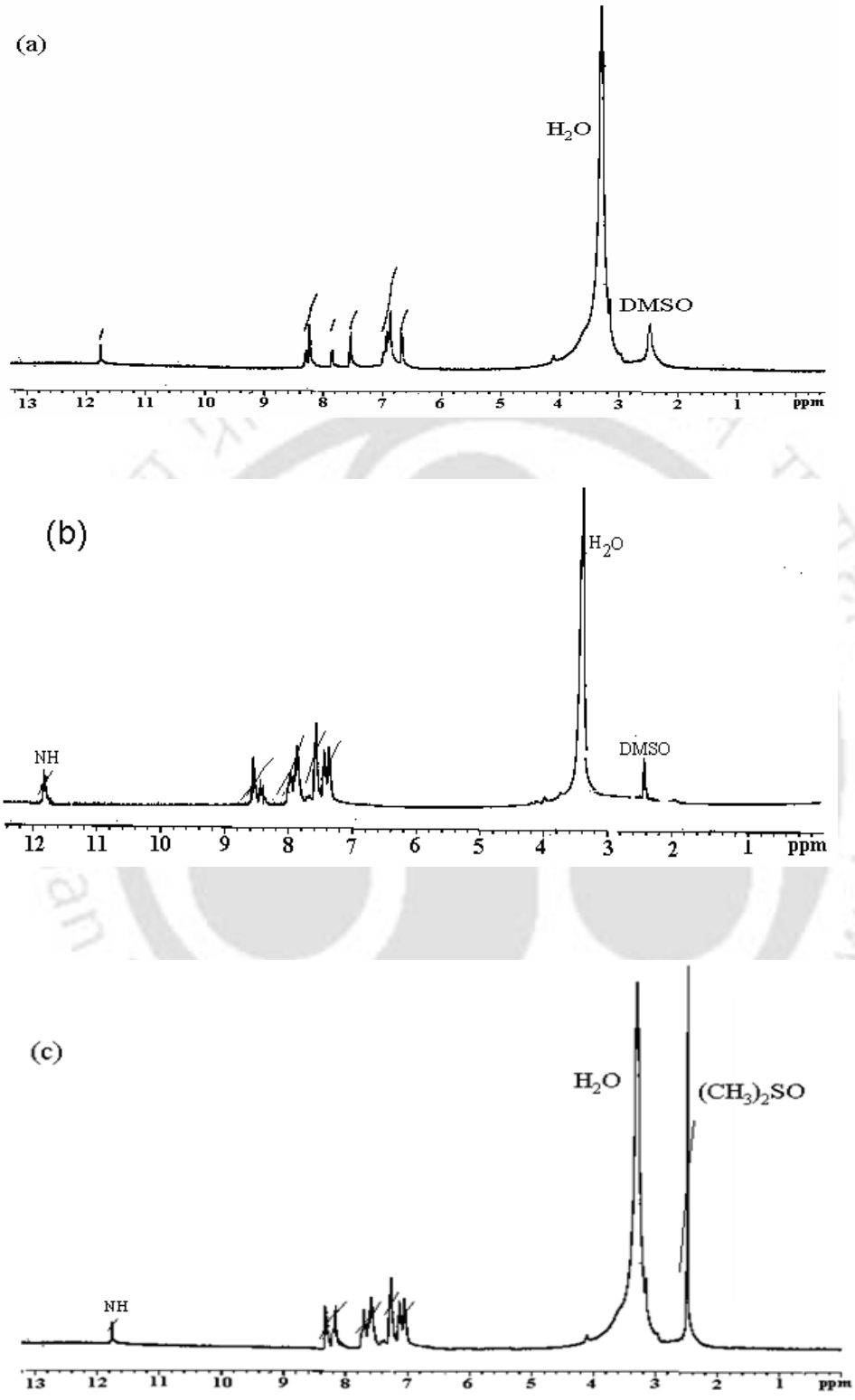

Figure 6.6: ^{1}H-NMR spectrum of complex (a) **10**, (b) **11** and (c) **12** in $(CD_3)_2SO$ solvent at room temperature.

6.2.6 Electrochemical studies

Redox properties of the complexes **10**, **11** and **12** have been studied in DMF solvent using glassy carbon platinum working electrode at 298K. Representative voltammograms are shown in figure 6.7. All potentials are referenced to the SCE. The complexes **10**, **11** and **12** display reversible Ru(III)/Ru(II) couples at 0.49 V, 0.55 V and 0.63 V, respectively. The one electron nature of the couples is confirmed by constant potential coulometry. The Ru(III)/Ru(II) couple of $[Ru(trpy)(L)Cl]^{2+}$ appears at 0.64 V.[25] Hence, the Ru(III)/Ru(II) couple of the chloro complex **10** appears at 0.50 mV lower potential than that of the previously reported analogous complexes, $[Ru^{II}(trpy)(L)Cl]^{+}$.[25] The better σ-donor nature of bbp compared to trpy is believed to be the primary contributing factor.[26] In the positive side of SCE, both the complexes display one more one electron quasi reversible couple at higher potential, at 1.30 V, 1.33 V and 1.35 V for **10**, **11** and **12**, respectively. These are assigned to the L_{sq}/L_q process.[27]

The complexes display two one-electron reductions at the negative side of SCE. The one-electron nature of these couples has been established by differential pulse voltammetry, which shows all the reduction waves to have the same height as that of the oxidation wave. Since both the coordinating ligands, bbp and L are known to accept electrons in their lowest unoccupied molecular orbitals,[10] the observed reductions are considered to be ligand based processes. Although there is no direct experimental evidence to assign the observed reductions corresponding to specific ligands, bbp and L, the first reduction couple is assigned to be associated with L. The reduction at the higher potential is assumed to be bbp based reductions. Very less solubility of the aqua-complex, **11** in water has precluded it's electrochemical study in aqueous solution at various pH.

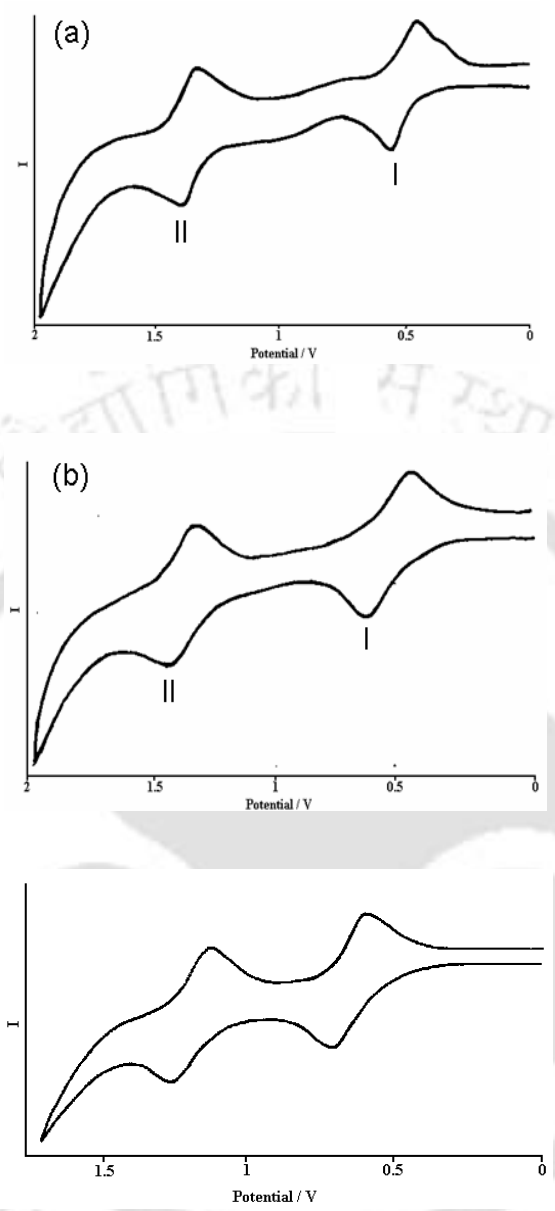

Figure 6.7: Cyclic voltammograms of complexes **10, 11** and **12** in DMF solvent at scan rate 50 mV/s under N_2 (SCE: Reference electrode; Glassy Carbon: Working electrode; Supporting electrolyte: TBAP).

6.3 Conclusion

Thus the present chapter described the stepwise synthesis of a set of complexes, [Ru(bbp)(L)(X)], [X = Cl (**10**), H_2O (**11**) and DMSO (**12**)]. The complexes have been characterized using various spectroscopic methods and single crystal X-ray structure determination. The physical and electrochemical properties of the complexes have been

studied in details. The electrochemical properties of complexes have been compared with the earlier reported complex **3a** (Chapter 3) and it has been observed that due to strong back bonding from the metal *d*-orbital to π^*-orbital of coordinated acetonitrile, the ruthenium(III)/ruthenium(II) couple in complex **3a** appears at higher potential than complexes **10**, **11** and **12**.

6.4 Experimental Section

6.4.1 Materials

Reagent-grade chemicals were used in all experiments and solvents were purified using standard procedures. The anciallry ligand, 2,6-*bis*(benzimidazol-2-yl)pyridine (bbp) and the starting complex, $[Ru(bbp)Cl_3]$ were synthesized using procedures reported previously.[9] *o*-phenylenediamine was purchased from Loba Chemie, Mumbai, India and purified before use.

6.4.2 Physical Measurements

Elemental analyses (C, H, N) were carried out using a Perkin-Elmer 240C elemental analyzer. Electronic and FT-IR spectra were recorded on Perkin-Elmer Lambda 25 and Perkin-Elmer spectrophotometer, respectively. Magnetic susceptibility measurements were made using PAR 155 vibrating sample magnetometer interfaced with a walker L75FBAL magnet. ^{1}H-NMR spectra were obtained from a 400 MHz Varian FT Spectrometer. Solution electrical conductivity was checked using a Systronic 305 conductivity bridge. Electrochemical measurements were made using CH Instruments 660A potentiostat. A glassy carbon working electrode, Pt wire auxiliary electrode and an aqueous saturated calomel reference electrode were used in a three-electrode configuration. All electrochemical measurements were done at 298

K under nitrogen atmosphere in methanol and aqueous solution containg TBAP as supporting electrolyte. The scan rate used was 50 mV/s. The half- wave potential E^0_{298} was set equal to $0.5(E_{pa} + E_{pc})$, where E_{pa} and E_{pc} are anodic and cathodic cyclic voltammetric peak potentials respectively.All the electrochemical data are uncorrected for junction potential. X-ray quality crystals were grown by slow diffusion followed by slow evaporation technique**.** The intensity data were collected using a Bruker SMART APEX-II CCD diffractometer, equipped with a fine focus 1.75 kW sealed tube MoK_α radiation (λ = 0.71073 Å) at 273(3) K, with increasing ω (width of 0.3° per frame) at a scan speed of 3 s/frame. The SMART software was used for data acquisition. Data integration and reduction were undertaken with SAINT and XPREP software. [28] Multi-scan empirical absorption corrections were applied to the data using the program SADABS.[29] Structures were solved by direct methods using SHELXS-97 and refined with full-matrix least squares on F^2 using SHELXL-97.[30] All non-hydrogen atoms were refined anisotropically. The hydrogen atoms were located from the difference Fourier maps and refined. Structural illustrations have been drawn with ORTEP-3 for Windows.[31]

6.4.2 Synthesis of complex [Ru^{II}(bbp)(L)(Cl)], 10

The precursor complex $Ru(bbp)Cl_3$ (300 mg, 0.58 mmol) is taken in 20 ml of ethanol and added 1,2 phenylenediammine (63 mg, 0.58 mmol) and NEt_3 (0.4 ml) and heated to reflux for 5h. The initial dark brown color of the solution was changed gradually to dark red. After that the volume of reaction mixture was reduced to 5 ml. It was then kept in freezer for 5h and solid precipitate thus obtained was filtered off and washed with cold water. The product was dried in vacuo over P_2O_5. It was then purified by using neutral alumina column. The complex was eluted by CH_2Cl_2/CH_3OH (4:1) solvent mixture.

Removal of the solvent under reduced pressure afforded the pure solid product. Yield: compound **10**; 210 mg (70%).

Anal. Cald.(%)($C_{25}H_{17}N_7ClRu$): C: 54.40; H: 3.10; N: 17.76. Found (%) C: 54.42; H: 3.11; N: 17.14. ^{1}H-NMR[$(CD_3)_2SO$, δ, ppm]: 8.34(m, 4H), 7.82(d, 2H), 7.57(t, 2H), 6.99(m, 4H), 6.70(t, 2H), 11.8(s, NH). ESI-Mass: 553.67.

6.4.3 Synthesis of complex [Ru^{II}(bbp)(L)(H_2O)], 11

The complex [Ru^{II}(bbp)(L)(Cl)], **10** (100 mg, 0.18 mmol) dissolved in ethanol:water (1:4, v/v) solvent mixture and treated with aqueous solution of $AgNO_3$ (in excess) and refluxed for 3h. After cooling down to room temperature, the precipitated AgCl was removed by filtration through a sintered crucible; the filtrate was then dried to solid mass. The crude solid upon purification using neutral alumina column and CH_2Cl_2/CH_3OH solvent mixture, afforded the pure aqua complex, **11** as dark colored solid. Yield: 30 mg (30%).

Anal. Calcd.(%)($C_{25}H_{19}N_7ORu$): C: 56.17; H: 3.58; N: 18.34. Found (%) C: 56.12; H: 3.60; N: 18.37. ^{1}H-NMR[$(CD_3)_2SO$, δ, ppm]: 8.51(t, 2H), 7.46(d, 2H), 7.71(m, 4H), 7.47(t, 2H), 7.18(m, 4H), 11.8(s, NH). ESI-Mass: 535.42.

6.4.4 Synthesis of complex [Ru^{II}(bbp)(L)(CH_3CN)], 3a

The complex **3a** has been synthesized in a following a different procedure earliar.[10] The complex **11** (50 mg, 0.093 mmol) was dissolved in 20 ml aectonitrile. It was heated to reflux for 5h. The solvent was then removed under reduced pressure to get the crude product. Upon purification using silica gel column and (4:1) CH_3CN/CH_3OH solvent mixture, the desired complex **3a** is obtained. Yield: 15 mg (30%). Elemental analyses and ^{1}H-NMR studies are reported in chapter 3.

6.4.4 Synthesis of complex [Ru^{II}(bbp)(L)(DMSO)], 12

The complex **11** (50 mg, 0.093 mmol) was dissolved in 10 ml ethanol:dimethyl sulfoxide (1:3, v/v). It was heated to reflux for 5h and kept in freezer; after a week the complex **12** is found to be crystallized out as dark colored rectangular shaped crystals. These are then separated from the solution and dried under vacuum. Anal. Calcd.(%)($C_{27}H_{23}N_7OSRu$): C: 54.53; H: 3.90; N: 16.49. Found (%): C: 54.59; H: 3.87; N: 16.51. ^{1}H-NMR[$(CD_3)_2SO$, δ, ppm]: 8.55(t, 2H), 8.41(d, 2H), 7.78(m, 4H), 7.44(t, 2H), 7.19(m, 4H), 2.50(s, 6H), 11.8(s, NH). ESI-Mass: 596.07.

6.5 References

1. (a) Abrahamsson, M.; Wolpher, H.; Johansson, O.; Larsson, J.; Kritikos, M.; Eriksson, L.; Norrby, P.-O.; Bergquist, J.; Sun, L.; Åkermark, B.; Hammarström, L. *Inorg. Chem.* **2005**, *44*, 3215. (b) Kalyanasundaram, K. *Photochemistry of Polypyridine and Porphyrin Complexes*; Academic Press: London, **1992**. (c) Scandola, F.; Chiorboli, C.; Indelli, M. T.; Rampi, M. A. In *Electron Transfer in Chemistry*; Balzani, V., Ed.; Wiley-VCH: Weinheim, Germany, **2001**; Vol. III.
2. (a) Barigelletti, F.; Flamigni, L. *Chem. Soc. Rev.* **2000**, *29*, 1. (b) Sauvage, J.-P.; Collin, J.-P.; Chambron, J.-C.; Guillerez, S.; Coudret, C.; Balzani, V.; Barigelletti, F.; De Cola, L.; Flamigni, L. *Chem. Rev.* **1994**, *94*, 993. (c) (5) Meyer, T. J. *Pure Appl. Chem.* **1986**, *58*, 1193. (d) Thummel, R. P.; Jhang, Y. *Inorg. Chem.* **1986**, *25*, 2527. (e) Calvert, J. M.; Caspar, J. V.; Binstead, R. A.; Westmoreland, T. D.; Meyer, T. J. *J. Am. Chem. Soc.* **1982**, *104*, 6620.
3. (a) Wolpher, H.; Johansson, O.; Abrahamsson, M.; Kritikos, M.; Sun, L.; Akermark, B. *Inorg. Chem. Commun.* **2004**, *7*, 337. (b) Medlycott, E. A.; Hanan, G. S. *Chem. Soc. Rev.* **2005**, *34*, 133. (c) Abrahamsson, M.; Jäger, M.; Österman, T.; Eriksson, L.; Persson, P.; Becker, H.-C.; Johansson, O.; Hammarström, L. *J. Am. Chem. Soc.* **2006**, *128*, 12616.
4. (a) Balzani, V.; Scandola, F.; *Supramolecular Photochemistry*, Horwood, Chichester, U.K. **1991.** (b) Kalyanasundaram, K. *Coord. Chem. Rev.* **1989**, *28*, 2920 (c) Meyer, T. J. *Pure Appl. Chem.* **1986**, *58*, 1193.
5. F. Scandola, C. A. Bignozzi and M. T. Indelli, *Photosensitization and Photocatalysis Using Inorganic and Organometallic Compounds*, eds. K. Kalyanasundaram and M. Gratzel, Kluwer, Dordrecht **1993**, p161.
6. (a) Balzani, V.; Juris, A.; Venturi, M.; Campagna, S.; Serroni, S. *Chem. Rev.* **1996**, *96*, 759. (b) Bignozzi, C. A.; Schoonover, J. R.; Scandola, F. *Prog. Inorg. Chem.*

1997, *44*, 1. (c) De Cola, L.; Belser, P. *Coord. Chem. Rev.* **1998**, *177*, 301. (d) Barigelletti, F.; Flamigni, L. *Chem. Soc. Rev.* **2000**, *29*, 1.

7. (a) Harriman, A.; Ziessel, R. *Chem. Commun.* **1996**, 925. (b) Barigelletti, F.; Flamigni, L.; Collin, J.-P.; Sauvage, J.-P. *Chem. Commun.* **1997**, 333.
8. (a) Haga, M.-a.; Hong, H.-Gi.; Shiozawa, Y.; Kawata, Y.; Monjushiro, H.; Fukuo, T.; Arakawa, R. *Inorg. Chem.* **2000**, *39*, 4566. (b) Haga, M.-a.; Takasugi, T.; Tomie, A.; Ishizuya, M.; Yamada, T.; Hossain, M. D.; Inoue, M. *J. Chem. Soc., Dalton Trans.* **2003**, 2069. (c) Terada, K.; Kobayashi, K.; Haga, M.-a. *J. Chem. Soc*., *Dalton Trans.* **2008**, 4846.(d) Vaidyanathan, V. G.; Nair, B. U. *J. Inorg. Biochem.* **2002**, *91*, 405. (e) Vaidyanathan, V. G.; Nair, B. U. *J. Chem. Soc., Dalton Trans.* **2005**, 2842.
9. (a) Addison, A. W.; Burke, P. J. *J. Heterocycl. Chem.* **1981**, *18*, 803. (b) Haga, M.; Kato, N.; Monjushiro, H.; Wang, K.; Hossain, M. D. *Supramol. Sci.* **1998**, *5*, 337.
10. Singh, A.; Pramanik, A.; Das, G.; Mondal, B. *Organometaliics* **2008**, *27*, 6403 and unpublished work.
11. (a) Mondal, B.; Puranik, V. G. ; Lahiri, G. K. *Inorg. Chem.* **2002**, *41*, 5831. (b) Chanda, N.; Mondal, B.; Puranik, V. G.; Lahiri, G. K. *Polyhedron* **2002**, *21*, 2033. (c) Mondal, B.; Paul, H.; Puranik, V. G. ; Lahiri, G. K. *J. Chem. Soc., Dalton Trans.* **2001**, 481 (d) Sarkar, S.; Sarkar, B.; Chanda, N.; Kar, S.; Mobin, S. M.; Fiedler, J.; Kaim, W.; Lahiri, G. K. *Inorg. Chem.* **2005**, *44*, 6092.
12. Pramanik. N. C.; Pramanik, K.; Ghosh, P.; Bhattacharya, S. *Polyhedron* **1998**, *17*, 1525
13. Singh, A.; Das, G.; Mondal, B. *Polyhedron* **2008**, *27*, 2563.
14. Boelrijk, A. M. E.; Reedijk, J. *J. Mol. Catal.* **1994**, *89*, 63.
15. Mondal, B.; walawalkar, M. G.; Lahiri, G. K. *J. Chem. Soc., Dalton Trans.* **2000**, 4209.

16. Cathey, C. J.; Constable, E. C.; Hannon, M. J.; Tocher, D. A.; Ward, M. D. *J. Chem. Soc., Chem. Commun.* **1990**, 6.

17. Forster, R. J.; Boyle, A.; Vos, J. G.; Hage, R.; Dijkhuis, A. H. J.; DeGraff, R. A. G.; Haasnoot, J. G.; Prins, R.; Reedijk, J. *J. Chem. Soc., Dalton Trans*. **1990**, 121.

18. Rachford, A. A.; Petersen, J. L.; Rack, J. J., *Inorg. Chem*. **2006**, *42*, 5953.

19. Calligaris, M.; Carugo, O. *Coord. Chem. Rev*, **1996**, *153*, 83.

20. Calligaris, M.; *Coord. Chem. Rev*, **2004**, *248*, 351.

21. (a) DeLearie, L. A.; Haltiwanger, R. C.; Pierpont, C. G. *Inorg. Chem.* **1989**, *28*, 644. (b) Karsanov, I. V.; Ivakhnenko, Y. P.; Khandkarova, V. S.; Prokofev, A. I.; Rubezhov,A. Z.; Kabachnik, M. I. *J. Organomet. Chem.* **1989**, *379*, 1. (c) Bhattacharya, S.; Pierpont, C. G.; *Inorg. Chem*. **1992**, *31*, 2020. (d) Bhattacharya, S.; Pierpont, C. G. *Inorg. Chem.* **1994**, *33*, 6038. (e) Whalen, A. M.; Bhattacharya, S.; Pierpont, C. G. *Inorg.Chem*. **1994**, *33*, 347. (f) Speier, G.; Whalen, A. M.; Cishony, J.; Pierpont, C. G. *Inorg. Chem.* **1995**, *34*, 1355. (g) Speier, G.; Whalen, A. M.; Csihony, J.; Pierpont, C. G. *Inorg. Chim. Acta* **1996**, *245*, 1.

22. (a) Verani, C. N.; Gallert, S.; Bill, E.; Weyhermuller, T.; Weighardt, K.; Chaudhuri, P. *Chem. Commun*. **1999**, 1747. (b) Chaudhuri, P.; Verani, C. N.; Bill, E.; Weyhermuller, T.; Weighardt, K. *J. Am. Chem. Soc.* **2001**, *123*, 2213. (c) Chun, H.; Verani, C. N.; Chaudhuri, P.; Bothe, E.; Bill, E.; Weyhermuller, T.; Weighardt, K. *Inorg. Chem*. **2001**, *40*, 4157. (d) Chun, H.; Weyhermuller, T.; Bill, E.; Weighardt, K. *Angew. Chem., Int. Ed. Engl.* **2001**, *40*, 2489. (e) Chun, H.; Chaudhuri, P; Weyhermuller, T.; Weighardt, K. *Inorg. Chem.* **2002**, *41*, 790. (f) Sun, X.; Chun, H.; Hildenbrand, K.; Bothe, E.; Weyhermuller, T.; Weighardt, K. *Inorg. Chem.* **2002**, *41*, 4295.

23. (a) Chanda, N.; Paul, D.; Kar, S.; Mobin, S. M.; Dutta, A.; Puranik, V. G.; Rao, K. K.; Lahiri, G. K. *Inorg. Chem.* **2005**, *44*, 3499. (b) Patra, S.; Sarkar, B.; Ghumaan, S.;

Patil, M. P.; Mobin, S. M.; Sunoj, R. B.; Kaim, W.; Lahiri, G. K. *J. Chem. Soc., Dalton Trans.* **2005**, 1188.

24. Mondal, B.; Walawalkar, M. G.; Lahiri, G. K.; *J. Chem. Soc., Dalton Trans.* **2000**, 4209.
25. (a) Maji, M.; Patra, S.; Chakraborty, S.; Janardanan, D.; Mobin, S. M.; Sunoj, R. B.; Lahiri, G. K. *Eur. J. Inorg. Chem*. **2007**, 314.
26. Singh, A.; Chetia, B.; Mobin, S. M.; Das, G.; Iyer, P. K.; Mondal, B. *Polyhedron* **2008**, *27*, 1983.
27. Ebadi, M.; Lever, A. B. P. *Inorg. Chem.* 1**999**, *38*, 467.
28. SMART, SAINT and XPREP, Siemens Analytical X-ray Instruments Inc., Madison, Wisconsin, USA, **1995**.
29. Sheldrick, G. M. SADABS: software for Empirical Absorption Correction, University of Gottingen, Institut fur Anorganische Chemieder Universitat, Tammanstrasse 4, D-3400 Gottingen, Germany, **1999–2003**.
30. Sheldrick, G. M. SHELXS-97, University of Gottingen, Germany, **1997**.
31. Farrugia, L. J. *J. Appl. Crystallogr.* **1997**, *30*, 565.

Abstract

A series of substituted ligands DBL [2,6-*bis*(1-benzylbenzimidazol-2-yl)pyridine], DEL [2,6-*bis(*1-ethylbenzimidazol-2-yl)pyridine], DML [2,6-*bis*(1-methylbenzimidaz ol-2-yl)pyridine] have been synthesized and characterized by spectroscopic techniques as well as single crystal X-ray structure. These substituted ligands have been used to synthesize the ruthenium oxolene complexes. It is interesting to note that the oxolene ligands are coordinated to metal in catecholato form rather than quinone and semiquinonate form.

7.1 Introduction

The photophysical and photochemical properties of ruthenium complexes incorporating polypyridyl ligands have been thoroughly investigated during the last decade.[1-5] Unlike the polypyridyl ligands, substituted 2,6-*bis*(benzimidazol-2-yl)pyridine, (bbp) ligands act as a hybrid having both strong σ–donor (benzimidazole unit) and π–accepter (pyridine ring) properties.[6] The substitution by alkyl and aryl group at the imidazole nitrogen center of bbp framework will allow one to tune the electron donor-/acceptor properties of bbp ligand. Thus, by the appropriate choice of substituent on the imidazole nitrogen, it is possible to modulate the spectro-electrochemical properties of the metal complexes of bbp based ligands in a predictable manner. The transition metal complexes with various bbp derivatives have been reported for their structural and spectro-chemical properties investigations.[7-9] Grätzel et al. reported the ruthenium(II) complexes of the type [Ru(dmbip)(Hdcbpy)X], [Ru(dmbip)(Hdcbiq)X] and [Ru(dhbip)-(Hdcbpy)X], where dmbip = 2,6-*bis*(1-methylbenzimidazol-2-yl)pyridine, dhbip = 2,6-*bis*(1-hexadecyl benzimidazol-2-yl)pyridine, H_2dcbpy = 4,4′-dicarboxy-2,2′-bipyridine, H_2dcbiq = 4,4′-dicarboxy-2,2′-biquinoline and X = Cl^-, NCS^-, CN^- or H_2O. They are known to act as efficient charge-transfer sensitizers when anchored onto nanocrystalline TiO_2 films.[10] Haga and co-workers reported the proton coupled electron transfer reaction of self assembled mono layers of ruthenium(II) complex containing tridentate bbp and substituted bbp ligand on gold surface.[11] The mononuclear ruthenium chemistry of substituted bbp ligand in combination with ancillary ligands are not much explored though it's chemistry with some transition metals like chromium, iron, cobalt and rhenium have been studied well.[12,15] Apart from this, the substituted bbp ligands can play an important role in ruthenium-dioxolene complexes to control the binding mode of the dioxolene type ligands.

This chapter deals with the synthesis of three substituted bbp ligands with benzyl,

ethyl and methyl groups, a new set of their ruthenium complexes and the study of the effect of absence of dissociable proton in bbp framework on the binding, spectral, electrochemical properties of their complexes.

7.2 Results and Discusssion

The bbp ligand has been modified by substituting the benzyl, ethyl and methyl group on N-center in it's frame work (Scheme 7.1). The substituted ligands have been synthesized using a modified reported procedure and the ligands have been characterized by various spectroscopic techniques as well as single crystal X-ray structure determination (Figure 7.1).

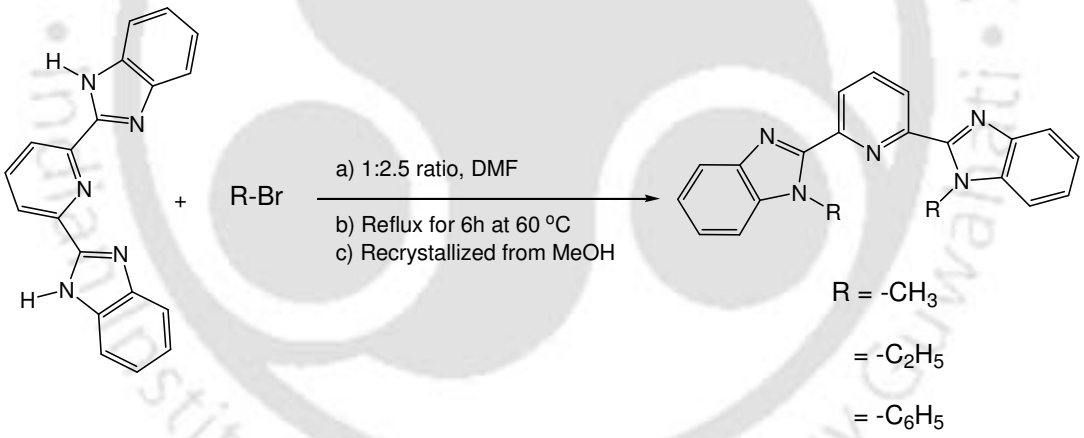

Scheme 7.1

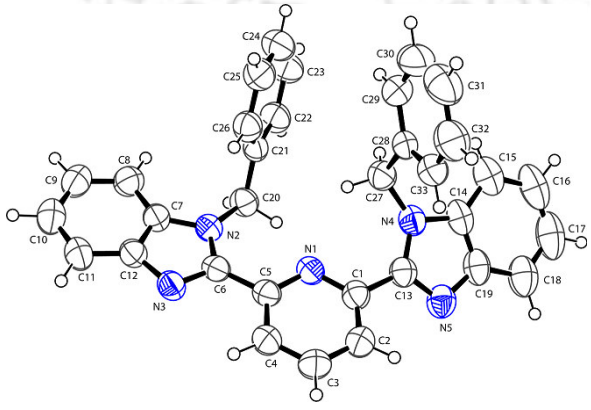

Figure 7.1: ORTEP diagram of **DBL** ligand (50% thermal ellipsoids plot).

The X-ray quality crystals of DBL were grown from the methanol solution. Figure 7.1 represents the ORTEP diagram of DBL. The crystallographic data are listed in table 7.1. From the crystal structure it is evident that both the N-H centers of the imidazole ring are substituted by the benzyl group. As a result the N(2)-C(7); 1.397(1), N(2)-C(6); 1.379(1) Å, N(4)-C(13); 1.383(1) Å and N(4)-C(14); 1.390(1) Å bond lengths are increased by an average of 0.023 Å compared to the unsubstituted bbp. On the other hand, the average bond length of N(3)-C(6); 1.323(1) Å and N(5)-C(13); 1.322(1) Å are decreased by 0.001 Å. This difference in bond lengths are attributed to the increase of localized single and double bond character of the corresponding bonds, respectively. The important bond lengths are given in table 7.2. The formation of all the ligands have been authenticated by comparing their ^{1}H-NMR (Figure 7.2), ^{13}C-NMR, FT-IR spectra with the earlier reported ones.[13]

Table 7.1: Crystallographic data for ligand **DBL**

	DBL
Formulae	$C_{33}H_{25}N_7$
Mol. wt.	491.00
Crystal system	Monoclinic
Space group	C2/c
Temperature /K	298(2)
Wavelength /Å	0.71073
a /Å	29.9824(8)
b /Å	10.9698(2)
c /Å	15.8551(3)
α/°	90.00
β/°	103.513(2)
γ/°	90.00

V/ $Å^3$	5070.40(19)
Z	8
Density/Mgm^{-3}	1.690
Abs. Coeff. /mm^{-1}	0.775
F(000)	2608
Total no. of reflections	5690
Reflections, I > 2σ(I)	2903
Max. 2θ/°	28.19
Ranges (h, k, l)	-24 <= h <= 24 -14 <= k <= 14 -20 <= l <= 21
Complete to 2θ (%)	98.3
Refinement method	Full-matrix least-squares on F^2
Data/ Restraints/Parameters	5690/0/344
WR_2(all data)	0.0998
Goof (F^2)	3.032
R indices [I > 2σ(I)]	0.0577
R indices (all data)	0.0998

Table 7.2: Selected bond lengths (Å) of ligand **DBL**

Bond lengths (Å)	**DBL**
N(1)-C(1)	1.345(1)
N(1)-C(5)	1.347(4)
N(2)-C(6)	1.379(1)
N(2)-C(7)	1.397(1)
N(2)-C(20)	1.467(1)
N(3)-C(6)	1.323(1)
N(3)-C(12)	1.323(1)
N(4)-C(13)	1.383(3)
N(4)-C(27)	1.454(3)
N(5)-C(13)	1.322(3)
N(5)-C(19)	1.392(3)
C(1)-C(13)	1.487(1)
C(5)-C(6)	1.480(4)
C(7)-C(12)	1.393(5)
C(11)-C(12)	1.393(1)
C(20)-C(21)	1.512(4)

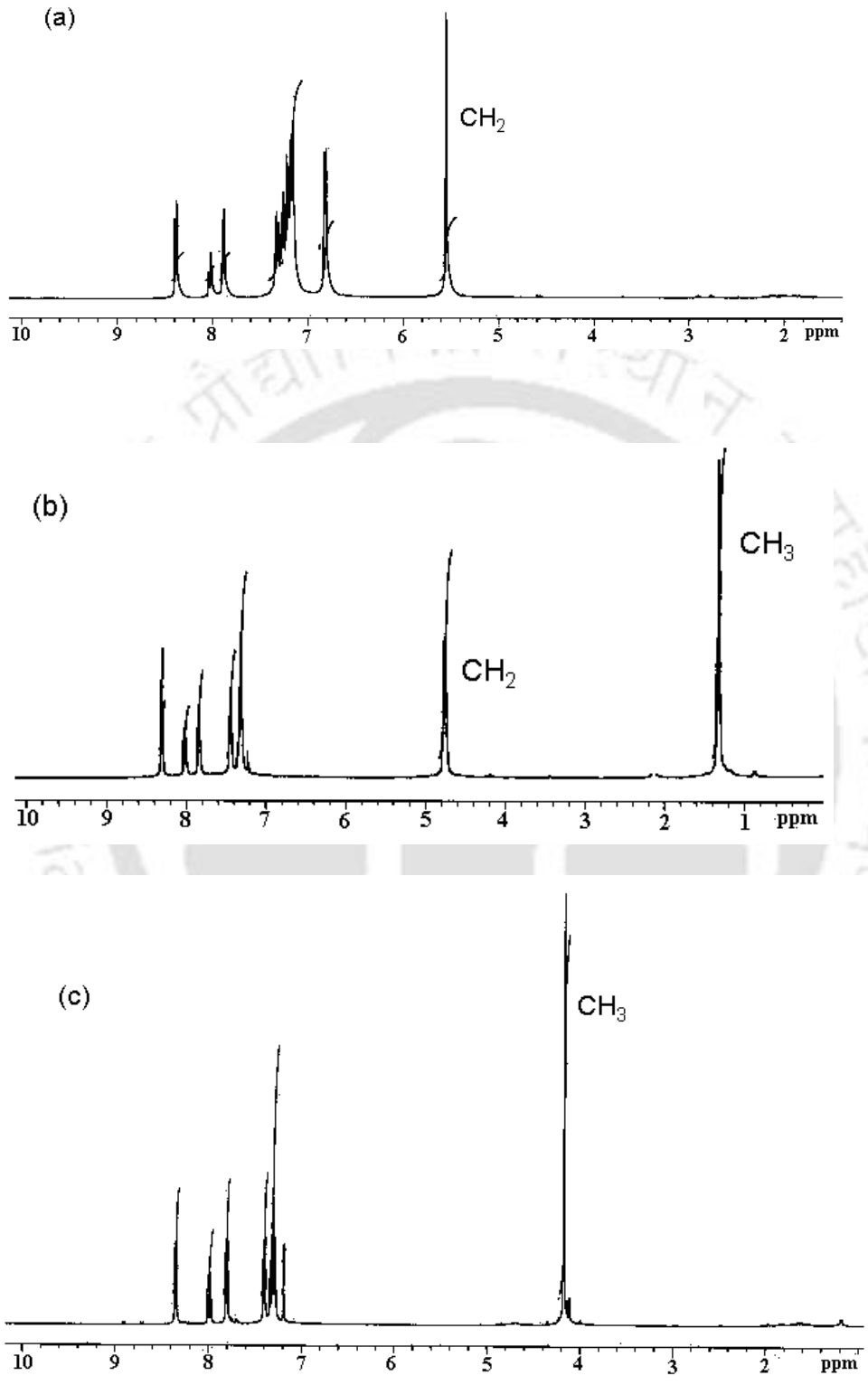

Figure 7.2: ^{1}H-NMR Spectra for (a) **DBL** (b) **DEL** and (c) **DML** ligand in $CDCl_3$ solvent.

These substituted ligands have been used to synthesize the corresponding ruthenium oxolene complexes [Ru(DBL)(L)CH_3CN)] (**13**), [Ru(DBL)(L)CH_3CN)] (**14**) and [Ru(DBL)(L)CH_3CN)] (**15**), [L = *o*-phenylenediamine] by the reaction of [Ru(DBL)Cl_3], [Ru(DBL)Cl_3] and [Ru(DBL)Cl_3], repectively with L in presence of NEt_3 in refluxing ethanolic medium. Chromatographic purification on silica gel column using (4:1) CH_2Cl_2/CH_3CN solvent mixture results into the pure products.

The complexes, **13-15** are found to be neutral and nonconducting in acetonitrile solvent. All the complexes exhibit satisfactory microanalysis (see Experimental Section).

7.2.1 Mass Spectroscopy

The ESI-mass spectra for all the complexes are recorded in acetonitrile/water (50:50) with 0.1% formic acid. The (m+1) molecular ion peaks for complexes **13-15** appear at 741.51, 613.39 and 592.04 respectively, which support the formation of the complexes (Figure 7.3).

Room temperature magnetic moment measurements reveal the diamagnetic nature of the all the three complexes. The observed diamagnetism of the complexes can be attributed either to the absence of any paramagnetic center in the molecule or to the spin coupling of multiple paramagnetic centers present in the complex.[16,17] Hence, in the present case, the charge distribution on both the redox active ligand and metal have become of interest. The diamagnetism can be explained on the basis of the following three combinations: (i) Ru^{II}-catecholate (ii) Ru^{III}-semiquinonate and (iii) Ru^{II}-quinonate. The neutral nature of the complexes precludes the possibility of Ru^{III}-semiquinonate or Ru^{II}-quinonate distribution. Hence, the Ru^{II}-catecholate distribution is the most probable one.

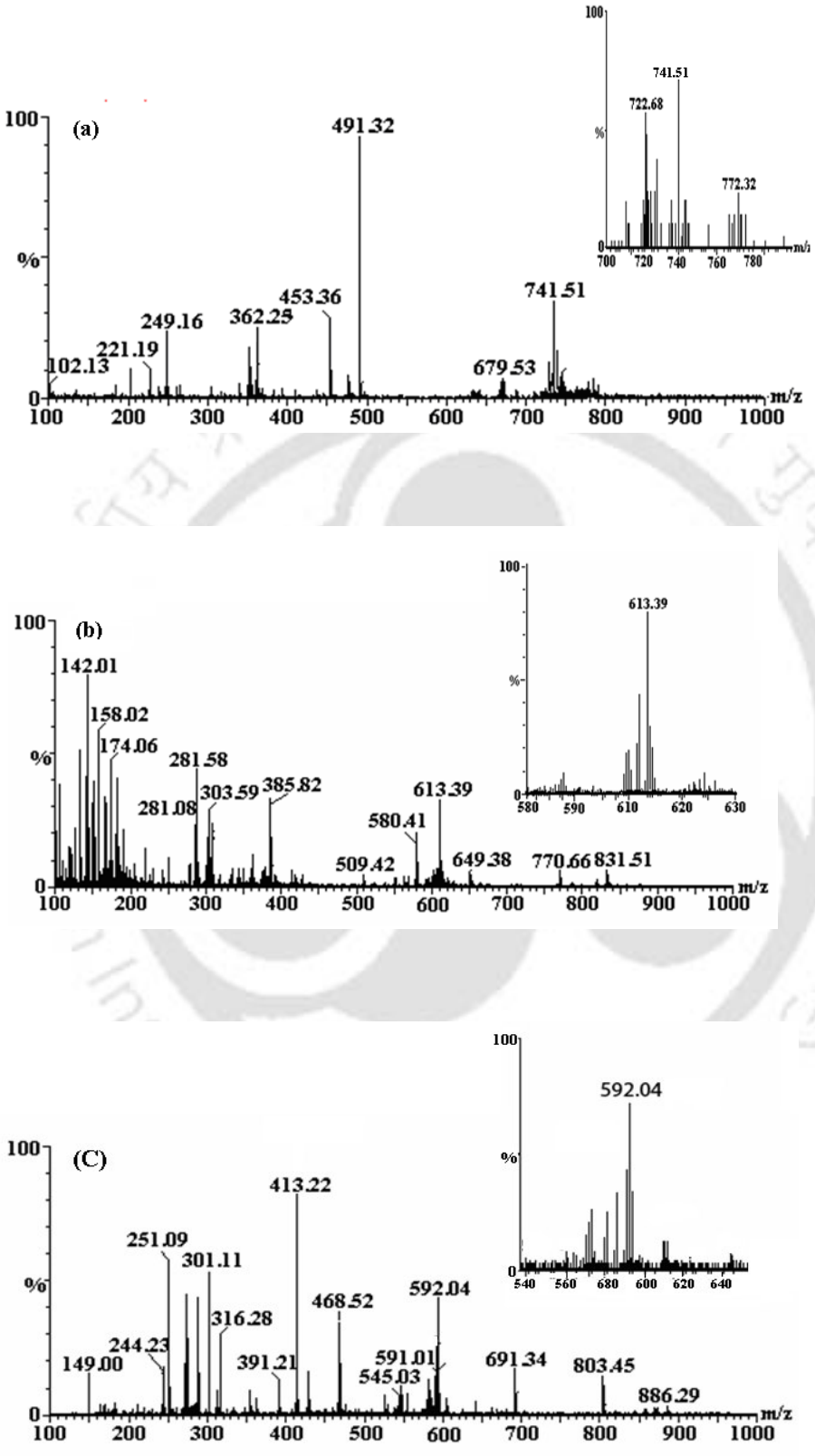

Figure 7.3: ESI-Mass spectra for complexes (a) **13**, (b) **14** and (c) **15** in CH_3CN/H_2O (50:50) with (0.1%) formic acid

7.2.2 UV-visible Spectroscopy

The UV-visible spectra of all the complexes were recorded in acetonitrile solvent. The spectra for all complexes are shown in figure 7.4. The complexes **13-15** exhibit a number of strong electronic absorption bands in the UV-visible region (Table 7.3).

Table 7.3

Complex	$\lambda_{max/nm}$ (ε/dm^{3}mol^{-1}cm^{-1})
13	237(22815), 313 (21130), 337 (21713), 349 (22144), 511(9498)
14	233(22249), 310 (19890), 335 (21160), 344 (21943), 514 (8558)
15	236 (22871), 312 (16522), 352 (20954), 510 (9460)

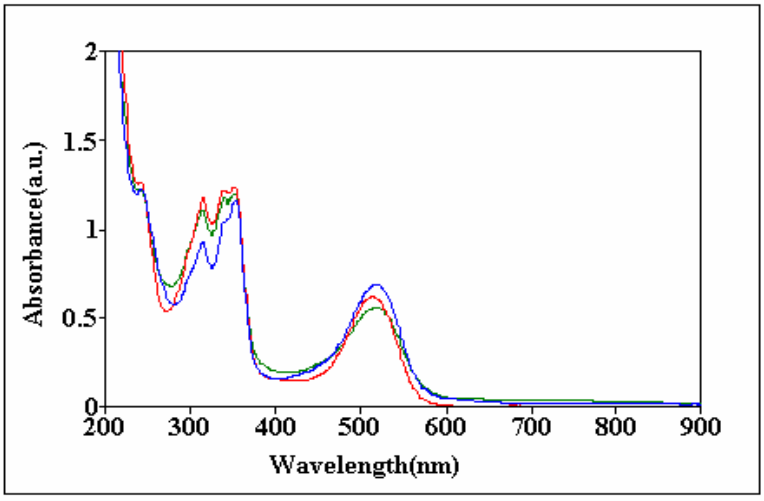

Figure 7.4: UV-visible spectra of complexes **13**(red), **14**(green) and **15**(blue) in acetonitrile solvent.

7.2.3 ^{1}H-NMR Spectroscopy

The ^{1}H-NMR spectra of complexes **13-15** were recorded in $(CD_3)_2SO$ at room temperature. In all the complexes, the NH protons of the oxolene moiety appear in the down field region in between δ 12.1-12.2 ppm. The aromatic protons appear in the region from δ 5.5 to 9.5 ppm. The aliphatic proton signal for the benzyl-CH_2 of complex **13**

appears at δ, 4.99 ppm (s, 2H); ethyl protons of complex **14**, at 1.30 (s, 2H) and 4.45 ppm (q, 2H) and methyl signal in case of complex **15**, at 4.60 ppm (s, 3H). In all the cases, the coordinated acetonitrile signal appears near δ, 2.20 ppm as sharp singlet corresponding to three protons. The similar signal for coordinated acetonitrile in [Ru(bbp)(*o*-phen)(CH_3CN)] and [Ru(trpy)(PAP)(CH_3CN)] {*o*-phen: *o*-phenylenediamine in quinone form; trpy: 2,2′:6′,2″-terpyridine; PAP: phenylazopyridine} was found to appear at 2.03 and 1.87 ppm, respectively.[18]

6.2.4 Cyclic Voltammetry

The cyclic voltammetric studies of the complexes **13–15** have been done in acetonitrile solvent using glassy carbon as working, Pt as auxiliary and SCE reference electrode in a three electrode configuration. The voltammograms of the complexes **13-15** show a quasi-reversible couple at 0.78 V, 0.71 V and 0.76 V, respectively (Figure 7.6). This couple has been found to be followed by another at 1.28 V, 1.18 V and 1.16 V for complexes **13**, **14** and **15**, respectively (Figure 7.6). One electron nature of all the couples were established by constant potential coulometry. The first couples are attributed to the Ru^{II}/Ru^{III} process and the next higher potential ones are to the sequential oxidation of semiquinone to quinone form of the oxolene moiety. While moving from complex **13** to **15**, the shift in potential of the Ru^{II}/Ru^{III} couple can be attributed to the better electron donor ability of DML ≈ DEL compared to DBL. The same couple was observed to appear at 0.84 V *vs* SCE in case of [Ru(bbp)(L)(CH_3CN)].[19] This is because of the change of binding mode of the bbp ligand to the metal center. In the present case the bbp binds the metal center as a neutral π-donor ligand. At the negative side of SCE, three one electron quasi-reversible processes are observed for all the complexes. The couple near -0.50 V and -0.47 V is assigned to the

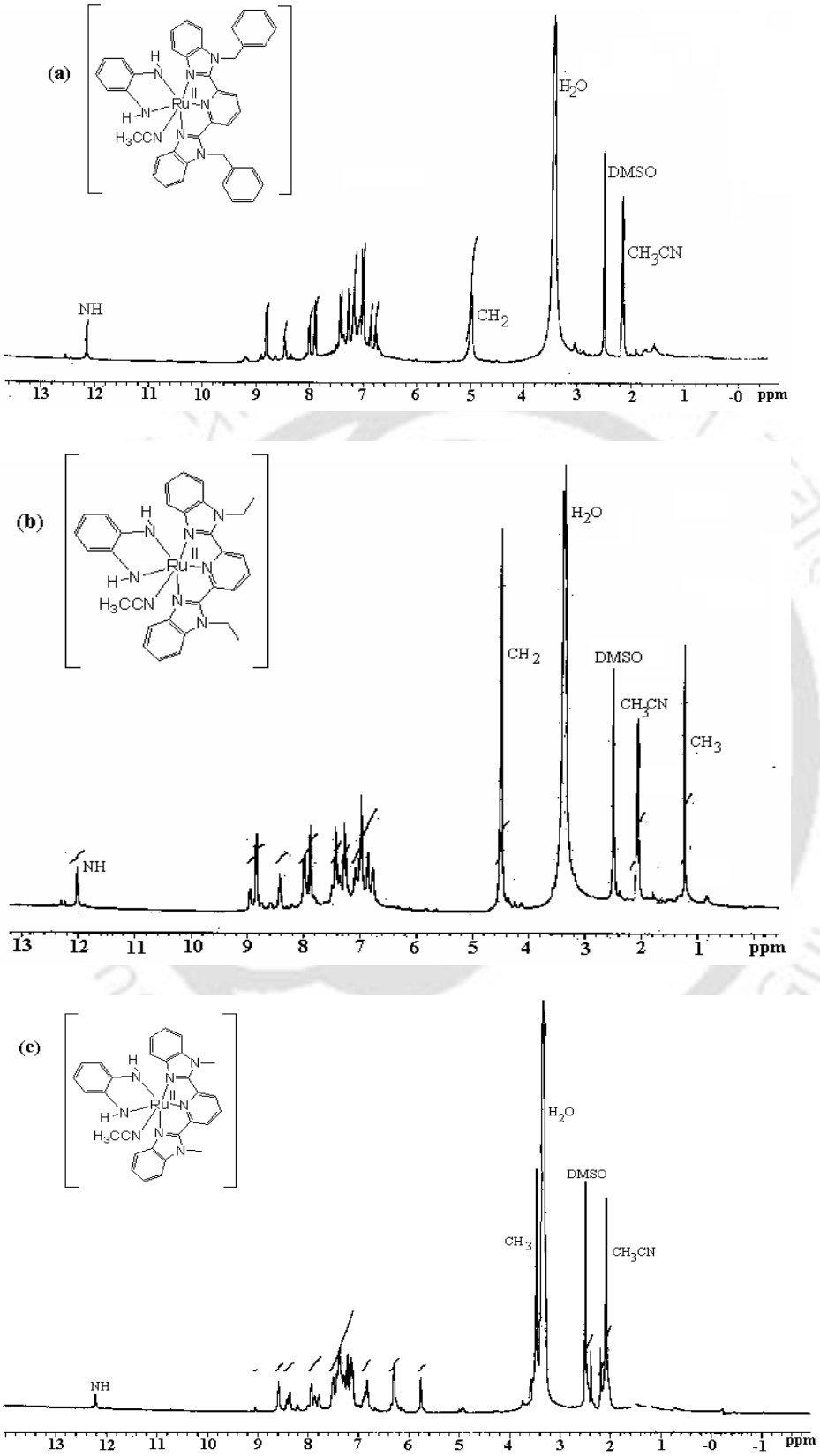

Figure 7.5: ^{1}H-NMR spectra for complexes (a) **13**, (b) **14** and (c) **15** in $(CD_3)_2SO$ solvent.

semiquinonate/catecholate reduction.[19,20] Other two lower potential reductions are attributed to the bbp reduction.[19]

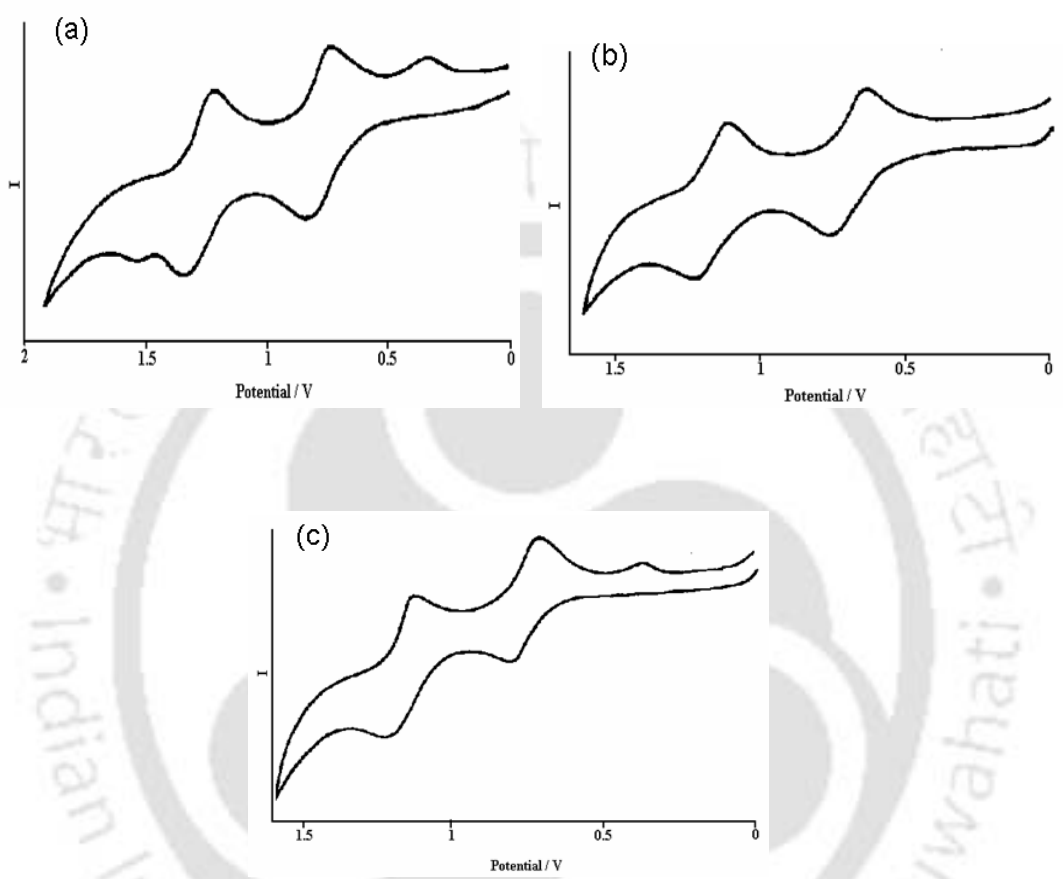

Figure 7.6: Cyclic voltammograms of complexes (a) **13**, (b) **14** and (c) **15** in acetonitrile solvent at scan rate 50 mV/s (SCE: Reference electrode Glassy Carbon: Working electrode; Supporting electrolyte: TBAP)

7.3 Conclusion

In summary, a new set of ruthenium complexes with substituted bbp ligands have been synthesized. All the complexes have been characterized using various spectroscopic techniques. The complexes reveal the difference in their redox potential on the basis of donor ability of substituents. The spectroscopic data of complexes **13-15** indicate that the dioxolene ligand bind to metal in catecholate form instead of the semiquinonate and quinine form which were observed in cases with bbp ligand in earlier cases (Chapter 3).

7. 4 Experimental Section

7.4.1 General

All reagents and solvents were purchased from commercial sources and were of reagent grade. Acetonitrile was distilled from calcium hydride. UV-visible spectra were recorded on a Perkin Elmer Lambda-25 spectrophotometer. FT-IR spectra were taken on a Perkin Elmer spectrophotometer with samples prepared as KBr pellets. Solution electrical conductivity was checked using a Systronic 305 conductivity bridge. ^{1}H-NMR spectra were obtained with a 400 MHz Varian FT spectrometer. Chemical shifts (ppm) were referenced to the residual solvent peaks. Elemental analyses were obtained from a Perkin Elmer Series II Analyzer. The Mass spectral studies were observed on Water Mass spectrometer.

7.4.2 Synthesis of substituted ligands

All the substituted ligands were synthesized following the same synthetic route. The 2,6-bis(benzimidazol-2-yl)pyridine (bbp) ligand was prepared using the reported process.[21] The ligands **DML**, **DEL** were prepared in high yields through simple alkylation of bbp with methyl bromide and ethyl bromide respectively, in DMF at room temperature; while the alkylation of bbp with benzyl for **DBL** ligand proceeds at higher temperature (60 °C).[13, 22]

Synthesis of DML

The powdered KOH (280 mg, 5 mmol) was added to a stirring suspension of bbp ligand (311 mg, 1 mmol) in DMF. After a few minute, methyl iodide (1.42 g, 10 mmol) was added to the reaction mixture with vigorous stirring. After 6h, the mixtures were added to cold water. The precipitate was filtered off and was recrystallized from methanol and brownish white crystals were obtained with a yield of 70% (211 mg).

All the other substituted ligands synthesized were confirmed by elemental analysis and NMR spectral data also.

Characterization

DBL: ^{1}H-NMR (400MHz, $CDCl_3$): δ(ppm); 8.38(d, 1H, *J* = 6.4Hz), 8.02(t, 4H, *J* = 6.3Hz), 7.88(d, 4H, *J* = 8.0Hz), 7.20(m, 8H, *J* = 7.6Hz), 8.15(d, 4H, *J* = 7.2Hz), 5.55(s, 4H)

DEL: ^{1}H-NMR (400MHz, $CDCl_3$): δ(ppm); 831(d, 2H, *J* = 8Hz), 8.02(t, 2H, *J* = 7.8Hz), 7.84(t, 2H, *J* = 6.8Hz), 7.45(t, 2H, *J* = 6.8Hz), 7.32(m, 4H, *J* = 5. 6Hz), 4.77(q, 2H, *J* = 7.2Hz), 1.33(t, 3H, *J* = 6.8Hz)

DML: ^{1}H-NMR (400MHz, $CDCl_3$): δ(ppm); 8.34(d, 2H, *J* = 8Hz), 7.98(t, 1H, *J* = 8Hz), 7.80(d, 2H, *J* = 7.2Hz), 7.41(d, 4H, *J* = 7.6Hz), 7.29(m, 4H, *J* = 6.8Hz), 4.17(s, 6H)

7.4.3 Synthesis of complex [Ru(DBL)(L)(CH_3CN)], 13

The [Ru(bbp)(DBL)Cl_3] (300 mg, 0.43 mmol) and *o*-phenylenediamine (46 mg, 0.43 mmol) is taken in 20 ml of ethanol and added NEt_3 (0.5 ml) and heated to reflux for 4h. After that the volume of reaction mixture was reduced to 5 ml. It was kept in freezer for overnight and solid precipitate thus obtained was filtered off and washed with cold water and diethylether. The product was dried in vacuo over P_2O_5. It was then purified by using silica gel column by using CH_2Cl_2:CH_3CN (4:1) as eluent. The solvent was dried under reduced pressure which affords a pure, dark colored solid. Yield 210 mg (70%). Anal. Calcd. (%)($C_{41}H_{34}N_8Ru$): C: 66.56; H: 4.63; N: 15.35. Found (%) C: 66.58; H: 4.62; N: 15.35. ^{1}H-NMR[$(CD_3)_2SO$, δ, ppm]: 11.8(s, 1NH), 8.58(d, 2H), 8.41(t, 2H), 7.94(d, 2H), 7.39(t, 2H), 7.09(d, 2H), 6.99(d, 2H), 6.84(t, 5H), 6.74(d, 2H), 5.01(s, 2H), 2.07(s, 3H). ESI-Mass: 741.51

7.4.4 Synthesis of complex [Ru(DEL)(L)(CH_3CN)], 14

The [Ru(bbp)(DEL)Cl_3] (300 mg, 0.43 mmol) and *o*-phenylenediamine (53 mg, 0.43 mmol) is taken in 20 ml of ethanol and added NEt_3 (0.5 ml) and heated to reflux for 5h. The volume of reaction mixture was reduced to 5 ml and was kept in freezer for overnight to get solid precipitate. The precipitate obtained was filtered off and washed with cold water followed by diethylether. The product was dried in vacuo over P_2O_5. It was then purified by using silica gel column by using CH_2Cl_2:CH_3CN solvent mixture. Removal of the solvent under reduced pressure afforded the pure solid. Yield 180 mg (60%). Anal. Calcd. (%)($C_{31}H_{30}N_8Ru$): C: 60.47; H: 4.91; N: 18.20. Found (%) C: 60.44; H: 4.91; N: 18.35. ^{1}H-NMR[$(CD_3)_2SO$, δ, ppm]: 12.2(s, NH), 8.81(d, 2H), 8.45(t, 3H), 7.98(d, 2H), 7.88(d, 2H), 7.42(t, 2H), 7.27(t, 2H), 7.16(d, 2H), 7.01(d, 2H), 6.98(t, 2H), 4.55(q, 2H), 1.44(t, 3H), 2.01(s, 3H). ESI-Mass: 613.39.

7.4.5 Synthesis of complex [Ru(DML)(L)(CH_3CN)], 15

The [Ru(bbp)(DML)Cl_3] (300 mg, 0.43 mmol) and *o*-phenylenediamine (55 mg, 0.43 mmol) is taken in 20 ml of ethanol and added NEt_3 (0.5 ml) and heated to reflux for 5h. After that the volume of reaction mixture was reduced to 5 ml, it was kept in freezer for overnight and solid precipitate thus obtained was filtered off; washed with cold water and diethylether. The crude product was dried in vacuo over P_2O_5. Purification of the crude product using silica gel column and CH_2Cl_2:CH_3CN solvent, yielded the desired product. Yield:195 mg (65%). Anal. Calcd. (%) ($C_{29}H_{26}N_8Ru$): C: 59.27; H: 4.46; N: 19.07. Found (%) C: 59.30; H: 4.44; N: 19.05. ^{1}H-NMR[$(CD_3)_2SO$, δ, ppm]: 11.99(s, NH), 8.88(d, 2H), 8.38(t, 2H), 7.99(t, 2H), 7.41(m, 4H), 6.98(t, 2H), 6.45(d, 2H), 5.93(d, 2H), 3.87(s, 3H), 2.02(s, 3H). ESI-Mass: 592.04

7.5 References

1. Ferraudi, G. J. *Elements of Inorganic Photochemistry*, Wiley-Interscience, New York, **1988**.

2. Roundhill, D. M. *Photochemistry and Photophysics of Metal Complexes*, Plenum, New York, **1994**.

3. Juris, A.; Balzani, V.; Barigelletti, F.; Campagna, S.; Belser, P.; von Zelewsky, A. *Coord. Chem. Rev.*, **1988**, *84*, 85.

4. Opperman, K. A.; Mecklenburg, S. L.; Meyer, T. J. *Inorg. Chem.*, **1994**, *33*, 5295.

5. (a) Scandola, F.; Inddelli, M. T.; Bignozzi, C. A. *Top. Curr. Chem.*, **1990**, *158*, 73. (b) Scandola, F.; Bignozzi, C. A.; Inddelli, M. T. *Photosensitization and Photocatalysis Using Inorganic and Organometallic Compounds*, Kluwer, Dordrecht, **1993**, pp. 161–216.

6. Ashwell, G. J. *Molecular Electronics*, RSP Ltd., Taunton, **1991**.

7. (a) Breslow, R.; Hunt, J. T.; Smiley, R.; Tarnowski, T. *J. Am. Chem. Soc.* **1983**, *105*, 5337. (b) Beer, R. H.; Tolmann, W. B.; Bott, S. G.; Lippard, S. J. *Inorg. Chem.* **1989**, *28*, 4557. (c) Wu, F.-J.; Kurtz, D. M., Jr.; Hagen, K. S.; Nyman, P. D.; Debrunner, P. G.; Vankai, V. A. *Inorg. Chem.* **1990**, *29*, 5174. (d) Kimblin, C.; Allen, W. E.; Parkin, G. *J. Chem. Soc., Chem. Commun.* **1995**, 1813. (e) Sorrell, T. N.; Allen, W. E.; White, P. S. *Inorg. Chem.* **1995**, *34*, 952.

8. (a) Chatlas, J.; Kaizaki, S.; Kita, E.; Kita, P.; Sakagami, N.; Van Eldik, R. *J. Chem. Soc., Dalton Trans.* **1999**, 91. (b) Winter, J. A.; Caruso, D.; Shepherd, R. E. *Inorg. Chem*. **1988**, *27*, 1086. (c) Bocarsly, J. R.; Chiang, M. Y.; Bryant, L.; Barton, J. K. *Inorg. Chem*. **1990**, *29*, 4898.

9. Ceniceros-Go´meza, A. E.; Barba-Behrensa, N.; Quiroz-Castro, M. E.; Berne`s, S.; No¨th, H.; Castillo-Blum, S. E. *Polyhedron* **2000**, *19*, 1821.

10. Naseeruddin, M. K.; Mullar, E.; H-Baker, R.; Vlachopoulos, N.; Grätzel, M. *J. Chem. Soc., Dalton Trans.* **1997**, 4571.

11. Haga, M.-a.; Hong, H.-Gi.; Shiozawa, Y.; Kawata, Y.; Monjushiro, H.; Fukuo, T.; Arakawa, R. *Inorg. Chem.* **2000**, *39*, 4566.

12. Ghosh, S.; Nanda, K. K.; Addison, K. A. W.; Butcher, R. J. *Inorg. Chem.* **2002**, *41*, 2243.

13. Zhang, W.; Sun, W-H.; Zhang, S.; Hou, J.; Wedeking, K.; Schultz, S.; Fro¨hlich, R.; Song, H. *Organometallics* **2006,** *25,* 1961.

14. Gelling, A.; Orrel, K. G.; Osborne, A. G. Sik. V.; Hurstouse, M. B.; Hibbs, David, E.; Malik, K. M. A. *Polyhedron*, **1998**, *17*, 2141.

15. Shklover, V.; Eremenko, I. L.; Berke, H.; Nesper, R.; Zakeeruddin, Nazeeruddin. M. K.; Grätzel. M. *Inorg. Chim. Acta*, **1994**, *219*, 11.

16. (a) DeLearie, L. A.; Haltiwanger, R. C.; Pierpont, C. G. *Inorg. Chem.* **1989**, *28*, 644. (b) Karsanov, I. V.; Ivakhnenko, Y. P.; Khandkarova, V. S.; Prokofev, A. I.; Rubezhov, A. Z.; Kabachnik, M. I. *J. Organomet. Chem.* **1989**, *379*, 1. (c) Bhattacharya, S.; Pierpont , C. G. *Inorg. Chem.* **1992**, *31*, 2020. (d) Bhattacharya, S.; Pierpont, C. G. *Inorg. Chem.* **1994**, *33*, 6038. (e) Whalen, A. M.; Bhattacharya, S.; Pierpont, C. G. *Inorg. Chem.* **1994**, *33*, 347. (f) Speier, G.; Whalen, A. M.; Csihony, J.; Pierpont, C. G. *Inorg. Chem.* **1995**, *34*, 1355. (g) Speier, G.; Whalen, A. M.; Csihony, J.; Pierpont, C. G. *Inorg. Chim. Acta* **1996**, *245*, 1.

17. (a) Verani, C. N.; Gallert, S.; Bill, E.; Weyhermuller, T.; Weighardt, K.; Chaudhuri, P. *Chem. Commun.* **1999**, 1747. (b) Chaudhuri, P.; Verani, C. N.; Bill, E.; Weyhermuller, T.; Weighardt, K. *J. Am. Chem. Soc.* **2001**, *123*, 2213. (c) Chun, H.; Verani, C. N.; Chaudhuri, P.; Bothe, E.; Bill, E.; Weyhermuller, T.; Weighardt, K. *Inorg. Chem.* **2001**, *40*, 4157. (d) Chun, H.; Weyhermuller, T.; Bill, E.; Weighardt, K. *Angew. Chem., Int. Ed. Engl.* **2001**, *40*, 2489. (e) Chun, H.; Chaudhuri, P;

Weyhermuller, T.; Weighardt, K. *Inorg. Chem.* **2002**, *41*, 790. (f) Sun, X.; Chun, H.; Hildenbrand, K.; Bothe, E.; Weyhermuller, T.; Weighardt, K. *Inorg. Chem.* **2002**, *41*, 4295.

18. (a) Pramanik, N. C.; Pramanik, K.; Ghosh, P.; Bhattacharya, S. *Polyhedron*, **1998**, *17*, 1525.
19. Singh, A.; Pramanik, A.; Das, G.; Mondal, B. *Organometaliics* **2008**, *27*, 6403 and unpublished results.
20. Ebadi, M.; Lever, A. B. P. *Inorg. Chem.* **1999**, *38*, 467.
21. (a) Addison, A. W.; Burke, P. J. J. *Heterocycl. Chem*. **1981**, *18*, 803. (b) Muller, G.; Bu1nzli, J.-C. G.; Schenk, K. J.; Piguet, C.; Hopfgartner, G. *Inorg. Chem.* **2001**, *40*, 264.
22. Kikugawa, Y. synthesis **1981**, 124.

Research Publications

1. Ruthenium monoterpyridine complexes with 2,6-*bis*(benzimidazol-2-yl)pyridine: Synthesis, spectral properties and structure.

   Singh, A.; Chetia, B.; Mobin, S. M.; Das, G.; Iyer, P. K.; Mondal, B.

   Polyhedron, **2008**, *27*, 1983.

2. Ruthenium monoterpyridine complexes with 2,6-*bis*(benzoxazol-2-yl)pyridine as an ancillary ligand: Synthesis, structure and spectral studies.

   Singh, A.; Das, G.; Mondal, B.

   Polyhedron, **2008**, *27*, 2563.

3. Reduction of coordinated acetonitrile to ethylamine in Ruthenium complex by *p*-phenylenediamine or hydroquinone.

   Singh, A.; Pramanik, A.; Das, G.; Mondal, B.

   Organometallics, **2008**, *27*, 6403.

4. Reduction of copper(II) complex of a tripodal ligand by nitric oxide and reductive nitrosation of the ligand.

   Sarma, M.; Singh, A.; Gupta,G. S.; Das, G.; Mondal, B.

   Inorg. Chim. Acta, **DOI: 10.1016/j.ica.2009.09.048**

5. Solvent dependent disproportionation of Cu(II) complexes of N_2O_2-type ligands: Direct evidence of formation of phenoxyl radical.

   Debnath, R. K.; Singh, A.; Mondal, B. (***submitted***)

6. Proton dependent valance state distribution in ruthenium *o*-quinonoids with 2,6-*bis*(benzimidazol-2-yl)pyridine ancillary.

   Singh, A.; Mondal, B. (***submitted***)

7. Valance state distribution in ruthenium complexes of 2,6-*bis*(benzimidazol-2-yl)pyridine with catechol and acetylacetone as ancillary ligands.

Singh, A.; Mondal, B. (***submitted***)

8. Synthesis of ruthenium complexes Ru^{II}(bbp)(dioxolene)(Cl)], [Ru^{II}(bbp)(dioxolene)(H_2O)], [Ru^{II}(bbp)(dioxolene)(DMSO)] and [Ru^{II}(bbp)(dioxolene)(CH_3CN)]: Structural and spectral studies

   Singh, A.; Mondal, B. (***submitted***)